USE OF REMOTE SENSING FOR LAND USE POLICY FORMULATION

Annual Progress Report, June 1, 1982-May 31,1983

Prepared for:

Office of Space & Terrestrial Applications
National Aeronautics and Space Administration
Washington, D.C.

NASA Grant Number: NGL 23-004-083

Center for Remote Sensing
Michigan State University
East Lansing, Michigan 48824

Table of Contents

USE OF REMOTE SENSING FOR LAND USE POLICY FORMULATION

Page intentionally left blank

Page intentionally left blank

INTRODUCTION AND SUMMARY

Because of the numerous activities occurring in the Center this past year, this summary will attempt to highlight only the most salient points in each of the following areas:

1) publications and presentations resulting from research efforts;
2) new staff;
3) new space and equipment;
4) data base related activities and abilities to handle new types of remotely sensed data;
5) major new contracts in the Center;
6) general networking to provide technology transfer and application of research and development; and
7) an overview of the state of program on various research thrusts.

1. This year was good from the standpoint of publications and scientific presentations. Specifics are outlined on pages 52 to 55. The highlight was the 1983 William A Fischer Memorial Award presented to Ardeshir Goshtasby and William Enslin for their paper entitled "Registration of Rotated Images by Invariant Moments."

2. Scientific expertise is the key to a productive Center. This last year one of our Center specialists, Dave Lusch, obtained his Ph.D. in Geography. His research and disseration were on

"The Origin and Morphogenetic Significance of Patterned Ground in the Saginaw Lowland of Michigan." With his advanced degree, Dave is now providing much more leadership internally from a research standpoint and also is continuing his networking with other scientists on campus and at other agencies.

The highlight of new staff input is the addition of Dr. Kurt Pregitzer, Department of Forestry, who is very interested in biological productivity in forest ecosystems. Specifically, he provides a strong input into landform analysis and is using this concept as an input into a rational approach toward biological productivity. He has been very supportive of Center activities and many mutually beneficial relationships are evolving.

3) Space and equipment have also been expanded. An additional 800 square feet has been obtained for the Center. This has allowed us to separate the data processing area from the photointerpretation area. In addition, two IBM PC's have been obtained. One of these, with a color monitor and digitizer, has allowed us to significantly enhance the digital analysis capabilities within the Center. Also, two Harris minis are now being used extensively as part of the pre-processing capabilities that exist at MSU. These minis are widely used by our support staff in preparation of data for analysis. Coupled closely with this is increased data-based handling capabilities.

4) Close linkages with the Michigan Department of Natural Resources' data bases are being developed. They are digitizing extensive spacial information through the Resource Inventory Act in Michigan and their data can now be readily used in analysis within our Center for Remote Sensing.

New types of data obtained have included Landsat TM data, which has been examined and used both digitally and in analog form. This data has been found to be of extremely good quality and will aid us in addressing a number of additional fundamental questions. Also, in keeping with the Center's interest both in meteorological satellites and land resource inventory satellites, we have acquired a considerable number of NOAA digital tapes. We have evaluated these and are now using them in our research efforts.

5) We've received a contract from NASA Goddard "Temperature and Reflectance Monitored From Satellites as an Indicator of Shift and Impact of Vegetation Change," Jon Bartholic, Principal Investigator. This grew out of some preliminary work on the basic NASA university grant. Also, smaller grants on prime farmlands from the Soil Conservation Service and a contract from Dow Chemical to use multiple data bases for products targeting are but two examples in this area.

6) Networking is a key priority within the Center. To address many of the research efforts and certainly the priority areas associated with general global habitability science issues, team efforts are frequently needed. We continue to have a

very good working relationship with the Michigan Department of Natural Resources, Soil Conservation Service and numerous other groups. Also, this year, we've developed a much closer working relationship with the Corps of Engineers. The newsletters have continued to be published to keep the wide clientele of interested scientists up to date with new technologies and happenings within the Center.

7) Significant progress was made on numerous research areas.

A. Reports are provided on digital classification of coniferous forest types. Here, techniques for classifying forest-types were developed. Various analysis approaches and the accuracy of those techniques have been evaluated.

B. The project dealing with GOES data for radiant temperatures has moved forward. The data has been extensively reviewed and classified as to degree of cloudiness. Work on overlaying GOES information from different times of the day and different days of the year has moved ahead. Complimentary data bases dealing with surface conditions, vegetation and water-holding capacity have been digitized. The development of these statewide data bases has required a massive effort. With the data bases now operational, this project and many others requiring the data will move ahead rapidly.

C. Under land surface change detection, the potentials of the new TM data are being documented. Clearly, with the better resolution and increased informational content of the additional bands and better range, change detection is possible. This project is being underwritten cooperatively with the Michigan Department of Natural Resources as part of the Resource Inventory Act. Also, sophisticated programs were developed for geometrically correcting and overlaying different remotely sensed data.

D. Remote sensing of virus-infected blueberries (a prototype study) is nearing completion. That is reported on in detail later in this report. The use of the spectroradiometer has been very helpful in providing more detailed signatures of reflectance.

Again, the most significant completed results are reported in publications, pages 52 to 55.

PARTICIPATING FACULTY AND STAFF OF THE CENTER FOR REMOTE SENSING

Faculty

Jon F. Bartholic, Acting Director
Tony Bauer, Assistant Professor, School of Urban Planning and Landscape Architecture
Myles Boylan, Professor Emeritus, School of Urban Planning and Landscape Architecture
Stuart Gage, Associate Professor, Department of Entomology
Rene C. Hinojosa, Assistant Professor, School of Urban Planning and Landscape Architecture
Anil K. Jain, Professor, Department of Computer Science
Delbert L. Mokma, Associate Professor, Department of Crop and Soil Sciences
Fred Nurnberger, Associate Professor, Department of Agricultural Engineering
Kurt Pregitzer, Assistant Professor, Department of Forestry
Carl Ramm, Assistant Professor, Department of Forestry
Don Ramsdell, Professor, Department of Botany and Plant Pathology
Gene Safir, Associate Professor, Department of Botany and Plant Pathology
Ger Schultink, Assistant Visiting Professor, Department of Resource Development
Larry W. Tombaugh, Professor and Chairperson, Department of Forestry
Sylvan Wittwer, Associate Dean, Agriculture Experiment Station

Staff

William R. Enslin, Research Specialist and Manager
Elizabeth Bartels, Secretary
William D. Hudson, Research Specialist
Kyle Kittleson, Research Specialist
David P. Lusch, Research Specialist
Susan Perry, Systems Analyst
Andris Zusmanis, Systems Analyst

Brian Baer, Student Computer Assistant
David Crampton, Student Research Aide
Robin Freer, Student Research Aide
Ardeshir Goshtasby, Graduate Research Assistant
Richard Hill-Rowley, Graduate Research Assistant
Saiid Mahjoory, Graduate Research Assistant
Dwayne McIntosh, Student Research Aide
Robin Schneider, Student Research Aide

RESEARCH PROJECTS

DIGITAL CLASSIFICATION OF CONIFEROUS FOREST TYPES IN MICHIGAN'S NORTHERN LOWER PENINSULA FROM LANDSAT MULTISPECTRAL SCANNER DATA

Carl W. Ramm
Department of Forestry, MSU

William D. Hudson
Center for Remote Sensing, MSU
Department of Forestry, MSU

With over half of Michigan presently in forests (18.3 million acres), a large industrial capacity has become dependent upon a steady supply of industrial roundwood. The more than 2,000 firms in various forest industries provide nearly four billion dollars to the economy of the state. Decreases in the resource base are closely related to population growth, which results in increased highway, powerline, industrial, civic, and residential development. This situation is most evident in the northern Lower Peninsula, which is more than 60 percent forested and where the population growth rate has recently been 2.5 times that of the nation. Commercial forest land occupied 7.0 million acres in 1966, compared to 6.7 million acres in 1980, a 4 percent decline.

Approximately 30 percent of the northern Lower Peninsula consists of deep sandy soils, primarily the Rubicon, Roselawn, and Grayling series. Many of these sandy soils are covered with jack pine stands that were initiated after fire. Other conifers, aspen, and other hardwoods may be present in pure or mixed stands.

The Forest Management Division, Michigan Department of Natural Resources, which is responsible for developing a Statewide Forest Resources Plan, has expressed several concerns related to the jackpine (and associated species) resource in Michigan. These include:

1) Except for very general statistics, inventory information about the jackpine resource is unavailable.

2) Jack pine forms the critical habitat for an endangered bird species -- Kirtland's Warbler. The size, density, and location of jack pine stands are the major components of the habitat management program for the warbler.

3) Since the jack pine is such a fire-prone species, its size, density and location would be valuable to fire management personnel, not only for control purposes, but also for their fire planning activities.

4) There is a shortage of softwood fiber for the existing forest industries in the Lake States and, subsequently, jack pine has become the most valuable pulpwood species.

The status of Michigan's timber volumes is periodically assessed through the Resources Evaluation (formerly called Forest Survey). This inventory, conducted by the U.S. Forest Service, measures and evaluates timber conditions as well as the supply and drain situation. However, the inventory is conducted only every 10 to 15 years, it is not site-specific and it is statistically reliable only on a multi-county basis.

New developments in remote sensing techniques are providing foresters and other wildland managers unique opportunities for

earth-resource inventories. The Landsat (land satellite) system is the major component of NASA's land observation program. This program has generated considerable interest from the scientific community and resource managers. The Landsat system has provided readily available data on an unprecedented scale. The large aerial coverage (about 13,225 square miles per scene) and 18-day repetitive acquisition cycle provides a unique opportunity for large area mapping and inventory updating.

Researchers and resource management agencies have analyzed Landsat MSS data both visually (image interpretation) and by utilizing computer compatible tapes (automatic digital processing). Study locations, category definitions, and classification techniques are as nearly varied as the number of studies undertaken. Likewise, accuracies have varied between studies, from under 10 percent (rarely reported in the literature) to over 90 percent.

Several studies have been conducted by the Center for Remote Sensing using Landsat data to map forest resources in Michigan. A study utilizing visual interpretation of winter Landsat imagery, with snow cover on the ground, to map scattered woodlots obtained accuracies ranging from 74.0 to 98.5 percent. A second study analyzed Landsat computer enhanced imagery of an April (leaf-off) scene to map coniferous forest types. Overall classification accuracies were between 73 and 81 percent, whereas individual species interpretability accuracies ranged from 32 to 95 percent (the final report of this project is included n the appendix).

The major objective of the current study is the development and evaluation of automatic techniques (i.e. computer implemented classifications) for the identification and characterization of coniferous forest types in Michigan's northern Lower Peninsula. Specific research tasks designed to accomplish the overall objective include:

1. Evaluate several "standard" digital analysis techniques and determine accuracies.
2. Develop and test a linear-combination classifier from a model of characteristic response curves. Determine the ability of the classifier to identify coniferous forest types and to stratify forested areas into stocking classes.
3. Analyze the relative efficiency of the classifiers, including a comparative analysis of the magnitude and sources of errors.
4. Develop a multistage sampling procedure, which uses the Landsat data in the first stage, for conducting a coniferous forest inventory.

Two test sites in the northern Lower Peninsula were chosen to be representative of areas now supporting large acreages of conifers. Forest cover type maps for both sites have been compiled from aerial photography (1:24,000 color infrared). Additionally, both U.S. Forest Service and Michigan Department of Natural Resources forest cover type maps were consulted in conjunction with ground verification by field crews. A total of 136 stands were sampled throughout the study sites.

The cover type maps have been digitized into polygons, checked for errors, converted into grid files, and re-sampled to match the Landsat pixel size. The re-sampled maps were then rectified to overlay the digital Landsat files.

Unsupervised clustering has been implemented using default input parameters. A plot of the mean brightness values over the four Landsat bands for the 27 clusters produced for the Wexford County test site (Figure 1) and the Crawford County test site (Figure 2) were prepared. Clusters were assigned to cover types by comparison with the registered cover type maps. The registered cover type maps also permitted the production of error maps (Figure 3). These maps located stands which were omitted (area A in Figure 3 represents a very lightly stocked stand of red pine) and stands which were committed (area B in Figure 3 is a small stream and associated vegetation which was classified as forest). Additionally, having the two files (Landsat classification results and forest cover types) registered permitted us to run cross-tabluations of the files and create contingency tables (Table 1 and 2).

A sub-scene from each of the two test sites was utilized to test the effect of varying the values of the input parameters. After conducting numerous repetitive classifications, the only variable which consistently improved classification performance was the reduction of the maximum allowable cluster radius from 7 to 3 digital counts. Clusters were run on the entire test sites, the resulting cluster means were plotted (Figures 4 and 5) and .pa

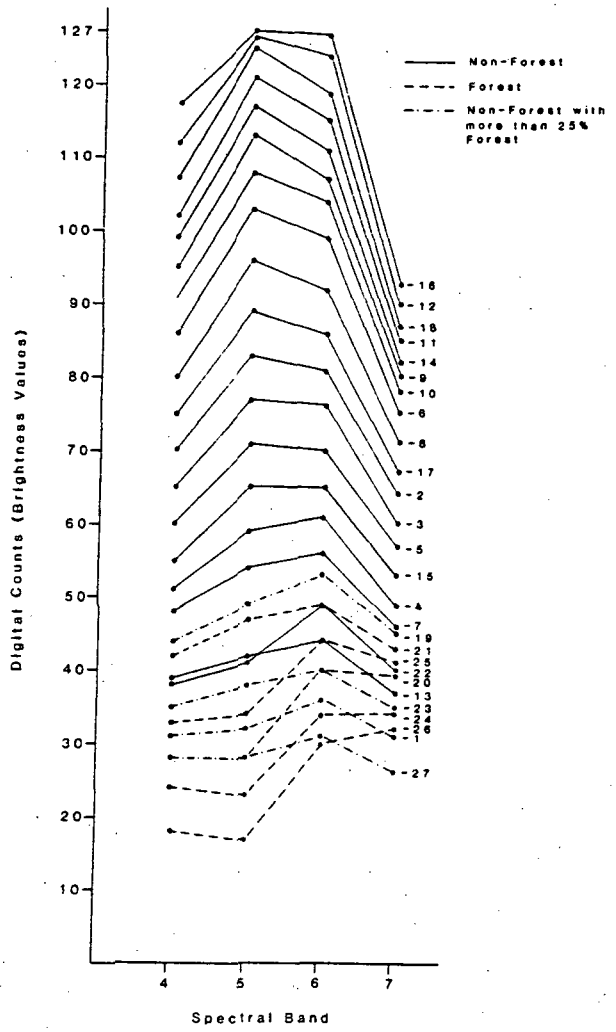

Figure 1. Wexford County Test Site, Default Clusters

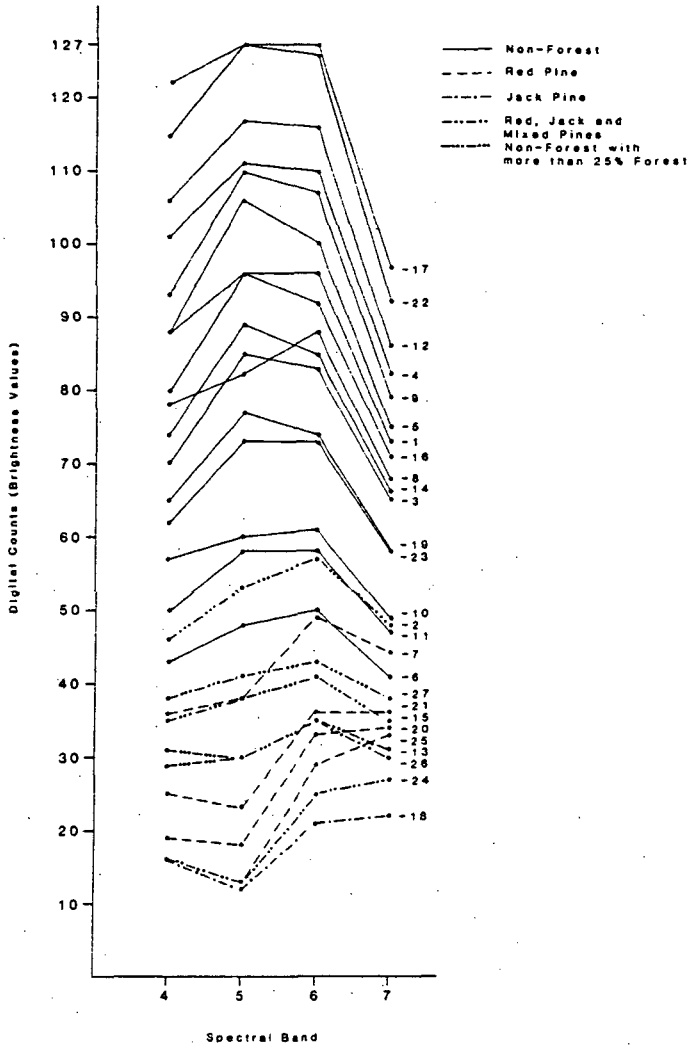

Figure 2. Crawford County Test Site, Default Clusters

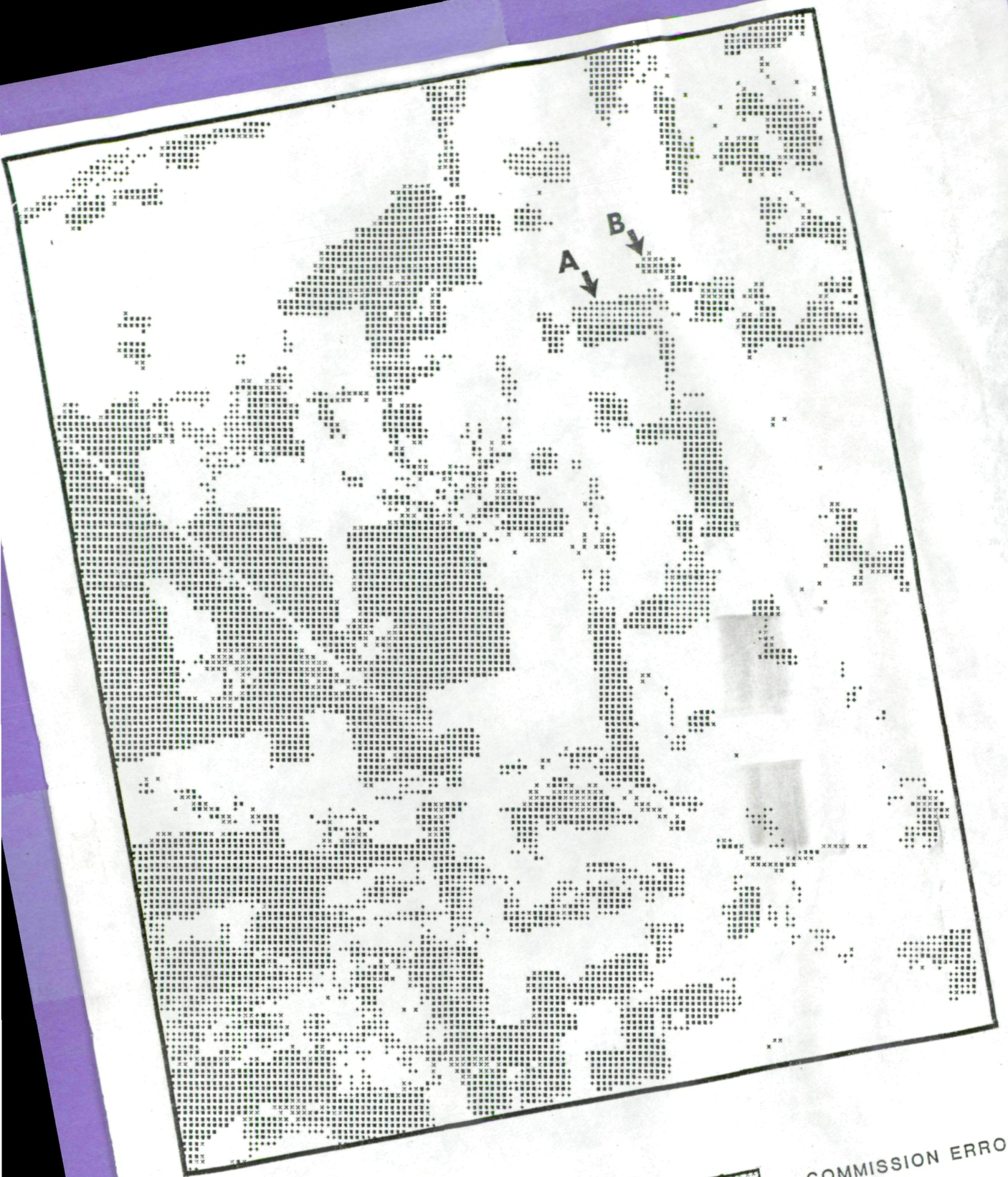

Figure 3. Example error map for the Wexford County Test Site

Table 1. Wexford County Test Site, Default Clusters

Cover type map	Number of Pixels Classified as -- Red pine	Jack pine	Pine mixtures	Swamp conifers	Non-forest	TOTAL	Percent correct
Red pine	4166	--	--	--	1201	5367	77.6
Jack pine	851	--	--	--	829	1680	0.0
Pine mixtures	973	--	--	--	238	1211	0.0
Swamp conifers	254	--	--	--	84	338	0.0
Non-Forest	738	--	--	--	13721	14459	94.9
TOTAL	6982	--	--	--	16073	23055	
Percent correct	59.7	0.0	0.0	0.0	85.4		77.6

Table 2. Crawford County Test Site, Defalut Clusters

Cover type map	Number of Pixels Classified as -- Red pine	Jack pine	Pine mixtures	Swamp conifers	Non-forest	TOTAL	Percent correct
Red pine	--	275	--	8	52	335	0.0
Jack pine	--	4757	--	95	1113	5965	79.7
Pine mixtures	--	550	--	13	167	730	0.0
Swamp conifers	--	853	--	525	38	1416	37.1
Non-Forest	--	1957	--	21	4181	6159	67.9
TOTAL	--	8392	--	662	5551	14605	
Percent correct	0.0	56.7	0.0	79.3	75.3		64.8

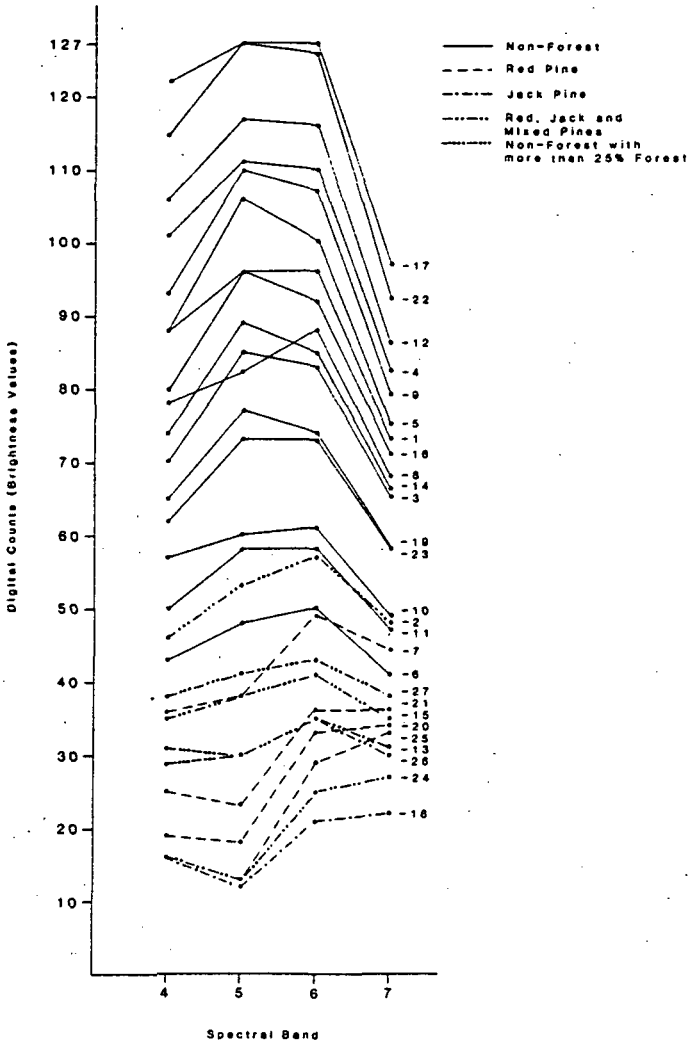

Figure 4, Wexford County Test Site with Smaller Cluster Radius

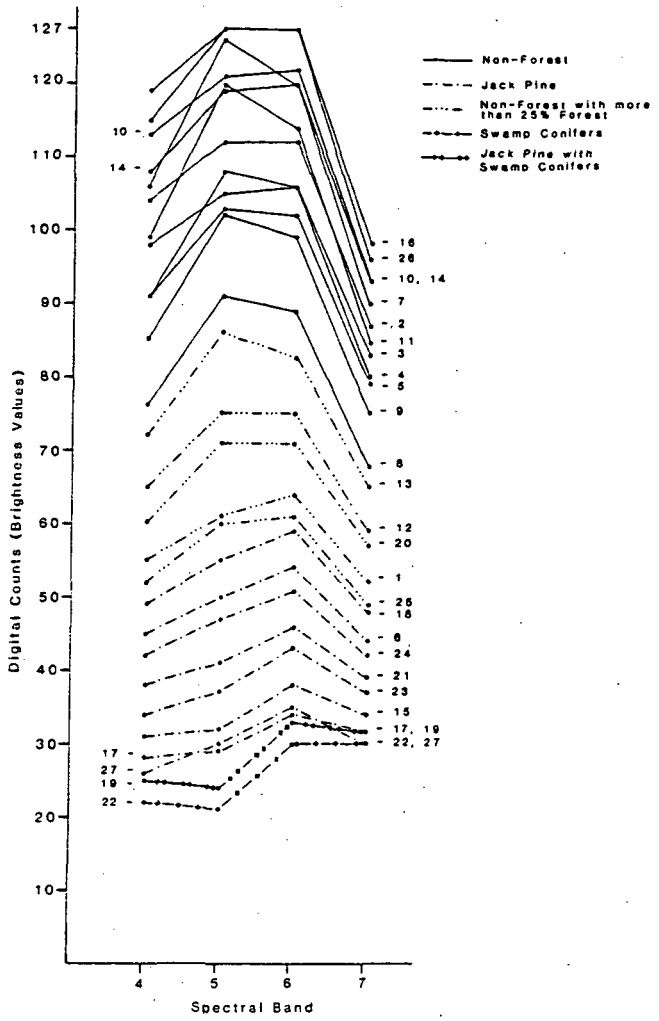

Figure 5. Crawford County Test with Smaller Cluster Radius

contingency tables constructed (Tables 3 and 4).

In an effort to minimize the effect of a large number of non-forest clusters, level slicing was used to pre-process the Landsat data. Two clusters, one using default parameteters and the other a smaller allowable cluster radius, were run on each test site with the results presented in Figures 6, 7, 8, and 9 and Tables 5, 6, 7, and 8.

Training site statistics were obtained for each cover type to be used as input for a minimum distance-to-means and maximum likelihood classifiers. An iterative procedure (input training site signatures, classify test site, evaluate accuracy, delete or add new signatures) were used to develop a final set of training site signatures. A total of 136 sites were sampled within the two

Table 3. Wexford County Test Site With Smaller Cluster Radius

Cover type map	Number of Pixels Classified as -- Red pine	Jack pine	Pine mixtures	Swamp conifers	Non-forest	TOTAL	Percent correct
Red pine	3931	37	--	--	1399	5367	73.2
Jack pine	452	459	--	--	769	1680	27.3
Pine mixtures	847	56	--	--	308	1211	0.0
Swamp conifers	181	41	--	--	116	338	0.0
Non-Forest	399	276	--	--	13784	14459	95.3
TOTAL	5810	869	--	--	16376	23055	
Percent correct	67.7	52.8	0.0	0.0	84.2		78.8

Table 4. Crawford County Test Site With Smaller Cluster Radius

Cover type map	Number of Pixels Classified as -- Red pine	Jack pine	Pine mixtures	Swamp conifers	Non-forest	TOTAL	Percent correct
Red pine	--	255	--	21	59	335	0.0
Jack pine	--	4451	--	281	1233	5965	74.6
Pine mixtures	--	516	--	35	179	730	0.0
Swamp conifers	--	695	--	674	47	1416	47.6
Non-Forest	--	1789	--	61	4309	6159	70.0
TOTAL	--	7706	--	1072	5827	14605	
Percent correct	0.0	57.8	0.0	62.9	73.9		64.6

Table 5. Wexford County Test Site, Default Cluster on Level Sliced Scene

Cover type map	Number of Pixels Classified as -- Red pine	Jack pine	Pine mixtures	Swamp conifers	Non-forest	TOTAL	Percent correct
Red pine	4027	147	--	--	1193	5367	75.0
Jack pine	262	677	--	--	741	1680	40.3
Pine mixtures	750	227	--	--	234	1211	0.0
Swamp conifers	161	95	--	--	82	338	0.0
Non-Forest	671	217	--	--	13571	14459	93.9
TOTAL	5871	1363	--	--	15821	23055	
Percent correct	68.6	49.7	0.0	0.0	85.8		79.3

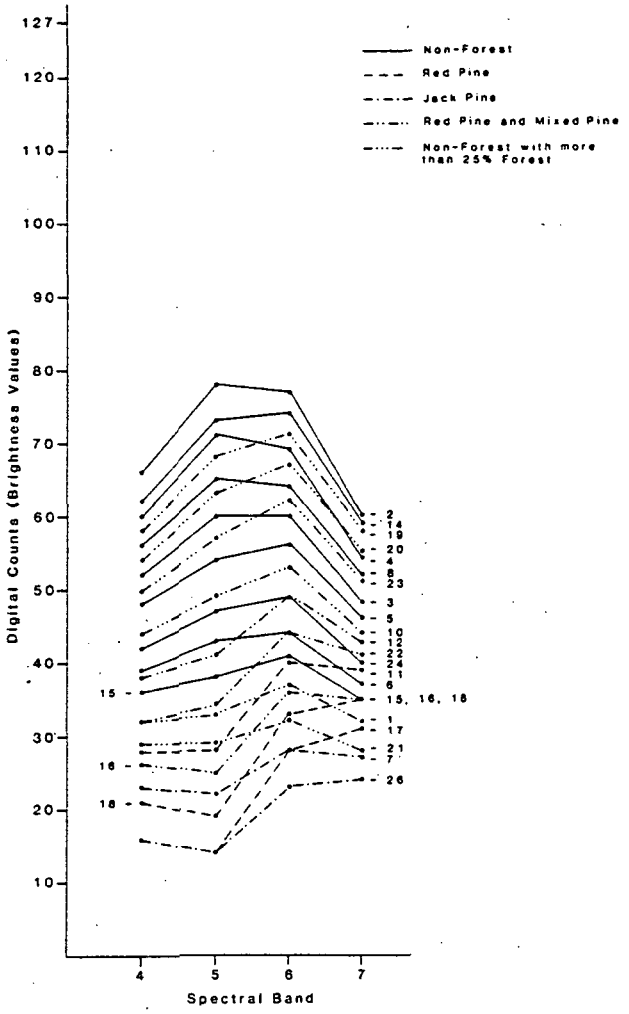

Figure 6. Wexford County Test Site, Default Cluster on Level Sliced Scene

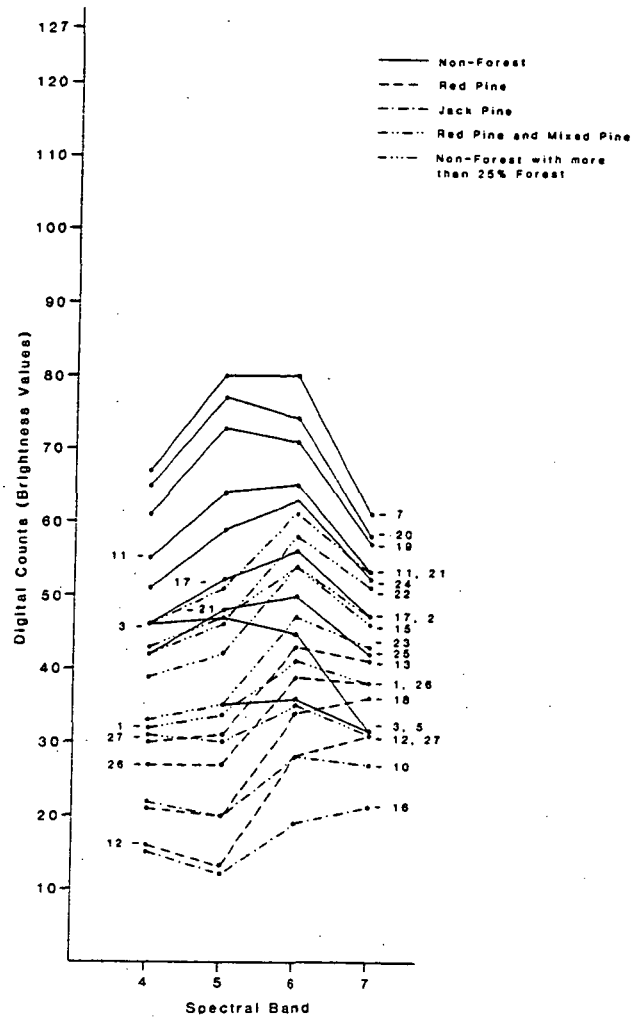

Figure 7. Wexford County Test Site, Cluster with Smaller Radius on Level Sliced Scene

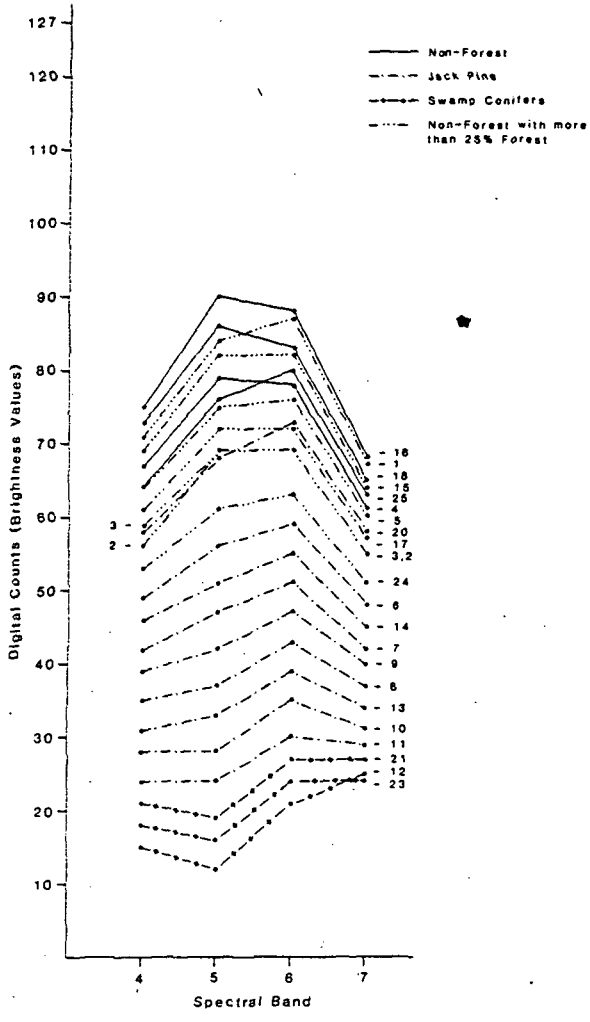

Figure 8. Crawford County Test Site, Default Cluster on Level Sliced Scene

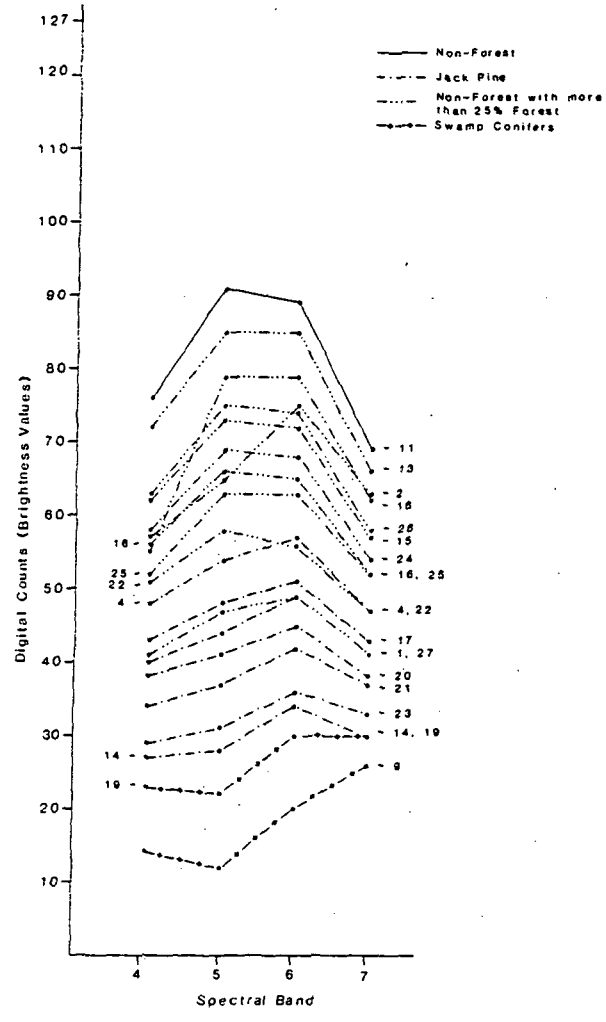

Figure 9. Crawford County Test Site, Cluster with Smaller Radius on Level Sliced Scene

Table 6. Wexford County Test Site, Cluster With Smaller Radius on Level Sliced Scene

Cover type map	Number of Pixels Classified as -- Red pine	Jack pine	Pine mixtures	Swamp conifers	Non-forest	TOTAL	Percent correct
Red pine	4193	168	--	--	1006	5367	78.1
Jack pine	180	697	--	--	803	1680	41.5
Pine mixtures	755	197	--	--	259	1211	0.0
Swamp conifers	128	93	--	--	117	338	0.0
Non-Forest	661	220	--	--	13578	14459	93.9
TOTAL	5917	1375	--	--	15763	23055	
Percent correct	70.9	50.7	0.0	0.0	86.1		80.1

Table 7. Crawford County Test Site, Default Cluster on Level Sliced Scene

Cover type map	Number of Pixels Classified as -- Red pine	Jack pine	Pine mixtures	Swamp conifers	Non-forest	TOTAL	Percent correct
Red pine	--	274	--	9	52	335	0.0
Jack pine	--	4768	--	109	1088	5965	79.9
Pine mixtures	--	551	--	19	160	730	0.0
Swamp conifers	--	832	--	546	38	1416	38.6
Non-Forest	--	2002	--	98	4059	6159	65.9
TOTAL	--	8427	--	781	5397	14605	
Percent correct	0.0	56.6	0.0	69.9	75.2		64.2

Table 8. Crawford County Test Site, Cluster With Smaller Radius on Level Sliced Scene

Cover type map	Number of Pixels Classified as -- Red pine	Jack pine	Pine mixtures	Swamp conifers	Non-forest	TOTAL	Percent correct
Red pine	--	237	--	35	63	335	0.0
Jack pine	--	4216	--	371	1378	5965	70.7
Pine mixtures	--	487	--	50	193	730	0.0
Swamp conifers	--	607	--	741	68	1416	52.3
Non-Forest	--	1572	--	77	4510	6159	73.2
TOTAL	--	7119	--	1274	6212	14605	
Percent correct	0.0	59.2	0.0	58.2	72.6		64.8

test sites with a total sample size of 7854. Results of the minimum distance-to-means classifications are given in Tables 9 and 10 while those for the maximum likelihood are given in Tables 11 and 12.

In order to evaluate the effect of the accuracy assessment procedure upon classification performance, a test was run using aerial photography as the "ground truth." Aerial photographs were enlarged and registered to a map showing forest cover types as classified by the maximum likelihood classifier for the Wexford County Test Site. A systematic sample of one-fourth of the classified pixels were compared with the aerial photography to determine errors of omission, commission, and species confusion. Overall misclassification appeared to be 2.7 percent lower (Table

13) when determined from aerial photography as compared to accuracy determined from the generalized forest cover type maps.

Table 9. Wexford County Test Site, Minimum Distance-to-Means Classification

Cover type map	Number of Pixels Classified as -- Red pine	Jack pine	Pine mixtures	Swamp conifers	Non-forest	TOTAL	Percent correct
Red pine	3850	208	102	--	1207	5367	71.7
Jack pine	256	737	42	--	645	1680	43.9
Pine mixtures	535	228	211	--	237	1211	17.4
Swamp conifers	119	114	39	--	66	338	0.0
Non-Forest	658	300	6	--	13495	14459	93.3
TOTAL	5418	1587	400	--	15650	23055	
Percent correct	71.1	46.4	52.8	0.0	81.0		79.3

Table 10. Wexford County Test Site, Maximum Likelihood Classification

Cover type map	Number of Pixels Classified as -- Red pine	Jack pine	Pine mixtures	Swamp conifers	Non-forest	TOTAL	Percent correct
Red pine	3701	222	146	--	1298	5367	69.0
Jack pine	203	709	77	--	691	1680	42.4
Pine mixtures	498	202	265	--	246	1211	21.9
Swamp conifers	113	105	50	--	70	338	0.0
Non-Forest	528	274	20	--	13637	14459	94.3
TOTAL	5043	1512	558	--	15942	23055	
Percent correct	73.4	46.9	47.5	0.0	85.5		79.4

Table 11. Crawford County Test Site, Minimum Distance-to-Means Classification

Cover type map	Number of Pixels Classified as -- Red pine	Jack pine	Pine mixtures	Swamp conifers	Non-forest	TOTAL	Percent correct
Red pine	--	261	--	28	46	335	0.0
Jack pine	--	4650	--	215	1100	5965	77.9
Pine mixtures	--	528	--	37	165	730	0.0
Swamp conifers	--	665	--	707	44	1416	49.9
Non-Forest	--	1936	--	51	4152	6152	67.7
TOTAL	--	8040	--	1038	5527	14605	
Percent correct	0.0	57.8	0.0	68.1	75.5		65.2

Table 12. Crawford County Test Site, Maximum Likelihood Classification

Cover type map	Number of Pixels Classified as -- Red pine	Jack pine	Pine mixtures	Swamp conifers	Non-forest	TOTAL	Percent correct
Red pine	--	248	--	45	42	335	0.0
Jack pine	--	4703	--	238	1024	5965	78.8
Pine mixtures	--	532	--	40	158	730	0.0
Swamp conifers	--	649	--	732	35	1416	51.7
Non-Forest	--	2035	--	56	4068	6159	66.0
TOTAL	--	8167	--	1111	5327	14605	
Percent correct	0.0	57.6	0.0	65.9	76.3		65.1

Table 13. Wexford County Test Site, Maximum Likelihood Errors As Determined from Aerial Photographs

Cover type map	Number of Pixels Classified as -- Red pine	Jack pine	Pine mixtures	Swamp conifers	Non-forest	TOTAL	Percent correct
Red pine	3862	232	152	--	1142	5388	71.7
Jack pine	212	740	80	--	609	1641	45.1
Pine mixtures	520	211	277	--	217	1225	22.6
Swamp conifers	118	110	52	--	62	342	0.0
Non-Forest	268	139	10	--	14042	14459	97.1
TOTAL	4980	1432	571	--	16072	23055	
Percent correct	77.5	51.7	48.5	0.0	87.4		82.1

ANALYSIS OF RADIANT TEMPERATURE DATA FROM THE GEOSTATIONARY OPERATIONAL ENVIRONMENTAL STAELLITES

David P. Lusch
Center for Remote Sensing, MSU
Department of Geography, MSU

Jay Harman
Department of Geography, MSU

Archival digital data from the thermal infrared scanner on board the GOES-East satellite were obtained from the Satellite Data Services Division, National Climatic Center. This data set included all available infrared records for 16 dates in the spring, summer, and fall of 1980. A subset of these data was chosen representing near-dawn (minimum temperature) and mid-afternoon (maximum temperature) thermal images. Only 13 of the 16 dates had digital images at the appropriate times (Table 1).

The pre-dawn and mid-afternoon records for each of the 13 dates were extracted from the tape data and displayed on a CRT monitor. Contrast enhancement of these thermal images was used to determine the presence of clouds in any of the scenes. Unfortunately, only four of the 13 days were determined to be cloud-free: 5/25/80, 5/26/80, 6/11/80, and 8/22/80. Additional data from 1981-1983 are being identified and will be acquired.

The two research tasks of this project are:

1. Mapping multi-temporal, minimum and maximum, radiant temperature patterns in the Lower Peninsula of Michigan.
2. Multi-temporal comparison of GOES radiant temperatures with data from the climatological station network.

Table 1. GOES-East digital data available for study.

Date	Time (EST)	Sunrise (EST)*	Comments
4/22/80	0500 1600	0545	no 0600 available
5/3/80	0400 1600	0530	no 0500 or 0600 available
5/4/80	0500 1600	0530	
5/5/80	0500 1600	0530	
5/25/80	0500 1600	0500	
5/26/80	0500 1600	0500	
6/11/80	0500 1600	0500	
6/12/80	0500 1600	0500	
7/23/80	0500 1600	0500	
7/24/80	0400 1600	0500	no 0500 available
8/22/80	0500 1600	0545	no 0600 available
8/23/80	0500 1600	0545	no 0600 available
9/29/80	0700 1600	0645	

*to the nearest 15 minutes for 45^{o}n, corrected to $84^{o}40'$W

Both of these tasks require that the GOES temperature data be related to variations of selected key surface phenomena such as land cover, available soil water capacity, topography, and distance to the Great Lakes. The majority of the effort to date on this project has been directed toward the development of a multi-level geographic information system (GIS) to facilitate such comparisons. A grid-cell size of $1km^2$ was decided upon for the GIS providing 88 environmental-factor cells within each GOES pixel (which in Michigan average 8 x 11 km in size).

The microcomputer-based GIS being compiled for this project contains 733 rows and 633 columns, and includes several master files as well as several derivative data sets. Under separate funding from a previous contract, the recently published Soil Association Map of Michigan (Extension Bulletin E-1550) was digitized and the polygon data were subsequently converted to a $1km^2$ grid-cell file. Each soil association map unit contains one to four separate soil series. Published estimates were available from the U.S.D.A., Soil Conservation Service of the available water capacity of each horizon in all of the soil series represented on the Soil Association Map. These horizon data were re-aggregated for each one-foot increment of depth and multiplied by the percent occurence of each soil series in a soil association to determine the average available water capacity of each association by one-foot increments of depth to five feet.

The land cover data for the GIS has been visually interpreted from diazo-enhanced Landsat imagery which was optically magnified and registered to 1:250,000 scale topographic maps. The following

nine categories of land cover were mapped for the Lower Peninsula of Michigan:

Urban and Built-up
Agriculture
Rangeland
Deciduous Forest
Coniferous Forest
Water
Forested Wetlands
Non-forested Wetlands
Barren

These interpretations were aided by a variety of ancillary data including topographic maps ($1^{o}x2^{o}$, 15' and 7.5', aerial photographs (B/W 1:20,000 and 1:40,000; CIR 1:24,000 and 1:60,000), and county soil survey reports. Also, wherever possible, Landsat images from several different dates were interpreted which facilitated a more accurate delineation of the agricultural, rangeland, and forest categores (Table 2). The 14 stable-base, land cover overlays produced by the image interpreters are being digitized for editing and entry into the GIS. The status of this task is shown in Figure 1.

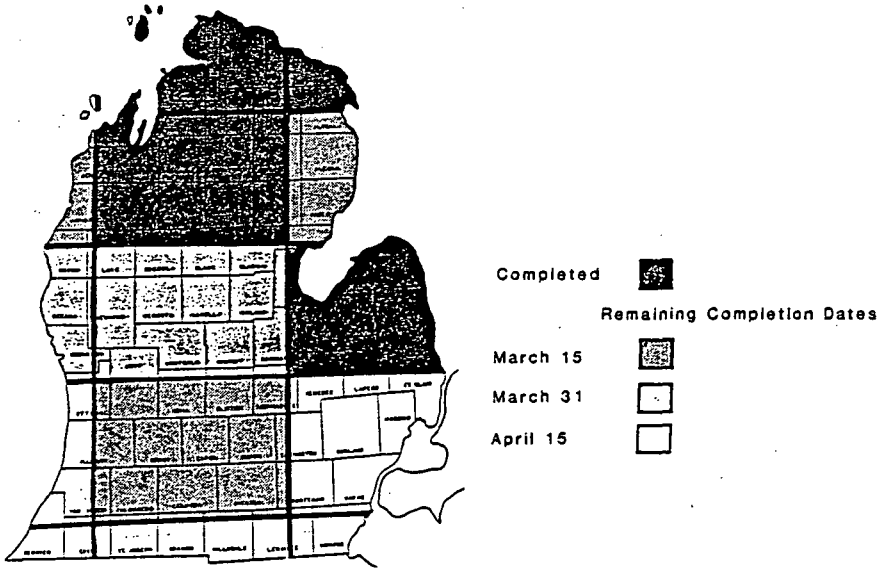

Figure 1. Status of digitization of land cover maps

Several topographic information layers for the data base are being compiled, including elevation, slope, and aspect. These elements of the GIS are being derived from the digital terrain data produced by the Defense Mapping Agency. Software to calculate local relief by grid-cell is being discussed at present.

The last file for the GIS, distance to the Great Lakes, has not been developed yet. Since the thermal patterns of the state will be analyzed with due regard for synoptic weather conditions at the time of GOES image acquisition, several files dealing with distance to the Great Lakes are necessary. It is envisioned that five such layers in the GIS will be produced -- one for each of the following mean wind-flow direction: northeast, north, northwest, west, and southwest. Others could be added as needed. Several programming alternatives are available to derive these data and will be evaluated.

Table 2. Landsat Imagery used, by Quadrangle.

	Path-Row	Date
Cheboygan NL 16-9	Multispectral Scanner (MSS)	
	023-028	17 June 80
	023-029	17 June 80
	024-028	24 June 79
	Thematic Mapper (TM)	
	021-029	27 Oct 82
	022-029	18 Oct 82
Alpena NL17-7	MSS	
	023-028	17 June 80
	TM	
	021-029	27 Oct 82
Manitowac NL16-11	MSS	
	024-029	22 Sept 79
	TM	
	022-029	18 Oct 82
Traverse City NL16-12	MSS	
	023-029	17 June 80
	024-029	22 Sept 79
	TM	
	021-029	27 Oct 82
	022-029	18 Oct 82
Tawas City NL17-10	MSS	
	022-029	13 June 79
	TM	
	021-029	27 Oct 82
Milwaukee NL16-2	MSS	
	023-030	12 Sept 79
	024-029	22 Sept 79
	024-030	22 Sept 79
Midland NK16-3	MSS	
	022-030	13 June 79
	023-030	17 June 80
	TM	
	021-030	27 Oct 82
Flint NK17-1	MSS	
	021-030	18 July 79
	022-029	13 June 79
	022-030	13 June 79
Racine NK16-5	MSS	
	023-030	12 Sept 79
	023-031	12 Sept 79
	024-030	22 Sept 79
Grand Rapids NK16-6	MSS	
	022-030	13 June 79
	022-031	20 Sept 79
	023-030	17 June 80
	023-031	12 Sept 79
	TM	
	021-030	27 Oct 82
Detroit NK17-4	MSS	
	021-030	18 July 79
Chicago NK16-8	MSS	
	023-031	12 Sept 79
Fort Wayne NK16-9	MSS	
	022-031	20 Sept 79
	023-031	12 Sept 79
Toledo NK17-7	MSS	
	022-031	20 Sept 79

LAND SURFACE CHANGE DETECTION USING SATELLITE DATA AND A GEOGRAPHIC DATA BASE

William R. Enslin
Center for Remote Sensing, MSU

Anil Jain and Ardeshir Goshtasby
Department of Computer Science, MSU

Richard Hill-Rowley
Department of Resource and Community Science
The University of Michigan - Flint

Michael Scieszka
Michigan Department of Natural Resources

The objective of this research is to develop methods and techniques for the detection, monitoring, and modeling of land surface change using data acquired by satellite sensor systems. Data from the Landsat multispectral scanner (MSS), weather satellites, and the new Landsat Thematic Mapper (TM) are being evaluated to determine the capability to accurately identify land cover types and to detect land surface change.

The research is being conducted in cooperation with the Michigan Resource Inventory Program, which is currently implementing a legislated statewide information system. The system includes digitized photo-derived land use information which will serve as the baseline data set for comparisons with computer-aided classifications of satellite digital images. The aim is to develop and evaluate techniques and methodologies for integrating and processing data obtained from satellite sensors with data layers in the geographic information system of the state.

Several research areas have been identified which will provide techniques needed as components of an overall system for

monitoring land cover/use changes and updating regional and statewide geo-referenced data bases. Other areas of research are being defined related to integrating and analyzing satellite data with selected earth surface attribute sets of the data base, particularly information on forest stand type, size, and density. A summary of the current efforts follows.

Image Registration

Accurate image registration is a prerequisite for most change detection and inventory update methods. Techniques to handle three types of image registration are required for this research, i.e., image to image, image to geographic data base, and image with ancillary data sets such as digital elevation data.

Several multi-image registration algorithms have been developed and evaluated (Goshtasby, Jain, and Enslin, 1982; Goshtasby and Enslin, 1982, Goshtasby and Stockman). Emphasis has been placed on automatic digital image registration procedures that will handle images with translational, rotational, and scaling differences.

A new technique (Goshtasby and Enslin, 1982) has been developed to register rotated images using invariant moments as the similarity measure (See Appendix for more detail). If circular windows with invariant moments are used, then the window search can be carried out on rotated images in the same manner that cross-correlation with rectangular window is used on translated images. It has been found that normalization of invariant moments provides a more accurate window similarity measurement than using the non-adjusted moments. The new approach

has been tested successfully against two images from different satellites (GOES and HCMM) that have translational and rotational differences.

Geographic Information System Data

During this reporting period, we have developed a series of computer programs that convert digital land cover data files from the Michigan Land Resource Information System (MIRIS) to the file structure of the ERDAS 400 Image Processing System at the Center. The programs provide the capability to: 1) sort polygons by areal extent (this prevents islands from being overwritten); 2) read area-sorted tape data and write out an ERDAS compatible disk file; 3) convert MIRIS polygon format to ERDAS polygon format; and 4) recode or regroup polygon labels.

The last program which allows regrouping labels is very useful since there are potentially 991 land cover classes in a MIRIS data file. Presently, there are nine standard coding schemes options available in the program for grouping the 991 land cover/use classes, (i.e. level I, level II, level III, level V, forest, conifers, broadleaf, forest stand size/stocking, and urban uses).

Our next effort will be to work on the registration of Landsat digital images and other satellite data to the MIRIS land use files that have been converted using the above programs. We will be evaluating existing computer routines that perform polygon to raster conversion and image-to-data base registration.

To date no work has begun on merging ancillary data sets with

digital images from satellite sensors. However, digital elevation data for two 1:250,000 topographic quadrangles has been received from the National Cartographic Information Center, and several programs have been written to read and reformat these data.

Computer programs have been developed on a Harris 500 superminicomputer to: 1) read DMA digital terrain tapes and reformat the elevation data so that it is commpatible with the ERDAS 400 system at the Center; 2) contour the data; 3) create a slope image, and 4) produce an aspect image file. Another routine will be developed that will calculate local relief within a specified resampling cell size.

Test Sites

Based upon the availability of MIRIS digital land cover/use data, three test areas have been selected within the Northwest Michigan area that was imaged by the Landsat Thematic Mapper on October 27, 1982 (ID E-40094-1554). We have received both visual (photographic) and digital data for this Landsat scene, which will be the primary remote sensing data used in the study. Test areas have been established to investigate deforestation (Northeast Manistee County), forest regeneration (Crawford County), and urbanization (Grand Traverse County). Currently, the Landsat Thematic Mapper data acquired in October, 1982, is being preliminarily classified and evaluated prior to exploring and developing change detection techniques.

REMOTE SENSING OF VIRUS-INFECTED BLUEBERRY FIELDS AND VINEYARDS IN MICHIGAN

Donald C. Ramsdell
Department of Botany and Plant Pathology, MSU

Adele M. Childress-Roberts
Department of Botany and Plant Pathology, MSU

Evaluation of the field-portable spectroradiometer (Spectron Inc.) as a rapid method of detecting virus-infected plants in commercial fields was continued during the 1983 growing season. Highbush blueberry fields that contained either blueberry shoestring virus (BBSSV) or blueberry leaf mottle virus (BBLMV) infected plants were selected for study. Vineyards with peach rosette mosaic virus (PRMV) infected vines were also surveyed. All tests plants were previously tested for virus infection using the Enzyme-Linked Immunosorbent Assay (ELISA) technique. Seven virus-infected plants were selected in each field and matched with a healthy plant located either next to the infected plant or in the same vicinity and subject to the sam environmental conditions.

Spectral readings were taken 24 June, 22 July, and 29 August, at various phenological stages. All specteral readings were reference to a $BaSO_4$ reflectance panel located in the field and at the same height as the top of the plant canopy.

Data obtained from the spectral readings will be processed by computer to utilize statistical packages available. Before further analysis of the data can be made, modifications in the programming must be implemented, therefore analysis of the 1983 data is still in progress.

OTHER ACTIVITIES

William A. Fisher Award Goes to MSU Researchers

Ardeshir Goshtasby of the Department of Computer Science and the Center for Remote Sensing and William R. Enslin of the Center for Remote Sensing were the recipients of the 1983 - William A. Fisher Award for the best contributed paper presented at the Seventeenth International Symposium on Remote Sensing of Environment. The panel of judges unanimously selected their paper entitled "Registration of Rotated Images by Invariant Moments" as most completely satisfying both the intent of this award and the evaluation criteria.

General Motors Corporation Donates a Thermal Scanner to the Center for Remote Sensing

In November, 1983, the Center for Remote Sensing received a thermal infrared scanner which was generously donated to Michigan State University by the General Motors Corporation. This instrument, a Dynarad model 810 Precision Thermal Imaging System, has the following specifications:

mimimum detectable ΔT	$0.1^{o}C$
IFOV	1.4 mrad
temperature measurement range	$-50^{o}C$ to $+500^{o}C$
detector type	HgCdTe
detector spectral range	8-14 micrometers
detector coolant	liquid nitrogen
frame time (sec/frame)	1 to 16 (in 5 steps)
scan rate (lines/sec)	60
field of view	$10^{o}x10^{o}$ to $25^{o}x25^{o}$ (in four steps)

The scanner will be used in a variety of research projects and to support laboratory instruction in remote sensing.

Important Farmlands Inventory

The Center for Remote Sensing continued work under contract with the Soil Conservation Service for the preparation of Important Farmlands maps for counties in Michigan. The mapping involves the delineation of prime soil areas from soil survey information and the identification of unique farmland, water, and urban built-up areas from aerial photography (U.S. Department of Agriculture, Secretary's memorandum number 1827, revised, October 30, 1978). Unique farmlands are lands other than those designated prime that are used for the production of specific high-value food and fiber crops (i.e., tree and bush fruits, vineyards, and vegetables).

The information is compiled onto a 1:50,000 base map of each county and area statistics per category are determined. The Important Farmland maps are being produced under the Land Inventory and Monitoring (LIM) program of the U.S. Department of Agriculture.

Important Farmland Maps for six counties were completed this reporting period. A contract for the preparation of an Important Farmland map for one additional county was received during the reporting period; which brings the total that have been under contract to 37 counties.

ASP Eastern Great Lakes Region Meeting

April 22, 1983

In spring 1983, the MSU Center for Remote Sensing hosted the Eastern Great Lakes Region of the American Society of Photogrammetry conference on "Recent Remote Sensing Applications in the Great Lakes Region." Tours of MSU's Center for Remote Sensing were given as well as tours of the Michigan Department of Natural Resources (DNR) Michigan Resource Inventory Program.

Remote sensing for geo-botany was discussed by Mathew Schwaller of the University of Michigan, who explained how changes in leaf reflectance in response to heavy metal stress may be useful indicators for geo-botanical exploration with remote sensing. Fred Tannis of the Environmental Research Institute of Michigan presented information on the use of the coastal zone color scanner in Great Lakes water quality monitoring.

Airborne thematic mapper data collection and processing for the Lake Ellen Kimberlite region in Iron County was presented by Dr. Robert K. Vincent, Paul Etzler, and Marc Wilson of Geospectra Corporation, and Tom Ory, Daedalus Enterprises, Inc. Mike Scieszka of the Michigan Department of Natural Resources discussed the Michigan Resource Inventory Program. Dr. David P. Lusch and William D. Hudson of the MSU Center for Remote Sensing presented information on the correlation of GOES temperature patterns with Michigan surface features, and discrimination and mapping of coniferous forest types from Landsat data.

The Eastern Great Lakes Region
of
AMERICAN SOCIETY OF PHOTOGRAMMETRY

Conference on

RECENT REMOTE SENSING APPLICATIONS IN THE GREAT LAKES REGION

April 22, 1983

CENTER FOR REMOTE SENSING MICHIGAN STATE UNIVERSITY

HCMM DAY-VIS 18APR79

THE EASTERN GREAT LAKES REGION
OF
AMERICAN SOCIETY OF PHOTOGRAMMETRY

"RECENT REMOTE SENSING APPLICATIONS IN THE GREAT LAKES REGION"

Date: Friday, April 22, 1983
Location: MSU Union, Parlors A, B, C
Michigan State University
East Lansing, MI

OPENING EVENTS

9:00-12:00 a.m.	Registration ($5.00 fee; students free) Exhibits and Displays
9:30-10:30 10:45-11:45	Tours: Center for Remote Sensing Michigan State University
9:30-10:30 10:45-11:45	Tours: Michigan Resource Inventory Program Department of Natural Resources
12:00- 1:15 p.m.	Open Lunch Period (Lunch may be purchased at the MSU Union Cafeteria)

TECHNICAL PRESENTATIONS

1:15- 1:30	Welcome. Dr. Jon F. Bartholic, Coordinator, Center for Remote Sensing, MSU
1:30- 2:00	REMOTE SENSING FOR GEO-BOTANY Mathew R. Schwaller, University of Michigan
2:00- 2:30	COASTAL ZONE COLOR SCANNER: A SENSOR FOR GREAT LAKES WATER QUALITY MONITORING Fred Tanis and Jackie Ott, Environmental Research Institute of Michigan
2:30- 3:00	CORRELATION OF GOES TEMPERATURE PATTERNS WITH MICHIGAN SURFACE FEATURES Dr. David P. Lusch, MSU Center for Remote Sensing
3:00- 3:30	Break
3:30- 4:00	AIRBORNE THEMATIC MAPPER DATA COLLECTION AND PROCESSING FOR THE LAKE ELLEN KIMBERLITE REGION, IRON COUNTY, MICHIGAN Dr. Robert K. Vincent, Geospectra Corporation Tom Ory, Daedalus Enterprises, Inc. Paul Etzler, Geospectra Corporation Marc Wilson, Geospectra Corporation
4:00- 4:30	THE MICHIGAN RESOURCE INVENTORY PROGRAM Michael Scieszka, Michigan Department of Natural Resources
4:30- 5:00	DISCRIMINATION AND MAPPING OF CONIFEROUS FOREST TYPES FROM LANDSAT DATA William D. Hudson, MSU Center for Remote Sensing

"RECENT REMOTE SENSING APPLICATIONS IN THE GREAT LAKES REGION"

Advance Registration and Fees--You MUST register in advance. A fee of $5.00 for non-students (no fees for students) may be sent with registration or paid on the meeting day. Make checks payable to: Eastern Great Lakes Region, ASP.

____ Yes, I plan to attend

Name _____

Organization _____

Address _____

Phone _____

____ No, I do not want a tour/____ Yes, register me for the following tours(s). Transportation to tour sites is not provided.

Center for Remote Sensing
302 Berkey Hall
Michigan State University
East Lansing

____ 9:30 a.m.

____11:45 a.m.

Michigan Resource Inventory Program (limited to 15 per tour)
Land Resource Programs Division, Dept. of Natural Reosurces
7th Floor, Stevens T. Mason Building
Lansing

____ 9:30 a.m.

____11:45 a.m.

CALL FOR EXHIBITS AND POSTER DISPLAYS

Please reserve space (no charge) for an exhibit/poster display:

Name/Organization _____

Address _____

Phone _____

Special requirements _____

MAIL TO: William R. Enslin, Center for Remote Sensing, 302 Berkey Hall, Michigan State University, East Lansing, MI 48824-1111 (517) 353-7195

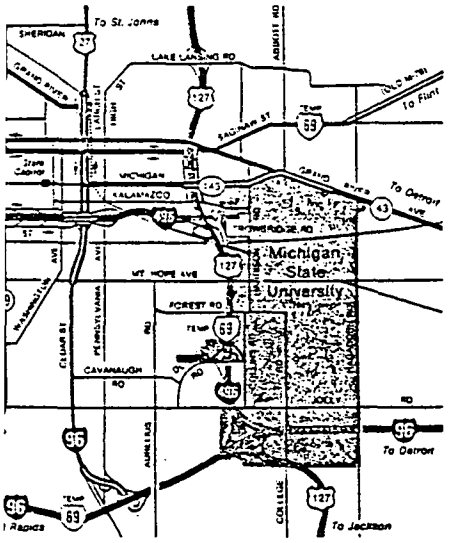

Lansing and MSU area

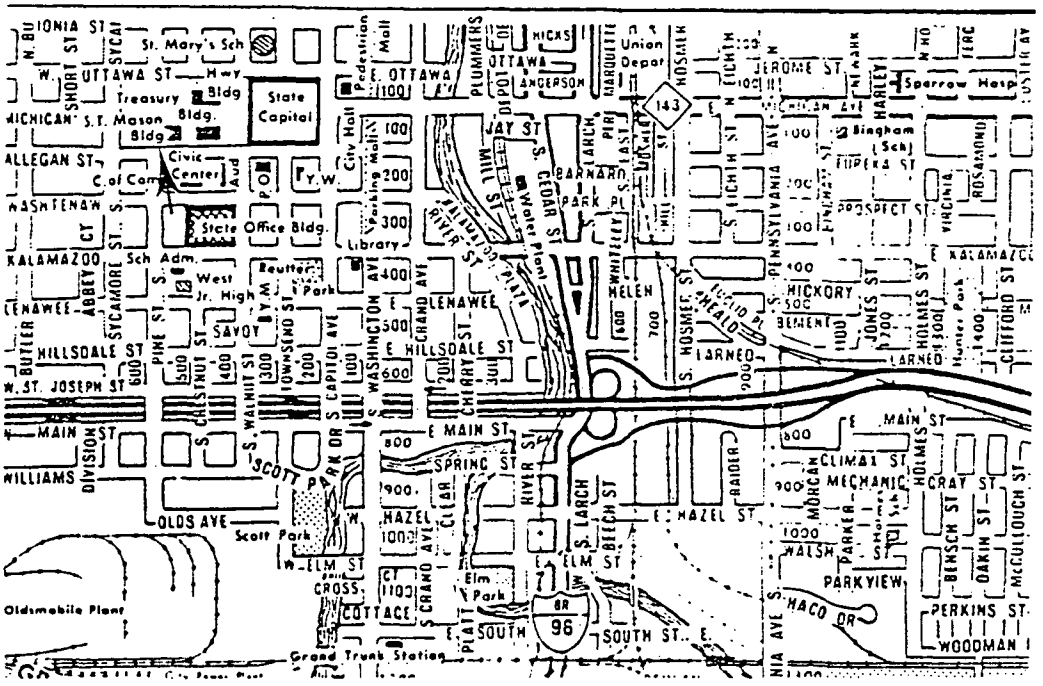

Downtown Lansing--Stevens T. Mason Building

MSU Campus--Union Building and Berkey Hall

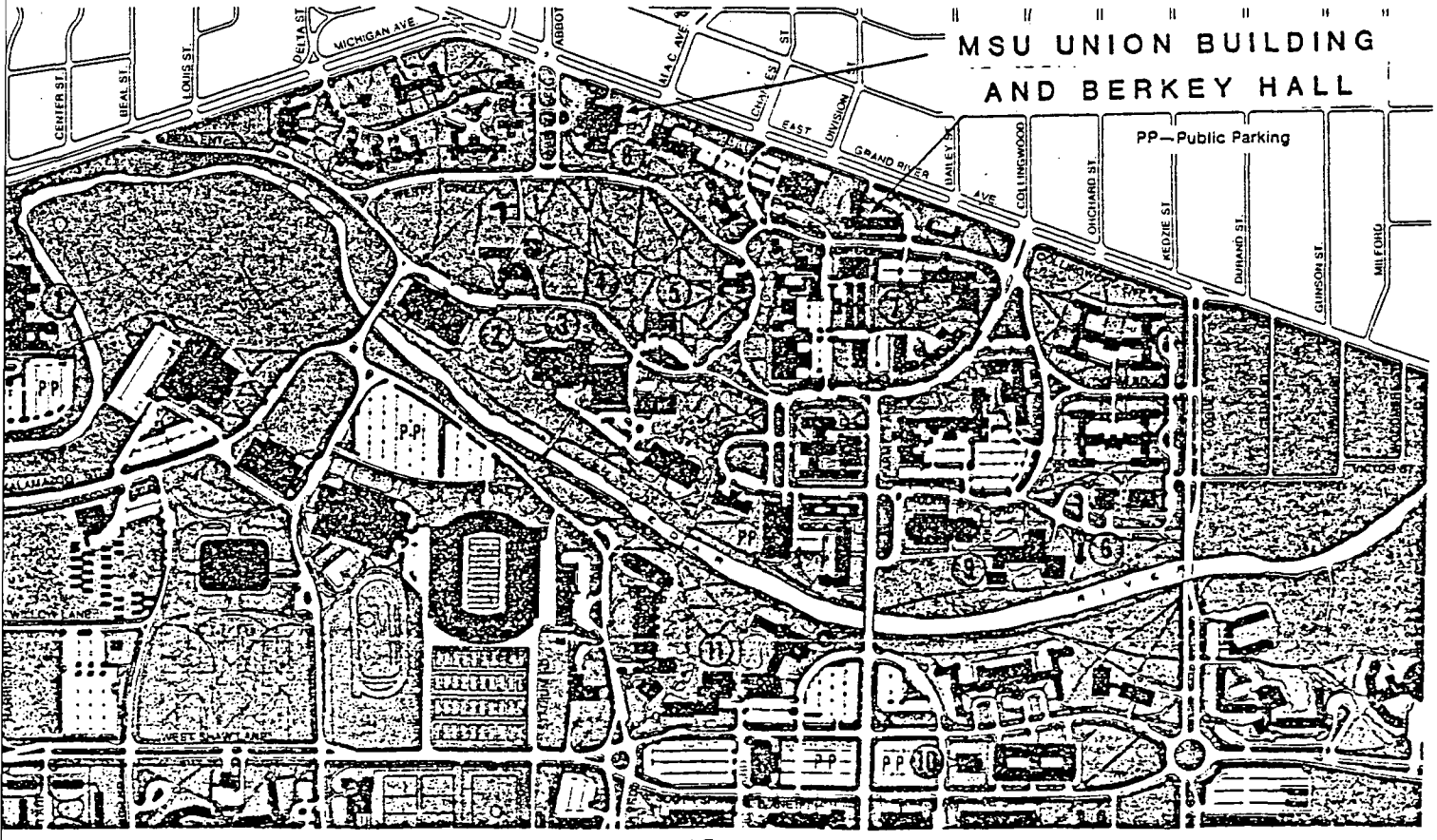

Education and Training Activities

Interpretation of Color Infrared Airphotos for Forest Resource Inventories

September 27-30, 1982 Grayling, Michigan

This three-day shortcourse introduced its participants to the application of medium-scale (1:24,000) color infrared aerial photography to forest cover type mapping. In addition to lectures, ample time was allotted for discussion, demonstrations, and practical exercises. A half-day session was devoted to field verification of the interpretation exercise.

Staff members William D. Hudson and David P. Lusch were the instructors.

Remote Sensing for Land Use Analysis

Geography 411 or Urban Planning 800, 4 credit hours

August 2-6, 1982

Three staff members from the Center for Remote Sensing, W.R. Enslin, W.D. Husdon, and D.P. Lusch, conducted this 5-day, 4-credit course which emphasized the use of remotely sensed data to inventory land cover/use. Thirty-six hours of classroom instruction, including numerous exercises, were supplemented with 4 hours of field work collecting ground-truth information. As part of the course materials prepared for this class, the instructors wrote the Photo Interpretation Key To Michigan Land Cover/Use. (Enslin, Hudson, and Lusch, 1983) Thirty-six students attended this course.

Land Use Mapping From Aerial Photography

August 10-12, 1982

This three-day shortcourse was sponsored by the Center for Remote Sensing, in cooperation with the Departments of Geography, Urban Planning, and Forestry, the Agricultural Experiment Station, and the Cooperative Extension Service at Michigan State University, as well as the Michigan Resource Inventory Program, Department of Natural Resources. Emphasis was placed on the practical application of airphoto interpretation for land cover/use inventories with special reference to 1:24,000 CIR imagery and the Michigan Current Use Inventory. The 20 participants included representatives from the following agencies or firms:

Planning Commissions	10
Consulting Agencies	3
Utilities	2
State Government	2
Soil Conservation Service	1
Miscellaneous	2

Introduction to Color Infrared Aerial Photography

This 1.75 hour tutorial session by David P. Lusch, Center for Remote Sensing, was an invited presentation to the "Soil Scientists' Workshop," August 23-25, 1983 at Lake Superior State College, Sault Ste. Marie, Michigan. This workshop was jointly sponsored by the Soil Conservation Service and the Forest Service, U.S.D.A., and the Michigan Department of Agriculture. More than 50 soil scientists currently involved in soil mapping projects in

the state were in attendance. The presentation highlighted the spectral reflectance characteristics of soil with regard to physical parameters such as texture, drainage, organic matter content, and iron oxide content.

Aerial Photography for Natural Resource Management -- A Remote Sensing Workshop

Under the auspices of the Comprehensive Resource Inventory and Evaluation System Project, funded by the U.S. Agency for International Development, a 3-month training activity for six visiting scientists from the Dominican Republic was conducted at Michigan State University June 15-September 15, 1983. The participants were staff members of the Department of Inventory and Department of Land and Water, Ministry of Agriculture Dominican Republic. David P. Lusch, Center for Remote Sensing, was the instructor during the period June 20-24, 1983. Topics covered in this phase of the training included:

- Historical overview of remote sensing
- Physical basis of remote sensing
- Energy interations with the atmostphere and earth surface features
- Photographic sensors
- Film technology
- Airphoto mission parameters
- Geometry of vertical airphotos
- Stereoscopy and photometrics
- Introduction to color and color infrared photography

William D. Hudson, Center for Remote Sensing, was the instructor during the period August 3-9, 1983. Topics covered in this phase of the training included:

Introduction to forest inventory

Planning a forest inventory

Classification of tropical vegetation

Holdridge life-zone model

Forestry photometrics

Photointerpretation of tropical forest types

Advanced Remote Sensing Techniques

This four-credit course, offered under the number Geography 424, was taught during the Spring, 1983, quarter by David P. Lusch, Center for Remote Sensing and Department of Geography. Thirty-two students participated in this course which deals with the theory, methodology, and applications of remote sensing. They were given a thorough understanding of the principles of electromagnetic radiation and its interactions with the earth's atmosphere and surface features. A major portion of the course was devoted to the characteristics of the multispectral sensor systems and data of the Landsat satellite program, including the Thematic Mapper on board Landsat 4. The students were also introduced to the computer processing of Landsat data and to the interpretation of thermal infrared and active microwave imagery.

Exhibit, Newsletter, and Brochure Available

A beautiful new exhibit on remote sensing techniques has been constructed by the Center for Remote Sensing for use at conferences, meetings, and educational activities. The exhibit is a 5-panelled, freestanding, portable display which illustrates several types of remotely sensed data in various formats. Included are samples of Heat Capacity Mapping Mission (HCMM) satellite images, Geostationary Operational Environmental Satellite (GOES) digital images, Landsat images, high-resolution color infrared photography, false-color composites, multispectral scanner images, and thematic mapper images. The data displayed includes Michigan forest cover types, surface temperature and reflectance, land use and vegetative cover, wildlife, geologic and water resources, rights of way, element sensitivity, and soil types.

The full-color exhibit is a self-explanatory introduction to the kinds and uses of remotely sensed data. It has been displayed at the National Agricultural Fair in Washington, D.C., the Michigan Technology Fair in Ann Arbor, MSU's Farmers' Week, and the International Symposium on Remote Sensing of Environment in Ann Arbor.

The Center produces a quarterly newletter (the first edition was March 1981) which is distributed pricipally in-state. The purpose of the newsletter is to keep state, regional, and local decision-makers informed about new remote sensing capabilities and application and to reach new potential users.

The Center has also prepared a new full-color Center for Remote Sensing brochure explaining the Center's purpose, organization, areas of research, facilities, and education and training opportunities.

New Facilities

The Center for Remote Sensing has relocated to Berkey Hall on the north end of Campus. Our new location consists of over 4,000 square feet of space on the third floor of Berkey, overlooking the MSU Horticulture Gardens.

Administrative offices are in 302 Berkey, and rooms 304, 310, and 311 contain equipment, labs, graduate and undergraduate student desk space, and photo archives. Room 305 is the permanent classroom for the Department of Geography undergraduate remote sensing class. The instructor for the class, Dr. Michael Chubb, also maintains an office at the Center. Room 306 has recently been secured by the Department of Geography for the Advanced Remote Sensing Course, taught by Dr. David P. Lusch, and for short courses, and international training session sponsored by the Center.

PUBLICATIONS

of the Michigan State University, Center for Remote Sensing

---

1. Automatic Digital Image Registration. A. Goshtasby, A.K. Jain, and W.R. Enslin. Proceedings 8th International Symposium on Machine Processing of Remotely Sensed Data, pp. 347-352. Purdue University, West Lafayette, Indiana, June, 1982.

2. Interpretation of Color Infrared Airphotos for Forest Resource Inventories. William D. Hudson and David P. Lusch. Center for Remote Sensing, Michigan State University. July, 1982. 55p.

3. Changes in Aquatic Vegetation in Quanicassee, Nayanquing Point, and Wildfowl Bay. Prepared for the East Central Michigan Planning and Development Region. Bill Enslin and Dwayne McIntosh. Center for Remote Sensing, Michigan State University. October, 1982.

4. An Evaluation of Digital Landsat Classification Procedures for Land Use Inventory in Michigan. Richard Hill-Rowley. Ph.D. dissertation, Michigan State University, 1982. 258p.

5. Visual Interpretation of Landsat Imagery for the Identification of Coniferous Forest Types in Michigan. Kathryn L. Franklin, William D. Hudson, Carl W. Ramm, Center for Remote Sensing and Department of Forestry, Michigan State University. Michigan State University Agriculture Experiment Station Research Report 448. Michigan State University. April, 1983.

6. Photo Interpretation Key to Michigan Land Cover/Use. William R. Enslin, William D. Hudson, and David P. Lusch. Center for Remote Sensing, Michigan State University. April, 1983. 61p.

7. Registration of Rotated Images by Invariant Moments. Ardeshir Goshtasby and William R. Enslin. Center for Remote Sensing, Michigan State University. Proceedings of the Seventeenth International Symposium on Remote Sensing of Environment, pp. 1033-1042. Ann Arbor, Michigan. May 9-13, 1983.

8. Point Pattern Matching by Selective Search. Aredeshir Goshtasby, Department of Computer Science, University of Kentucky and George C. Stockman, Department of Computer Science, Michigan State University. Submitted to the Journal of Photogrammetric Engineering and Remote Sensing.

9. Interpreting Michigan Forest Cover Types from Color Infrared Aerial Phogotraphs. William D. Hudson, Center for Remote Sensing, Michigan State University. Michigan State University Agriculture Experiment Station Research Report 452. Michigan State University. January, 1984.

PRESENTATIONS

of the Michigan State University, Center for Remote Sensing

---

1. "Fundamentals of Remote Sensing." Presented by David P. Lusch to the Geography and Map Division, Special Libraries Association, 73rd Annual Conference. Detroit, Michigan. June 5-10, 1982.

2. "Assessment of Modified Surface Temperatures and Solar Reflectance Using Meteorological Satellite and Aircraft Data." J. Bartholic, S. Gage, A. Goshtasby, C. Mason. Presented by J. Bartholic to the Symposium on Study of Land Transformation Processes from Space and Ground Observations. Ottawa, Canada, August, 1982.

3. "Correlation of GOES Temperature Patterns with Michigan Surface Festures." Presneted by David P. Lusch to the Eastern Great Lakes Regional Meeting of the American Society of Photogrammetry, Conference on Remote Sensing Applications in the Great Lakes Region. Michigan State University, East Lansing, Michigan. April 22, 1983.

4. "Discrimination and Mapping of Coniferous Forest Types From Landsat Data." Presented by William D. Hudson to the Eastern Great Lakes Regional Meeting of the American Society of Photogrammetry, Conference on Remote Sensing Applications In the Great Lakes Region. Michigan State University, East Lansing, Michigan. April 22, 1983.

5. "Potential Use of Remote Sensing in Delimiting Areas of Virus Infection in Vineyards and Blueberry Fields in Michigan." A.M. Childress-Roberts, D.C. Ramsdell, and David P. Lusch. Presented by A.M. Childress-Roberts to the Annual Meeting of the American Phytopathological Society. Ames, Iowa. June, 1983.

6. "Satellite Data for Estimates of Key Parameters for Calculating Evapotranspiration. Presented by Jon Bartholic at the American Geophysical Union Spring 1983 Meeting. Balitmore, Maryland. June, 1983.

7. "Late Wisconsinan Patterned Ground In the Sagniaw Lowland of Michigan." Presented by David P. Lusch at the Fourth International Conference on Permafrost. University of Alaska, Fairbanks, Alaska. July 18-22, 1983.

8. "The History and Development of Aerial Photography and Remote Sensing." Presented by David P. Lusch to the Lansing Camera Club. October 25, 1983.

9. "Interpretaton of Selected Glacial Features in Michigan From Landsat Imagery." Presented by David P. Lusch to the Geomorphology Section of the East Lakes Divisional meeting of the Association of American Geographers. University of Cincinnati, Cincinnati, Ohio. November 4-5, 1983.

10. "Digital Land Surface Information of Michigan." William R. Enslin and David P. Lusch. Presented by W.R. Enslin to the Eastern Great Lakes Regional meeting of the American Society of Photogrammetry. December 9, 1983.

11. "A Symbolically-Assisted Approach to Digital Image Registration with Application in Computer Vision." Ardeshir Goshtasby. Ph.D. dissertation, Michigan State University, 1983. 222 pages.

APPENDICES

Recipient of the 1983 William A. Fischer Memorial Award

REGISTRATION OF ROTATED IMAGES BY INVARIANT MOMENTS*

A. Goshtasby
Dept. of Computer Science
Michigan State University
E. Lansing, Michigan 48824

and

W. R. Enslin
Center for Remote Sensing
Michigan state University
E. Lansing, Michigan 48824

Abstract: A new technique for registration of rotated images using invariant moments as the similarity measure is given. If circular windows with invariant moments are used, then window search can be carried out on rotated images in the same manner cross-correlation with rectangular windows is used on translated images. Normalization of invariant moments for more accurate window similarity measurement is also given. The proposed approach is tested against two images from different satellites that have translational and rotational differences.

1. INTRODUCTION

Image registration is the process of determining the position of corresponding points in two images of the same scene. Usually image registration involves resampling of one of the images so that a point in the scene has the same coordinate values in both of the images. In this paper registration of images that have translational and rotational differences will be discussed.

Image registration has many applications. Some of the applications of image registration are in change detection, motion analysis, object tracking, and object recognition. Analysis of two or more images of the same scene often requires registration of the images.

One of the first attempts to register images digitally was made by Anuta [Anuta 69]. He used cross-correlation as the similarity measure to search for corresponding windows in the two images. The centers of the resultant matched windows were taken as corresponding control points for estimating the translational difference between the images.

Image registration by cross-correlation has proven to be very effective and it is still one of the best techniques in image registration. However, this technique can only register images that have translational differences. Computation of cross-correlation is also time consuming. To speed up the process, Anuta used the fast Fourier transform algorithm to compute the cross-correlation values [Anuta 70]. Sum of absolute differences has also been used as an alternative similarity measure to speed-up the window search process [Barnea 72].

* This work has been supported in part by NASA Grant NGL-23-004-083.

Most of the work in image translational registration has been centered on speed-up techniques rather than the accuracy of the registration. Dewdney has proposed a steepest-descent algorithm to limit the window search domain and thus achieve a higher speed [Dewdney 78].

A two-stage window search technique has also been used [Vanderburg 77]. In this technique, first a subwindow is used to locate possible locations for a match. Then the whole window is used to locate the best match position among the possible ones. This technique was later extended to the coarse-fine searching technique, where a coarse window is used first followed by a finer resolution window [Rosenfeld 77]. This window search process has been expanded to the multi-stage search technique in which in the first stage, the lowest resolution window is used and then higher resolution windows are successively used in each subsequent stage [Hall 76, Tanimoto 81]. Other similarity measures which have been used in the window search process are Haar transform coeffficients [Chandra 82], Walsh-Hadamard transform coefficients [Schutte 80], and invariant moments [Wong 78].

When the images are rotated with respect to each other, the above window search techniques for determination of corresponding points in images, will fail. This is because, even though the centers of two windows correspond, we may obtain low similarity measures due to the fact that other points in the windows may not correspond to each other. For example, Figure 1 shows two windows in which their centers correspond to each other but since other points in the two windows do not correspond, low similarity is obtained.

As a matter of fact, similarity measure is not the only problem. When two images are rotated with respect to each other, it is impossible for two rectangular windows to contain the same parts of the scene (except when the two windows are rotated by a multiple of 90 degrees with respect to each other). As shown in the two rotated windows of Figure 1, although the centers of the windows correspond to each other they don't contain the same parts of the scene.

This problem can be alleviated if we use circular windows. Then when the centers of two windows correspond to each other, the two windows will cover the same parts of the scene no matter what the rotational difference between the windows. Figure 2 shows two circular windows which are rotated with respect to each other and since their centers correspond to each other, they contain the same parts of the scene.

In this paper we will show that rotated images can be searched and matched by using circular windows and invariant moments as the similarity measure. Hu has derived a set of invariant moments such that if two windows contain the same pattern, they will have similar invarinat moments no matter what their rotational differences [Hu 62]. We will normalize 8 invariant moments and use them in the computation of the similarity measure between two windows.

In the following, invariant moments are first described and their use in template matching is given. Then the window search process using invariant moments with circular windows is discussed including a procedure for the determination of registration parameters. Finally, the result of the proposed approach on registration of multi-satellite images is presented.

2. INVARIANT MOMENTS

The two dimensional (p+q)th order moment of a digital image f is defined by

$$m_{pq} = \sum_x \sum_y x^p y^q f(x,y) \qquad (1)$$

where f(x,y) is the pixel value of image f at location (x,y) [Hu 62].

Measure m_{pq} changes if image f is translated. To make m_{pq} invariant with respect to translation of f, m_{pq} is modified as below,

$$u_{pq}= \sum_x \sum_y (x-x')^p (y-y')^q f(x,y) \qquad (2)$$

where

$$x'= \sum_x \sum_y x f(x,y) / \sum_x \sum_y f(x,y) = m_{10}/m_{00}$$

$$y'= \sum_x \sum_y y f(x,y) / \sum_x \sum_y f(x,y) = m_{01}/m_{00}$$

u_{pq} is called the (p+q)th order central moment of image f and is invariant with respect to translation of image f [Hu 62].

We still cannot apply u_{pq} in the template search process because u_{pq} varies with respect to the rotation of image f. Hu has been able to derive moments that are invariant with respect to rotation [Hu 62]. He has shown that an infinite number of such moments exist. The second-order and third-order moments which are invariant with respect to rotation (and translation) of f are given by,

$$a_1=u_{20}+u_{02} \qquad (3)$$

$$a_2=(u_{20}-u_{02})^2+4u_{11}^2 \qquad (4)$$

$$a_3=(u_{30}-3u_{12})^2+(3u_{21}-u_{03})^2 \qquad (5)$$

$$a_4=(u_{30}+u_{12})^2+(u_{21}+u_{03})^2 \qquad (6)$$

$$a_5=(u_{30}-3u_{12})(u_{30}+u_{12})[(u_{30}+u_{12})^2-3(u_{21}+u_{03})^2]+ (3u_{21}-u_{03})(u_{21}+u_{03})[3(u_{30}+u_{12})^2-(u_{21}+u_{03})^2] \qquad (7)$$

$$a_6=(u_{20}-u_{02})[(u_{30}+u_{12})^2-(u_{21}+u_{03})^2]+4u_{11}(u_{30}+u_{12})(u_{21}+u_{03}) \qquad (8)$$

$$a_7=(3u_{21}-u_{03})(u_{30}+u_{12})[(u_{30}+u_{12})^2-3(u_{21}+u_{03})^2]- (u_{30}-3u_{12})(u_{21}+u_{03})[3(u_{30}+u_{12})^2-(u_{21}+u_{03})^2] \qquad (9)$$

Usually more than one moment is used in decision making. One way to measure similarity between two windows is to compute the distance between two vectors of moments. The smaller the distance, the more similar the two windows [Giuliano 61]. This method however requires that the feature elements in the vectors be of the same unit (or scale). Moments of different orders do not have the same scale. Table 1.a shows a 16x16 window whose moments upto order 5 are shown in Table 1.b. As can be seen, moments of different order are in different magnitudes because of scale differences.

The correlation of the logarithm of moments has been used by Wong to measure the similarity between two windows [Wong 78]. Again, the moments of different orders have different scales and using the logarithm of the moments does not solve the problem. Note that in Table 1.b, the logarithm of the moments increase with the order of the moment. If the correlation of logarithm of moments are determined, high correlation values will always be obtained regardless of the dissimilarity between the two windows. So, the correlation of the moments is not an appropriate measure of similarity either. The correlation between two sets of numbers is defined when the numbers in each set

are in the same scale. When features of different scales are used in the computation of correlation value, the feature with the largest scale dominates the correlation value.

Garrett has proposed the concept of pairing function where the similarity between two sets of features is determined by quantizing the features and counting the number of quantized features that are equal [Garrett 76]. In this technique, since the features in the two sets are quantized into the same number of levels, it is as if the features in the two sets are in the same scale. This alleviates the problem of scale differences but this similarity measure does not provide information about how closely two features match. When the feature values are quantized, critical information needed in similarity measurement might disappear. So, the pairing function is also not appropriate for measuring the similarity between two windows when moments are used as features.

To overcome the above problems, we normalize the moments so that they all have the same scale. The normalized moment of order (p+q) for image f with diemensions N by N is defined by,

$$M_{pq} = \sum_{x=1}^{N}\sum_{y=1}^{N} (x/x'')^p (y/y'')^q f(x,y)$$

where

$$x'' = (1/N) \sum_{x=1}^{N} x = N(N+1)/2N = (N+1)/2$$

$$y'' = (1/N) \sum_{y=1}^{N} y = (N+1)/2$$

So, actually $M_{pq} = \sum_{x=1}^{N}\sum_{y=1}^{N} \{x/[(N+1)/2]\}^p \{y/[(N+1)/2]\}^q f(x,y)$

$$= [2/(N+1)]^{p+q} \sum_{x=1}^{N}\sum_{y=1}^{N} x^p y^q f(x,y)$$

$$= [2/(N+1)]^{p+q} m_{pq}$$

So, the normalized (p+q)th order moment is equal to the (p+q)th order moment multiply the scaling factor $[2/(N+1)]^{p+q}$. Table 1.b shows the normalized moments for the window of Table 1.a. As can be seen, moments of all orders have the same scale now.

To determine the normalized central moments, we replace x by x/[(N+1)/2] and y by y/[(N+1)/2] in formula (2).

$$U_{pq} = \sum_{x=1}^{N}\sum_{y=1}^{N} \{(x-x')/[(N+1)/2]\}^p \{(y-y')/[(N+1)/2]\}^q f(x,y)$$

$$= [2/(N+1)]^{p+q} \sum_{x=1}^{N}\sum_{y=1}^{N} (x-x')^p (y-y')^q f(x,y)$$

$$= [2/(N+1)]^{p+q} u_{pq}$$

In the same manner we can determine the normalized invariant moments (formulas (3) to (9)), in which each is multiplied by only a scaling factor. We will be using the normalized invariant moments from two circular windows as features and by computing the cross-correlation between these feature values, the similarity of windows will be determined.

3. DETERMINATION OF REGISTRATION PARAMETERS

The ultimate goal is to determine the translational and rotational differences (registration parameters) between two images. A minimum of two pairs of corresponding points from the two images are required to determine the registration parameters. To determine a pair of corresponding points in two

images, a small window called a template, is taken from one image and a larger window, called a search area, is extracted from the other image. The template is shifted in the search area until the position where the template best matches in the search area is determined. At the best match position, the center of the template corresponds to the center of the window in search area over which the template lies.

In order to make the window-matching procress more reliable, templates should be taken in a high variance (high information) area in the image. An automatic procedure for selection of high information templates has been defined [Davis 78]. This procedure selects windows that are well separated and have a large number of high gradient, high curvature, connected edges in the image. The search area should be selected such that the window corresponding to the template is not missed.

Given a circular template and a search area, the following algorithm determines the position where the template best matches in the search area using invariant moments.

Algorithm A: Template matching by invariant moments.

1. Select template W of size NxN from a high information area in one image.
2. Select search area S of size MxM in the other image such that it contains the template.
3. Determine the n normalized invariant moments of the template, let them be a1, a2, . . an.
4. For I = N/2 to M-N/2+1
5. | For J = N/2 to M-N/2+1
6. | | Determine the n normalized invariant moments of the window cantered at (I,J) in the search area and size NxN, let them be a1', a2', . . an'.
7. | | Find the cross-correlation between {a1, a2, . . an} and {a1', a2'. . , an'}, let it be r(I,J).
8. Let (I',J') be that (I,J) such that r(I',J')=Max r(I,J). Then (I',J') would be the coordinates of the center of the window in the search area which best matches with the template.
9. The center of the template corresponds to location (I',J') in the search area. By this, a pair of corresponding points from the two images are found.

Template size NxN, search area size MxM, and the number of invariant moments n are specified by the user. If the template size is too small, it may not contain enough information to carry out a reliable search. If the template size is too large, the search process becomes costly. So, selecting the right size template is very important.

Usually, smooth areas of an image require larger template sizes than detailed ones. Since an image may contain both smooth and detailed areas, a constant template size may not be adequate and different size templates may have to be used. Dynamically determining template size at every step, however, is time consuming and it adds overhead to the already slow search process.

Traditionally, template size has been selected heuristically. We have followed the tradition and have tried different template sizes. The smallest size which gave reasonable accuracy was taken as the template size. For the images we had, templates of size 16x16 turned out to be appropriate.

Search area size is another parameter which should be given by the user and it should be taken in such a way that it contains the template. Another parameter is the number of invariant moments required in the matching process. The greater the number of moments the more accurate the matching but the slower

the search process. We have used 8 normalized invariant moments. These are the zeroth order, second order, and third order normalized invarinat moments. The zeroth order moment is equal to the sum of intensity values in a window.

$$a_0=U_0=M_{00}=m_{00}= \sum_x \sum_y f(x,y)$$

Using Algorithm A, a number of corresponding points from the two images can be obtained. There are possibilities of mismatches in the process and some of the corresponding points may not actually correspond to each other. Non corresponding points should be eliminated before registration parameters are computed.

An effective method for detection of points that do not correspond to each other is given in [Fischler 81]. In this method, for each two pairs of corresponding points in the two images the transformation parameters are estimated from formula (10). Then a clustering is performed in the parameters space. Correct matches tend to make a cluster while mismatches tend to scatter randomly in the parameter space. Those points which produce parameter values larger than a given threshold value from the cluster center are taken as mismatches and are eliminated from the set.

Once a number of valid corresponding points from the two images are determined, the estimation of registration parameters is straight forward. Two images that have translational and rotational differences can be related to each other by

$$x'=x\cos\theta-y\sin\theta+h \qquad (10)$$
$$y'=x\sin\theta+y\cos\theta+k$$

where (x',y') and (x,y) are the coordinates of corresponding points in the two images. If we replace cosθ by a and sinθ by b we get,

$$x'=ax-by+h$$
$$y'=bx+ay+k$$

Now if coordinates of n corresponding points from the two images are given, we can estimate a, b, h, and k by minimizing the following sum of squared errors.

$$E= \sum_{i=1}^{n} \{[xi'-(axi-byi+h)]^2+[yi'-(bxi+ayi+k)]^2\}$$

To minimize E with respect to a, b, h, and k, we find the partial derivatives of E with respect to a, b, h, and k. Set them equal to zero, and solve the system of linear equations.

$$\begin{bmatrix} \sum_i(xi^2+yi^2) & 0 & \sum_i xi & \sum_i yi \\ 0 & \sum(xi^2+yi^2) & \sum_i yi & -\sum_i xi \\ \sum_i xi & \sum_i yi & n & 0 \\ \sum_i yi & -\sum_i xi & 0 & n \end{bmatrix} \begin{bmatrix} a \\ b \\ h \\ k \end{bmatrix} = \begin{bmatrix} \sum_i(xi'xi+yi'yi) \\ -\sum_i(yi'xi-xi'yi) \\ \sum_i xi' \\ \sum_i yi' \end{bmatrix} \qquad (11)$$

where (h,k) is the translational difference and $\theta= \cos^{-1}a$ and $\theta=\sin^{-1}b$ is the rotational difference between the images. Knowing h, k, and θ, we can map one image into another by the transformation functions of (10).

4. RESULTS

Two images from two different satellites were used to test the above image registration technique. Figure 3 shows a thermal-infrared image of Michigan

obtained by the Geostationary Operational Environment Satellite (GOES) on 24 June 79 at 3:00 PM. Figure 4 is a day-visible image of approximately the same area obtained by the Heat Capacity Mapping Mission (HCMM) satellite on 26 Sept. 79. Both GOES and HCMM images were already geometrically corrected. The original HCMM image has 500x500 meter resolution. Since the GOES image has 8x11 km resolution, the HCMM image was smoothed in 16x22 neighborhoods and was resampled to the same resolution as the GOES image. The two images now have the same scale but have translational and rotational differences.

Since two windows with similar pattern but different intensity values result in different invariant moments, we have used the gradient of the two images rather than the images themselves in the registration. This reduces the effect of intensity difference between the two images.

Six points from the GOES image was selected by hand. Circular templates with an 8 pixel radius were taken centered at the selected points. Search areas with a radius 16 pixels were selected from the HCMM image in such a way that they included the template areas. For each template and search area, Algorithm A was executed to determine the best match position of the template in the search area.

Transformation parameters were obtained by using the 6 pairs of corresponding points from the two images and solving the system of linear equations shown by (11). The rotational difference between the two images was 11.5 degrees and the translational difference between the two images was (9.4,-13.8). The GOES image was resampled by the nearest neighbor method and using the transformation,

$$x' = 0.98x - 0.20y + 9.4$$
$$y' = 0.20x + 0.98y - 13.8$$

where (x',y') and (x,y) are coordinates of corresponding points in the HCMM and GOES images, respectively. Figure 5 shows the resampled GOES image. GOES and HCMM images are subtracted in Figure 6 to visualize the registration.

5. CONCLUSION

A technique for registration of rotated images using normalized invariant moments was given. The technique first locates a number of corresponding points in two images by window searching and then estimates the registration parameters using the corresponding points and minimizing the sum of squared errors.

This technique can be used in registration of multi-satellite and multi-temporal images. If the images have scaling differeences, a low-pass filter can be used on the high resolution image and resample it to the same resolution as the low resolution image since resolution of satellite images are known. This alleviates the problem of scale difference between the images. The technique given above can then be used to determine the rotational and translational differences between the images. An example was given showing registration of HCMM and GOES images which had, known scaling difference but unknown rotational and translational differences.

REFERENCES

[Anuta 69] "Digital Registration of Multi-Spectral Video Imagery", Paul E.

Anuta, Soc. Photo-Optical Instrum. Engs. J., Vol. 7, Sept. 1969, pp 168-175.

[Anuta 70] "Spatial Registration of Multispectral and Multitemporal Digital Imagery Using Fast Fourier Transform Techniques," Paul E. Anuta, IEEE Trans. on Geoscience Electronics, Vol. GE-8, No. 4, Oct. 1970, pp 353-368.

[Barnea 72] "A Class of Algorithms for Fast Digital Image Registartion" Daniel I. Barnea and Harvey F. Silverman, IEEE Trans. on Computers, Vol. C-21, No. 2, Feb. 1972, pp 179-186.

[Chandra 82] "Feature Matching Multiple Image Registration Using Haar Coefficients," D. V. Satish Chandra, J. S. Boland, W. W. Malcolm, and H. S. Ranganath, Southcon, April 5-7, 1982, pp 549-552.

[Davis 78] "Automatic Selection of Control Points for the Registration of Digital Images", W. A. Davis and S. K. Kenue, 4th Int. Joint. Conf. on Pattern Recognition, 1978, pp 936-938.

[Dewdney 78] "Analysis of a Steepest-Descent Image-Matching Algorithm," A. K. Dewdney, Pattern Recognition, 1978, Vol. 10, pp 31-39.

[Garret 76] "Detection Threshold Estimation for Digital Area Correlation," Grier S. Garret, Edward L. Reagh, and Edwin B. Hibbs, Jr., IEEE Trans. on Syst., Man, Cybern., Jan. 1976, pp 65-70.

[Giuliano 61] "Automatic Pattern Recognition by Gestalt Method," Vincent E. Giuliano, Paul E. Jones, Goerge E. Kimball, Richard F. Meyer, and Barry Stein, Information and Control 4, 1961, pp 332-345.

[Hall 76] "Hierarchical Search for Image Matching," E. L. Hall, R. Y. Wong, and Lt. J. Rouge, IEEE Decision and Control Conf., 1976, pp 791-796.

[Hu 62] "Visual Pattern Recognition by Moment Invariants," M-K Hu, IRE Trans. on Information Theory, 1962, pp 179-187.

[Rosenfeld 77] "Coarse-Fine Template Matching", Azreil Rosenfeld and Gordon J. Varderburg, IEEE Trans. on Sys., Man, and Cybern., Feb. 1977, pp 104-107.

[Schutte 80] "Scene Matching with Translation Invariant Transforms," Holger Schcutte,, Stephen Frydrychowicz, and Johannes Schroder, Proc. 5th Int. Conf. on Pattern Recognition, 1980, pp 195-198.

[Tanimoto 81] "Template Matching in Pyramids," Steven L. Tanimoto, Computer Graphics and Image Processing 16, 1981, pp 356-369.

[Vanderburg 77] "Two-Stage Template Matching," Gordon J. Vanderburg and Azriel Rosenfeld, IEEE Trans. on Computers, Vol. C-26, No. 4, April 1977, pp 384-393.

[Wong 78] "Scene Matching with Invariant Moments," Robert Y. Wong and Ernest L. Hall, Computer Graphics and Image Processing 8, 1978, pp 16-24.

	0	1	2	3	4	5	6	7	8	9	10	11	12	13	14	15
0	71	65	65	68	67	64	65	65	65	65	66	65	68	64	60	59
1	68	65	67	67	62	62	66	67	67	63	61	60	55	50	44	43
2	68	67	66	62	60	64	66	66	61	51	45	44	41	38	38	38
3	66	66	62	65	67	60	56	51	40	35	33	33	34	36	38	37
4	64	67	65	67	60	46	39	40	35	38	40	42	45	40	43	43
5	64	66	60	49	38	32	33	40	46	53	51	54	56	61	62	65
6	66	60	45	33	30	35	38	45	49	57	59	57	65	73	74	77
7	54	39	34	30	29	34	36	44	52	55	59	68	71	72	75	77
8	42	28	26	28	30	31	35	37	43	49	53	57	64	70	73	74
9	35	31	29	31	30	28	32	34	39	44	49	53	60	65	71	72
10	37	38	33	34	35	29	27	30	33	35	42	50	56	59	63	70
11	42	41	38	37	35	31	30	33	32	35	35	40	48	52	59	67
12	44	42	44	39	36	35	37	38	33	35	34	36	42	47	53	61
13	49	45	48	46	40	38	39	35	36	35	38	35	37	38	45	48
14	52	56	51	47	41	41	40	37	36	37	36	37	35	37	41	46
15	63	56	53	48	46	44	46	44	39	40	39	35	36	39	39	42

(a)

MOMENTS	ORIGINAL	LOG10(ORIG)	NORMALIZED
M(0, 0)=	0.1241500E+05	0.4093947E+01	0.1241500E+05
M(0, 1)=	0.1071010E+06	0.5029794E+01	0.1127379E+05
M(1, 0)=	0.9822100E+05	0.4992205E+01	0.1033906E+05
M(0, 2)=	0.1208743E+07	0.6082335E+01	0.1339328E+05
M(1, 1)=	0.8615781E+06	0.5935295E+01	0.9546570E+04
M(2, 0)=	0.1046483E+07	0.6019732E+01	0.1159538E+05
M(0, 3)=	0.1527869E+08	0.7184086E+01	0.1782032E+05
M(1, 2)=	0.9858765E+07	0.6993823E+01	0.1149878E+05
M(2, 1)=	0.9134983E+07	0.6960708E+01	0.1065460E+05
M(3, 0)=	0.1274178E+08	0.7105230E+01	0.1486139E+05
M(0, 4)=	0.2049458E+09	0.8311639E+01	0.2516197E+05
M(1, 3)=	0.1259041E+09	0.8100039E+01	0.1545771E+05
M(2, 2)=	0.1043736E+09	0.8018591E+01	0.1281434E+05
M(3, 1)=	0.1097818E+09	0.8040530E+01	0.1347832E+05
M(4, 0)=	0.1667723E+09	0.8222124E+01	0.2047527E+05
M(0, 5)=	0.2851797E+10	0.9455119E+01	0.3685538E+05
M(1, 4)=	0.1701998E+10	0.9230959E+01	0.2199588E+05
M(2, 3)=	0.1333064E+10	0.9124851E+01	0.1722793E+05
M(3, 2)=	0.1245624E+10	0.9095387E+01	0.1609789E+05
M(4, 1)=	0.1416772E+10	0.9151299E+01	0.1830973E+05
M(5, 0)=	0.2283082E+10	0.9358521E+01	0.2950553E+05

(b)

Table 1. (a) A window and (b) its moments, logarithm moments, and normalized moments.

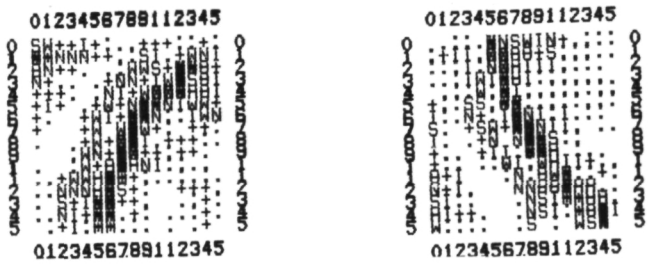

(a) (b)

Figure 1. Two rotated square windows with the same center point.

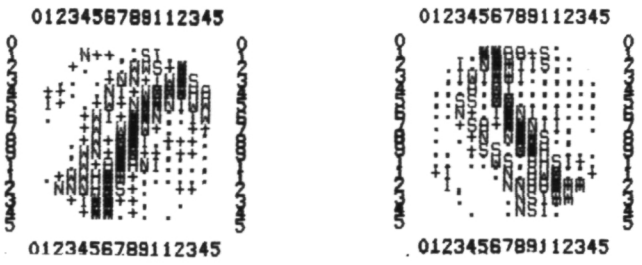

(a) (b)

Figure 2. Two rotated circular windows with the same center point.

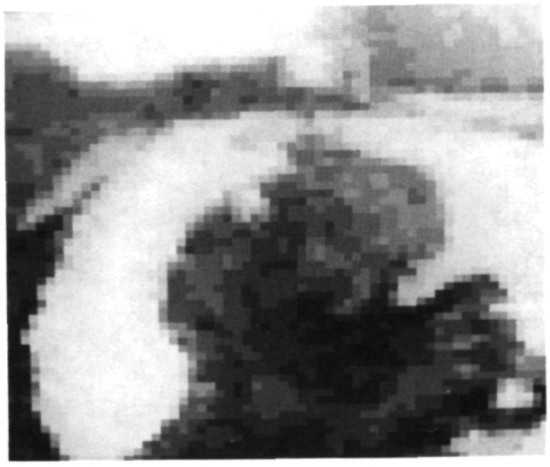

Figure 3. GOES thermal IR image of Michigan (24 Jun 79).

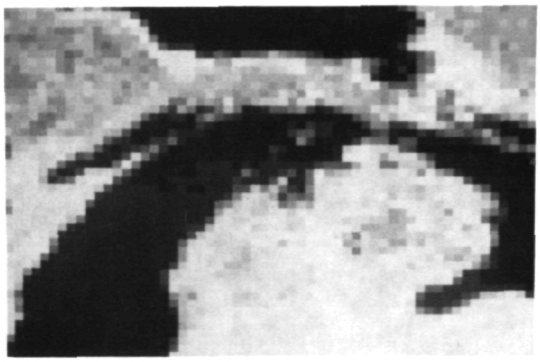

Figure 4. HCMM day-visible image of Michigan (26 Sep 79).

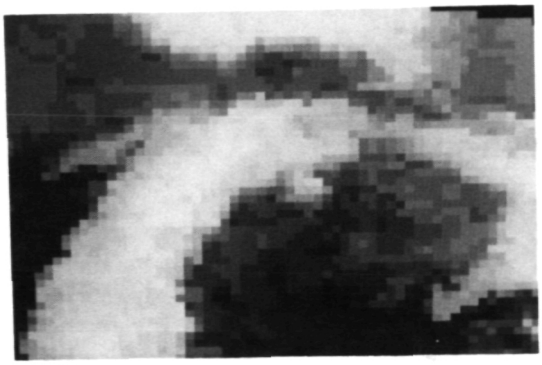

Figure 5. GOES image resampled to overlay with the HCMM image.

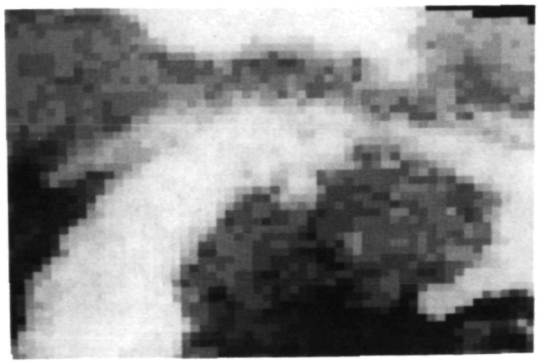

Figure 6. GOES and HCMM image difference.

APRIL 1983

RESEARCH REPORT 448 NATURAL RESOURCES

Landsat Imagery for Identifying Coniferous Forest Types in Michigan

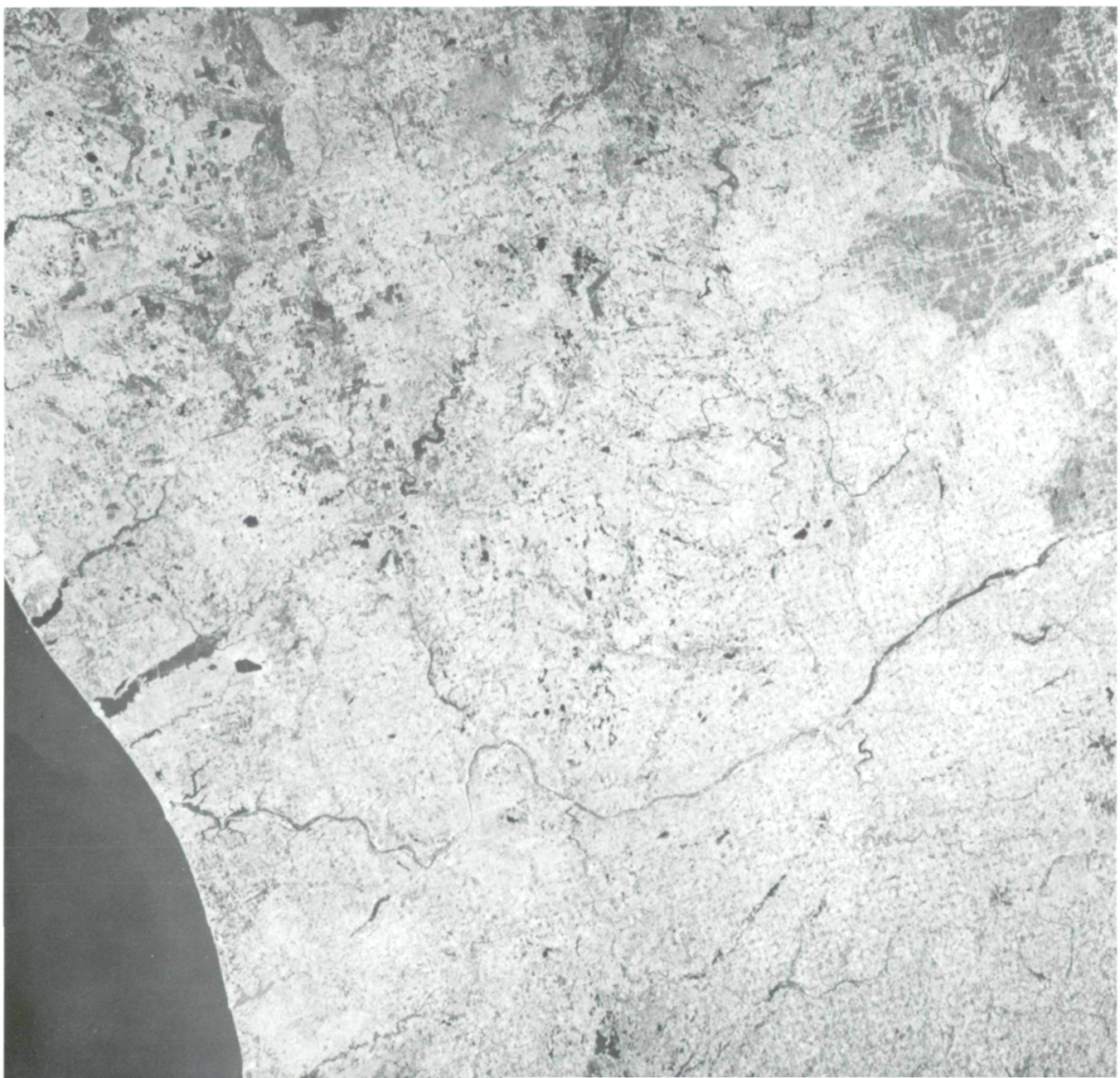

Landsat Imagery for Identifying Coniferous Forest Types in Michigan

by Kathryn L. Franklin, Student, Department of Forestry; William D. Hudson, Research Specialist, Center for Remote Sensing/Department of Forestry; and Carl W. Ramm, Assistant Professor, Department of Forestry

Summary

This study evaluated the use of Landsat computer enhanced imagery for mapping coniferous forest types in Michigan's northern Lower Peninsula. Visual interpretation procedures were developed and tested over two sites to determine the feasibility of identifying coniferous species. The accuracy achieved by two interpreters was compared and summarized in contingency tables.

Overall classification accuracies were 85 and 73 percent; individual species interpretability accuracies ranged from a low of 32 percent for mixed pine stands to 95 percent for jack pine plantations. Most of the errors in mapping the pines were accounted for by confusion between the individual pine species. The swamp conifer type had consistently low interpretation accuracies at both test sites. Other factors affecting interpretation accuracies were also identified and are reported.

Introduction

With more than half of Michigan presently in forests (19 million acres), a large industrial capacity depends on a steady supply of industrial roundwood. There is a possibility of losing a portion of this resource base because of population growth, highway and powerline construction, and residential development.

Michigan's timber volumes are assessed periodically through the Forest Survey, an inventory conducted by the U.S.D.A. Forest Service designed to measure and evaluate timber conditions and the supply and drain situation. However, the survey is conducted only every 10 to 15 years, is not site-specific, and is statistically reliable only on a multi-county basis. There is a need for detailed locational information on Michigan's forest types to supplement and update cover type maps produced from traditional field techniques and aerial photography.

New developments in remote sensing techniques are providing foresters and other wildland managers unique opportunities for earth-resource inventories. Although still considered by many to be in the developmental stage, the Landsat program has generated considerable interest from the scientific community and resource managers. The system has provided readily available data on an unprecedented scale. The large aerial coverage (about 13,225 square miles per image) and 18-day repetitive acquisition cycle provides a unique opportunity for large area mapping and inventory updating.

Several studies have been conducted on using Landsat data in mapping forest resources in Michigan. One of the first (4), conducted under a National Aeronautics and Space Administration ERTS-1 Project Grant, analyzed both visual and computer assisted interpretations.

A later attempt to map tree species and species groups from June data, using automated recognition techniques, did not produce a classification with acceptable accuracy (6). A study utilizing visual interpretation of winter Landsat imagery, with snow cover on the ground, to map scattered woodlots obtained accuracies ranging from 74.0 to 98.5 percent (2).

Study Area

The climate, physiography and soils of the northern Lower Peninsula combine to create a unique region, as compared to the southern Lower Peninsula or the Upper Peninsula. One of the most distinctive landscapes are high outwash plains near the center part of the region, which are dominated by stands of pines and oaks. These extensive, flat, sandy plains — where the large white pine forests of Michigan formerly grew — support much of the nearly 7 million acres of forest found in this unit.

Hardwood forests are more extensive than the softwoods with aspen-birch, a sub-climax type, the most common throughout the region. The northern hardwood type is most prevalent in the northwestern counties; lowland hardwoods are primarily restricted to riparian sites.

The softwoods, or coniferous forest types, occupy approximately 22 percent of the region. Three-fifths of these conifers are pines; jack pine, the most important pine sub-

* This research was supported by a National Aeronautics and Space Administration grant, NASA NGL 23-004-083, to Michigan State University, Center for Remote Sensing and by federal funds from the McIntire-Stennis Law (P.L. 87-788).

Figure 1. The northern Lower Peninsula of Michigan and the location of two test sites.

type, accounts for more than half the acreage. Jack pine occurs as a relatively pure type in a broad belt from the central northeastern area, south and west to the southwest central area. Significant areas are also found in the east and west central counties (5).

The swamp conifer types — consisting predominately of cedar with lesser areas of black spruce, balsam fir-white spruce, and tamarack — comprise less than 9 percent of the forest land. These swamp conifers occur most frequently as small patches of a few acres on wet lands. The exceptions are in the northeastern counties where these species are more frequent and exist as larger stands (5).

Two test sites were chosen in the northern Lower Peninsula (Figure 1) to be representative of areas now supporting large acreages of conifers. The first test site (Figure 2) was located in west central Wexford County (T. 22 and 23 N., R. 12 W.) and is underlain primarily by stratified sand and gravel outwash deposits confined to a broad valley (i.e., a valley train). Most of the area was cleared for agriculture at one time, but later was abandoned as unsuitable for sustained crop production.

The present forest covers more than 40 percent of the area and is predominately pine plantations. Red pine accounts for 60 percent of the plantations, jack pine is predominate in 29 percent and 11 percent are mixtures of red and jack pine. Ten percent of the forest land is composed of the swamp conifer type. These stands, composed of scattered northern white-cedar intermixed with lowland hardwoods, are concentrated along several creeks traversing the region.

Figure 2. High-altitude aerial photograph of test site number 1, west central Wexford County.

The second test site was located in northeastern Crawford County and southeastern Otsego County (T. 28 and 29 N., R. 1 W.). This area is part of an extensive outwash plain and is typical of the "jack pine flats" of the northern Lower Peninsula of Michigan. No evidence of land clearing for agriculture is present and the forest is entirely natural (i.e. there are no plantations).

The area is nearly entirely forested, with conifers dominant on 72 percent of the area, the remainder being predominately hardwoods, grass or brush. Pines are located throughout the site except for two large swamps which support lowland conifer species. Jack pine is by far the predominant species throughout the site and represents more than 70 percent of the softwood acreage.

Methodology

The Landsat (land satellite) system is the major component of NASA's land observation program. These satellites, orbiting the earth at an altitude of 570 miles, are configured to provide global coverage once every 18 days. This repetitive coverage capability, combined with the unexpected long life of the satellites, has prompted numerous investigations into the "operational" use of Landsat data.

The primary sensor aboard the satellite is a multispectral scanner. This instrument is an electronic imaging device which records sunlight reflected from the surface of the earth in four specific wavelength bands. Two of these bands are in the visible spectrum, at 0.5 to 0.6 μm (green) and 0.6 to 0.7 μm (red), and two are in the reflected infrared portion of the spectrum at 0.7 to 0.8 μm and 0.8 to 1.1 μm.

The analog signals from the detectors in each of the four bands are converted into digital electronic signals for transmitting to ground receiving stations. This digital information can then be processed and stored in a computer or converted to film images portraying the original scenes.

In 1977 the U.S. Geological Survey's EROS Data Center began producing a new Landsat image product, referred to as computer enhanced imagery (7). This product utilizes advanced digital image processing techniques and is produced from digitally preprocessed Landsat computer compatible tapes. Enhancement and restoration algorithms were designed to reveal more textural information and spectral contents to users.

Four techniques were applied to the imagery used in this study: 1) radiometric restoration — a histogram equalization technique to remove the striping effect; 2) contrast enhancement — a linear contrast stretch to provide improved contrast and maximum color variation; 3) edge enhancement — filtering to boost the high frequency content and thereby improve image sharpness; and 4) synthetic line generation — removing cosmetic defects caused by errors in data transmission.

After the digital data have been processed with these algorithms, the data for each Landsat band are printed on 9½" black-and-white film with a laser beam film recorder. False color composites are generated by successive exposure of three bands, using appropriate filters, onto color film. Standard composites are created by printing band 7 (0.8 to 1.1 μm) with a red filter, band 5 (0.6 to 0.7 μm) with a green filter, and band 4 (0.5 to 0.6 μm) with a blue filter. This combination produces a color composite which resembles a color infrared photograph.

Because the study dealt only with coniferous vegetation, a "leaf-off" scene was chosen (Figure 3) because of its sharp tonal (color) contrasts of several coniferous forest types (Figure 4). Based upon an initial analysis of this scene and the characteristics of the coniferous forest distribution in the northern Lower Peninsula, a classification scheme was developed.

Because of their large aggregate acreage and wide distribution, stands of jack pine, red pine, and mixed stands would be delineated; but white pine, which represents less than 1 percent of the forest land, would not be separated out. Lowland conifers, because of their small total acreage and tendency to form highly mixed stands, were grouped into a single category.

The resulting classification scheme utilizes portions of both Level IV and Level III of the Michigan Land Cover/Use Classification System (3). This classification is also compatible with the major forest types and subtypes used by the U.S.D.A. Forest Service in conducting the Forest Survey (1).

To faciliate interpretation and mapping functions, a pin-registered overlay system was utilized. For each test site, a base map was constructed from U.S. Geological Survey topographic maps. These maps, at a scale of approximately one inch to the mile, were registered, via punched holes aligned by a metal pin bar, with the "ground truth" maps and the Landsat interpretation maps. This system permitted precise overlaying and com-

Figure 3. Portion of Landsat false color composite E-2443-15415, April 6, 1976.

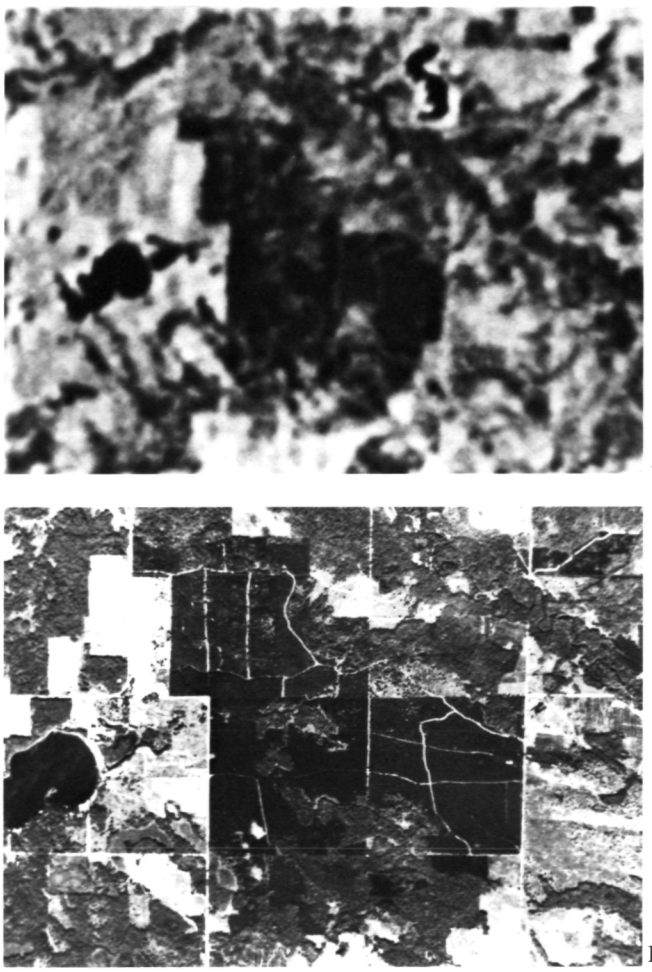

A

B

Figure 4. Landsat false color composite (A) and NASA high-altitude color infrared aerial photograph (B) showing several large pine plantations.

Table 1. Landsat classification performance, Wexford County test site.

Known Cover Type	Number of Sample Points Classified as — (a) Red Pine	Jack Pine	Pine Mixtures	Swamp Conifers	Non-Forest	Cover Type Total
Red pine	*774*	8	130	26	103	1,041
Jack pine	31	*391*	17	10	48	497
Pine mixtures	71	7	87	9	13	187
Swamp conifers	16	2	0	*143*	36	197
Non-forest	57	3	36	89	*2,590*	2,775
Total	949	411	270	277	2,790	*4,697*
Percent correct (b)	82	95	32	52	93	85 (c)

(a) Values along the diagonal represent correctly delineated and identified cover types.

(b) Ratio of diagonal value to the total count of that cover type as interpreted from the Landsat scene.

(c) Overall classification accuracy; ratio of the sum of diagonal values to the total number of sample points.

Table 2. Landsat classification performance, Crawford County test site.

Known Cover Type	Number of Sample Points Classified as — (a) Red Pine	Jack Pine	Pine Mixtures	Swamp Conifers	Non-Forest	Cover Type Total
Red pine	*23*	38	0	1	16	78
Jack pine	9	*1,500*	18	18	33	1,578
Pine mixtures	0	23	*33*	11	10	77
Swamp conifers	0	125	1	*398*	19	543
Non-forest	2	301	1	222	*307*	833
Total	34	1,987	53	650	385	*3,109*
Percent correct (b)	68	75	62	61	80	73 (c)

(a) Values along the diagonal represent correctly delineated and identified cover types.

(b) Ratio of diagonal value to the total count of that cover type as interpreted from the Landsat scene.

(c) Overall classification accuracy; ratio of the sum of diagonal values to the total number of sample points.

parison of two or more of the separate maps.

Prior to actual photo-interpretation, the two interpreters were given preliminary training, including the development of photo-interpretation training aids (Figure 5). These photo keys were prepared to illustrate the appearance of the different coniferous forest types on Landsat false-color composites. Additional training consisted of the systematic comparison of several examples of each forest type on high-altitude color infrared photography and on the Landsat color composite, coupled with specifically gathered forest stand inventory measurements.

The intrepretation entailed the enlargement of the Landsat color composite on a precision rear projector. Magnification was controlled by matching the enlarged Landsat scene to the previously prepared base map, and then replacing the base map with a blank sheet of polyester film. Utilizing the previous photo comparisons and photo keys, the interpreters identified and delineated the boundaries of all coniferous forest stands.

Tone, and in some cases, texture were the main interpretation criteria for the pine classes. Proximity to stream courses and water bodies were an additional aid in distinguishing between upland pine types and lowland swamp conifers.

To evaluate the accuracy of the visual interpretation procedure, the Landsat interpretations were compared with previously compiled cover type maps. These were prepared specifically for this project and were constructed from photo interpretation of medium-scale (1:24,000) color infrared photography. Additionally, both U.S.D.A. Forest Service and Michigan Department of Natural Resources (DNR) forest cover type maps were consulted in conjunction with ground verification by field crews.

Results

All errors in each Landsat interpretation map were identified by superimposing these maps on the cover type maps using the pin-registration system. In effect, a third, or composite, map resulted (Figure 6); which was used to categorize misclassified stands and determine accuracy of agreement.

The classification proceeded as follows, using as an example the stands in Figure 6: stands numbered 1 through 5 were correctly delineated and identified as to species; stands numbered 6 and 8 were correctly delineated, but misclassified as to species; stand number 7 represents a commission type error (i.e., a stand was delineated where, in fact, none existed); and stand number 9 represents an omission type error (i.e., the stand was not included in the delineation). The area of each of these stands was measured using a 160 dot/inch^2 grid and the results summarized in contingency tables (Tables 1 and 2).

These two-way cross-tabulations permit the results to be viewed from two approaches. By reading across a row, one may observe which categories, and to what degree of accuracy, a particular cover type was delineated. By reading down a column, one may observe the actual cover types composing each Landsat classification. For discussion purposes, accuracy was summarized as the ratio (expressed as a percent) of correctly delineated and classified stands to the total count of that cover type as interpreted from the Landsat scene.

Table 1 summarizes the Landsat interpretation accuracies for the Wexford County test site, which had an overall classification accuracy of 85 percent. The high accuracies obtained for both red and jack pine are probably a direct result of their high stocking levels and frequent occurrence in pure plantations.

Mixed plantations, where neither species represents more than 75 percent of the stocking, were consistently misclassified. Further investigation revealed that two-

LANDSAT SCENE 2443-15421
April 9, 1976
Oceana County, Michigan
T 16 N - R 15 W

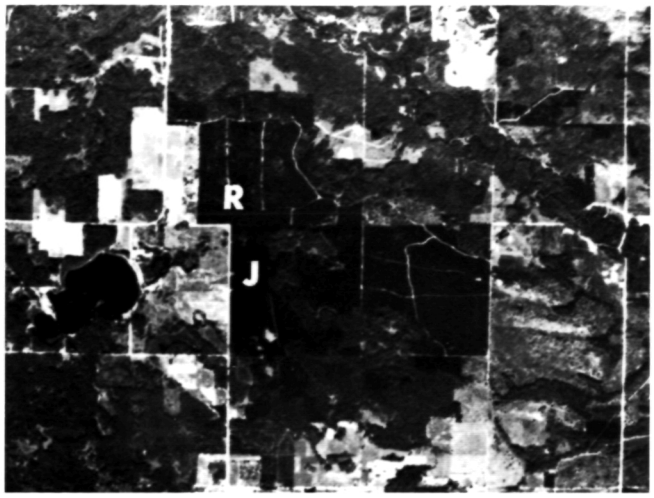

HIGH ALTITUDE COLOR IR
September 15, 1972
Classifications: R - Red Pine
J - Jack Pine
The high-altitude photo coverage is outlined on the Landsat photo.

DESCRIPTION

RED PINE		JACK PINE	
Stocking:	200 sq. ft. B.A./A	Stocking:	140 sq. ft. B.A./A
Av. d.b.h.:	7.3 in.	Av. d.b.h.:	7.0 in.
Av. ht.:	39 ft.	Av. ht.:	28 ft.

Figure 5. One of several photo interpretation training aids prepared to show coniferous forest types on high-altitude and Landsat photography.

thirds of these errors were accounted for by commission and omission errors to the red pine type. Additional cross checks confirmed that the majority of errors in the pine types were due to misclassifications among the several pine species.

Accuracies obtained without considering the within-pine variability, that is, utilizing a "pooled" pine category, shows that pines were correctly interpreted 93 percent of the time.

The swamp conifer type was correctly delineated and classified with approximately 73 percent accuracy. The lower reported accuracy (52 percent) resulted from a large commission type error. Upon examining the medium-scale photography, the majority of these errors occurred with swamp areas dominated by lowland brush and/or lowland hardwood species. Further "lumping" of species was attempted and indicated that forest land as a single category was interpreted with 90 percent accuracy.

Table 2 summarizes the Landsat interpretation accuracies for the Crawford County test site. The lower accuracies for both red and jack pine may be caused by their lower stocking levels, with many stands grading into non-forest categories (i.e., less than 25 percent stocked). The various forest types encountered at this site exhibited less contrast than those at the Wexford County site. Most errors in the pine categories occurred among the various

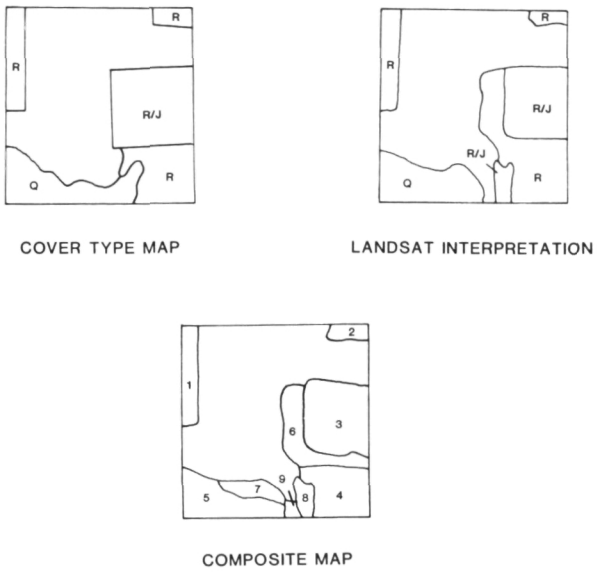

Figure 6. Method of comparing Landsat results with existing cover. Area shown is one square mile from the Wexford County test sites.

pine types, and in recognizing hardwoods intermixed with low density pines such as jack pine. Again, "pooling" the pine types increased overall interpretation accuracy to 77 percent for the pine category.

Errors in the swamp conifer type were similar to those found in the Wexford County site. Lowland brush, often with scattered trees, were the most frequently misinterpreted areas, although some confusion between jack pine and swamp conifers did occur. Overall forest/non-forest accuracies, 81 percent, were substantially below those obtained over the Wexford County site.

References

1. Chase, Clarence D., Ray E. Pfeifer and John S. Spencer, Jr. (1970). The growing timber resource of Michigan, 1966. U.S.D.A. Forest Service Resource Bulletin NC-9.
2. Karteris, Michael A., William R. Enslin and Jerry Thiede (1981). Area estimation of forestlands in Southwestern Michigan from Landsat imagery. In "Second Eastern Regional Remote Sensing Applications Conference," NASA Conference Publication 2198.
3. Michigan Land Use Classification and Referencing Committee (1975). Michigan land cover use classification system. Office of Land Use, Michigan Department of Natural Resources, Lansing, Michigan.
4. Myers, W.L., G.R. Safir, A.L. Andersen, D.L. Mokma, E.P. Whiteside, H.A. Winters, R. Rieck, W.A. Malila, J.E. Sarano, T.W. Wagner, J.T. Lewis and J.P. Erickson (1974). Use of ERTS data for a multidisciplinary analysis of Michigan resources. Michigan State University Agricultural Experiment Station Journal No. 7091.
5. Pfeifer, Ray E. and John S. Spencer, Jr. (1966). The growing timber resource of Michigan, Unit 3 — The northern Lower Peninsula. Michigan Department of Natural Resources, Lansing, Michigan.
6. Roller, Norman E.G. and Larry Visser (1980). Accuracy of Landsat Forest Cover Type Mapping in the Lake States Region of the U.S. In "Proceedings 14th International Symposium on Remote Sensing of Environment," San Jose, Costa Rica.
7. U.S. Geological Survey (1977). EROS digital image enhancement system (EDIES) "Fact Sheet." EROS Data Center, Sioux Falls, South Dakota.

Outlying Field Research Stations

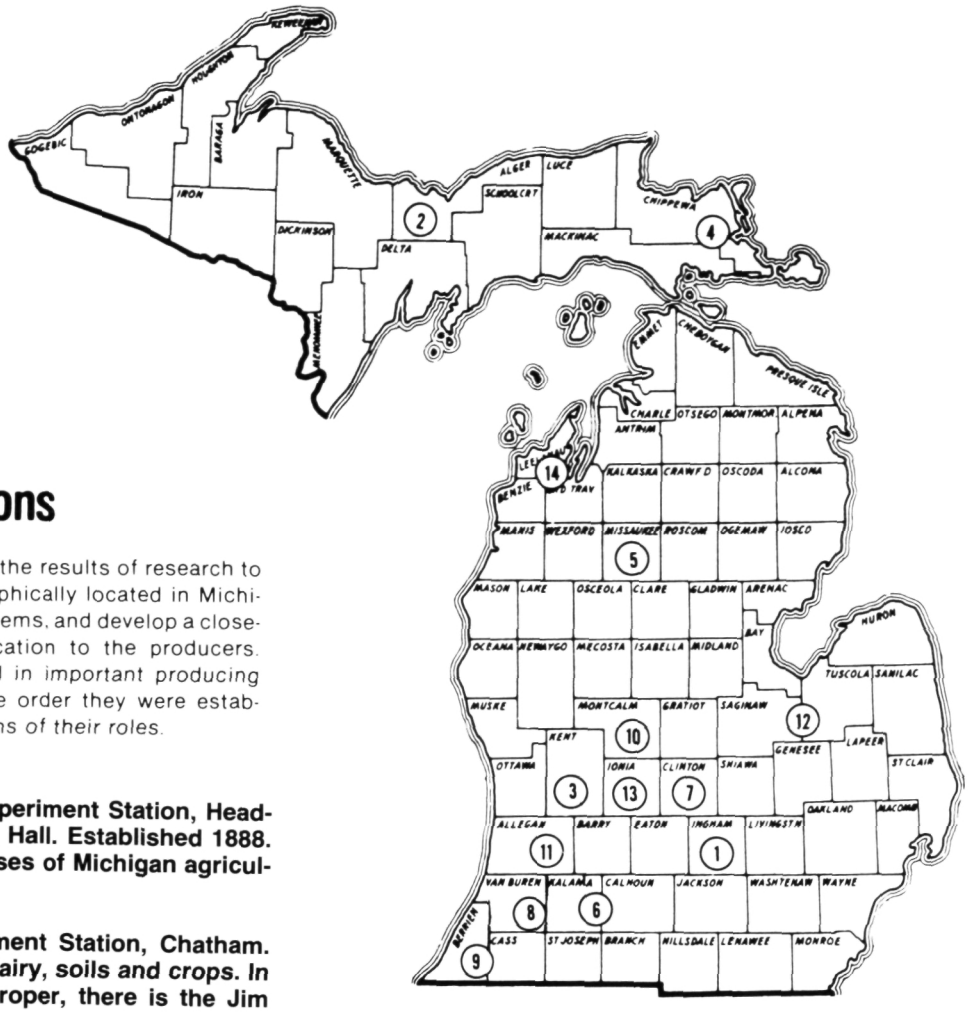

These research units bring the results of research to the users. They are geographically located in Michigan to help solve local problems, and develop a closeness of science and education to the producers. These 14 units are located in important producing areas, and are listed in the order they were established with brief descriptions of their roles.

1. **Michigan Agricultural Experiment Station, Headquarters, 109 Agriculture Hall. Established 1888. Research work in all phases of Michigan agriculture and related fields.**

2. **Upper Peninsula Experiment Station, Chatham. Established 1907. Beef, dairy, soils and crops. In addition to the station proper, there is the Jim Wells Forest.**

3. **Graham Horticultural Experiment Station, Grand Rapids. Established 1919. Varieties, orchard soil management, spray methods.**

4. **Dunbar Forest Experiment Station, Sault Ste. Marie. Established 1925. Forest, fisheries and wildlife management.**

5. **Lake City Experiment Station, Lake City. Established 1928. Breeding, feeding and management of beef cattle and fish pond production studies.**

6. **W. K. Kellogg Biological Station Complex, Hickory Corners. Established 1928. Natural and managed systems: agricultural production, forestry and wildlife resources. Research, academic and public service programs.**

7. **Muck Soils Research Farm, Laingsburg. Plots established 1941. Crop production practices on organic soils.**

8. **Fred Russ Forest Experiment Station, Decatur. Established 1942. Hardwood forest management.**

9. **Sodus Horticultural Experiment Station, Sodus. Established 1954. Production of small fruit and vegetable crops. (land leased)**

10. **Montcalm Experimental Farm, Entrican. Established 1966. Research on crops for processing with special emphasis on potatoes.**

11. **Trevor Nichols Experimental Farm, Fennville. Established 1967. Studies related to fruit crop production with emphasis on pesticides research.**

12. **Saginaw Valley Beet and Bean Research Farm, Saginaw. Established 1971, the farm is owned by the beet and bean industries and leased to MSU. Studies related to production of sugar beets and dry edible beans in rotation programs.**

13. **Clarksville Horticultural Experiment Station, Clarksville. Purchased 1974. First plots established 1978. Research on all types of tree fruits, small fruits, vegetable crops and ornamental plants.**

14. **Northwest Michigan Horticultural Experiment Station, Traverse City. Established 1979. Research and education for cherry and other horticultural crops in northwest Michigan.**

4-83 — 2.5M — File 24.2

A TWO-STAGE CROSS-CORRELATION APPROACH TO TEMPLATE MATCHING*

A. Goshtasby, S.H. Gage, and J. F. Bartholic
Michigan State University

Abstract: Two-stage template matching with sum of absolute differences as the similarity measure has been developed by Vanderburg and Rosenfeld [1,2]. This correspondence shows the development of two-stage template matching with cross-correlation as the similarity measure. The threshold value of the first-stage is derived analytically and its validity is verified experimentally. It is shown that considerable speed-up over the one-stage process is obtainable by introducing only a small false alarm probability.

Index terms: Cross-correlation, two-stage template matching, Fisher's Z-transform, fast Fourier transform, order statistics of correlated normal variables.

I. INTRODUCTION

Template matching is the process of locating the position of a subimage inside a larger image. The subimage is called the template and the larger image is called the search area. The template matching process involves shifting the template over the search area and computing the similarity between the template and the window in the search area over which the template lies. The next step is determining the shift position where the largest similarity measure is obtainable. This is the position in the search area where the template is most likely to be located.

* This work has been supported in part by NASA Grant NGL-23-004-083.

Major similarity measures which are used in template matching are the sum of absolute differences and the cross-correlation coefficient. Sum of absolute differences is a measure which is computationally fast and algorithms are available which make the template search process even faster [3]. The method of assessing similarity by the correlation coefficient measure on the other hand is more accurate [4], but is computationally slow.

Two-stage template matching is one method to increase the speed of the search process. In the first stage, a subtemplate is used to determine the good candidates for a match by determining those shift positions which result in a similarity measure above a threshold value. In the second stage, using those good candidates, the whole template is used to determine the best match position.

The difficulty in the two-stage template matching is the determination of an accurate threshold value during the first stage. If the threshold value is too low, the search process becomes slow. If the threshold value is too high, the optimal match position might be missed. In this correspondence, we derive the threshold value of the first stage, using the subtemplate size and the false alarm probability.

II. TEMPLATE MATCHING WITH CROSS-CORRELATION

The cross-correlation coefficient between two windows f and g of size NxN is defined by

$$r=\frac{\sum_{x=0}^{N-1}\sum_{y=0}^{N-1} f(x,y)\,g(x,y)}{\{\sum_{x=0}^{N-1}\sum_{y=0}^{N-1} f(x,y)^2 \sum_{x=0}^{N-1}\sum_{y=0}^{N-1} g(x,y)^2\}^{0.5}}$$

where $f(x,y)$ and $g(x,y)$ are pixel values at locations (x,y) of f and g, respectively. It is assumed that f and g are normalized so that they have a mean of zero. The value of r changes between -1 and +1 and the closer r is to +1, the more similar the two windows would be.

When the search area is MxM and the template size is NxN (N<M), we have to compute r for every shift position (which is $(M-N+1)^2$ shift positions).

$$r(u,v) = \frac{\sum_{x=0}^{N-1}\sum_{y=0}^{N-1} f(x,y)\,g(x+u,y+v)}{\{\sum_{x=0}^{N-1}\sum_{y=0}^{N-1} f(x,y)^2 \sum_{x=0}^{N-1}\sum_{y=0}^{N-1} g(x+u,y+v)^2\}^{0.5}} \qquad (1)$$

$u,v=0,1,2,\ldots M-N$

Among all the computed r's, the one with the largest value shows the cross-correlation coefficient for the best match.

The computational complexity of (1) involves computation of $\sum_{x=0}^{N-1}\sum_{y=0}^{N-1} f(x,y)^2$ which is computed once, $\sum_{x=0}^{N-1}\sum_{y=0}^{N-1} g(x+u,y+v)^2$ which if the squares of pixels in the search area are computed once, for the new shift positions, the corresponding squared pixels can be used. By this, the computation time of the denominator turns out to be negligible with respect to that of the numerator, which involves $N^2(M-N+1)^2$ additions and

$N^2(M-N+1)^2$ multiplications.

The computation time, for a search area with M=32 and Template with N=16 on a PDP 11/34 computer (where real addition time = 60 micro sec and real multiplication time = 85 micro sec) is 10.7 sec.

We know that an operation like

$$\sum_{x=0}^{N-1}\sum_{y=0}^{N-1} f(x,y)\,g(x-u,y-v) \qquad (2)$$

is a convolution operation and can be replaced by $FT^{-1}\{FT(f)\,FT(g)\}$. Where FT is the Fourier transform operation and FT^{-1} is the Fourier inverse transform operation and f and g are square windows with dimensions of a power of 2. The dimensions of f and g must be equal. If they are not, by appending the necessary number of zero rows and zero columns to the smaller window they are made equal.

If we compare the numerator of equation (1) to (2), we see that they are similar except for a change in sign. The numerator of (1) can be replaced by

$$FT^{-1}\{FT(f)\,FT^{*}(g)\} \qquad (3)$$

where * means the complex conjugate and takes care of the sign change in the numerator of (1) which is + instead of -. Since Fourier transforms and Fourier inverse transforms can be computed by the fast Fourier transform (fFt) algorithm, the computation time of (1) can be reduced considerably [5].

The computational complexity of operation (3) is $3M^2\log_2 M$ complex multiplications and $3M^2\log_2 M$ real additions or $12M^2\log_2 M$ real multiplications and $3M^2\log_2 M$ real additions. When M=32, computation time = 6.2 sec. We see the computation time is reduced. But still, the template search using the cross-correlation method is costly. However applying the two-stage template matching idea, we will see that increased speed is attainable.

III. TWO-STAGE TEMPLATE MATCHING

The principle idea behind the two-stage template matching method is to use a subtemplate to find the possible positions for a match and not to invest time on those positions where there is no evidence for a match. Once this is accomplished the objective is to find the best match position among the possible ones. In [1], a subarea of the template is used as the subtemplate, while in [2], a reduced resolution template is used as the subtemplate, in the first stage. We take the subtemplate to be a set of n randomly selected data points from a template with N^2 data points, in the first stage.

Two-stage template matching using the sum of absolute differences has resulted in reduced computation time. We will show that the cross-correlation coefficient as the more accurate similarity measure can also be used to reduce computation time, by introducing only a small false alarm probability.

IV. THRESHOLD ESTIMATION

Let the search area size and the template size be MxM and NxN, respectively. Then the number of positions where the template should be shifted in the search area to find the best match position is $k=(M-N+1)^2$. Since our subtemplate is a randomly selected set of n data points from the template, for a given shift position i (i=1, . . k) by selecting a random sample, we obtain correlation coefficients r_i. We assume that the data points in the template and the data points in the search area over which the template lies at a given shift position i, have normal distributions and their true correlation coefficient is ρ_i. Then at a given shift position i, r_i has a nearly normal distribution as long as its expected correlation coefficient ρ_i is near or equal to zero and the sample size, n, is large [6].

However, we wish to determine the shift position which gives the largest correlation coefficient, and the distribution of r_i when ρ_i is large is far from normal [6]. r_i can be transformed by the Fisher's Z-transfrom as below.

$$z_i=0.5\{\log_e(1+r_i) - \log_e(1-r_i)\} \qquad (4)$$

Now whatever the value of ρ_i, z_i are nearly normally distributed with mean ζ_i and variance $1/(n-3)$ even with sample size as small as 8 data points [6]. Where $\zeta_i=0.5\{\log_e(1+\rho_i)-\log_e(1-\rho_i)\}$.

Now let $Z_1, Z_2, \ldots Z_k$ be k normally and independtly distributed chance variables with unknown means $\zeta 1, \zeta 2, \ldots \zeta k$ and common standard deviation $\sigma = 1/\sqrt{n-3}$. Let

$$z_{[1]} < z_{[2]} < \ldots < z_{[k]}$$

denote the ordered z's after applying the observed r's into equation (4). We want to determine the population which has the largest mean.

Gupta [7] has formulated a subset selection procedure which can select a subset of the Z's so as to include the population with the largest mean with a minimum guaranteed probability $(1-\alpha)$. This procedure selects all Z_t such that

$$z_{[t]} > z_{[k]} - d\sigma \qquad (5)$$

where σ is the common standard deviation for the random variables, and d satisfies

$$\int_{-\infty}^{\infty} \Phi^{k-1}(z+d)\,\phi(z)\,dz = 1-\alpha \qquad (6)$$

Φ and ϕ are, respectively, the cumulative distribution function and density function of a standard normal random variable.

Note that formula (5) holds for random variables that are normally and independently distributed. So, we are assuming that data points in each window are normally distributed which is not unrealistic. What about the condition of independency?

Figure 1 shows those positions in the search area that have values equal to $z_{[t]}=z_{[k]}-d\sigma$. Now it may not be unrealistic to assume Z_t and Z_k as being independent because they are far apart and that we are using only a subset of the data from the two windows in computation of the z's.

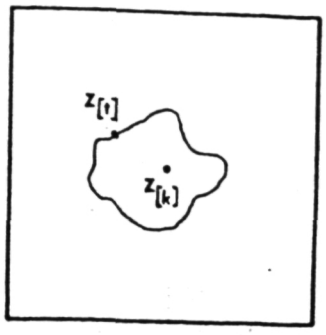

Figure 1. The line showing positions with values equal to $z_{[t]}$, in the search area.

A window which is near the window at $z_{[k]}$ may correlate with the window at $z_{[k]}$ but the fact is, those windows which are near $z_{[k]}$ will fall above the threshold value anyway and it doesn't matter if they correlate or are independent of the window at $z_{[k]}$.

Table of values for d are available for k=1, . .15 and α=0.100, 0.050, 0.010 in [7]. For other values of k and α, d can be computed directly from (6) by numerical methods [7].

To summarize, we determine the threshold value as below.

1. Compute r_1, r_2, . . r_k, using the subtemplate in the first stage (there is no need to order them).

2. Find $r_{max}=\max_i r_i$.

3. Compute $z_{[k]}=0.5\{\log_e(1+r_{max})-\log_e(1-r_{max})\}$.

4. Knowing $z_{[k]}$, compute $z_{[t]}$ from equation (5) for the given α and $\sigma = 1/\sqrt{(n-3)}$, where n is the number of data points in the subtemplate.

5. knowing $z_{[t]}$ inversely solve equation (4) for $r_{[t]}$.

$$r_{[t]} = \{\exp(2z_{[t]}) - 1\} / \{\exp(2z_{[t]}) + 1\}$$

6. $r_{[t]}$ is the threshold value and any position in the search area which has a correlation value larger than $r_{[t]}$ in the first stage, should be tested in the second stage.

V. RESULTS

To measure the performance of the two-stage template matching with cross-correlation and to verify the validity of the estimated threshold values, the following experiments were conducted. Heat Capacity Mapping Mission (HCMM) day-visible and day-IR data acquired on 26 Sept. 79 for an area over Michigan (Scene id: A-A0518-18110) were used (Figure 2). A 32x32 window from an area over Mackinaw city was extracted from the day-visible image as the search area, window a of Figure 2.a.

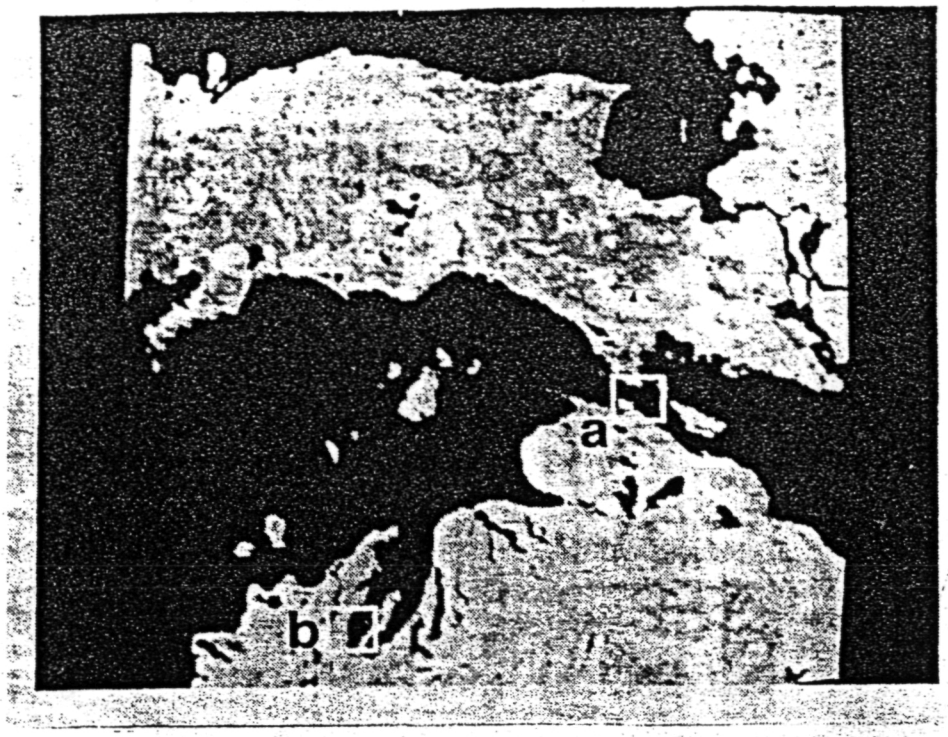

(a)

(b)

Figure 2. (a) Day-visible and (b) day-IR, satellite images of Michigan acquired by HCMM on 26 Sept. 1979 (scene id: A-A0518-18110). Windows a and b were used as the search areas and windows a' and b' were used as the templates.

A 16x16 window was extracted as the template from about the same area in the day-IR image, window a' of Figure 2.b. When using the whole template in the search process, window a' matches best at position (11,1) of window a.

Knowing the best match position, we then carried out the two-stage process for the search area a and window a' using n=16 randomly selected data points from the template as the subtemplate. The experiment was carried out 100 times, each time with different random sample. With false alarm probability α=0.05, 3 false matches were obtained.

Table 1 shows one case out of the 100 experiments. 35 positions have fallen above the threshold value which should be tested in the second stage. In the average, we obtained 34 positions above the threshold that had to be tested in the second stage, for the 100 experiments.

Table 1. Correlation values in the first stage, for search area a shown in Figure 2.a and template a' shown in Figure 2.b. The enclosed positions are those which fell above the threshold value. These positions are the only ones which should be tested in the second stage. The correst match is known to be at (11,1).

CORRELATION COEFFICIENTS IN THE FIRST STAGE

	0	1	2	3	4	5	6	7	8	9	10	11	12	13	14	15	1
0	-0.42	-0.47	-0.60	-0.53	-0.52	-0.35	-0.43	-0.53	-0.45	-0.41	-0.33	-0.34	-0.24	-0.18	-0.16	-0.26	-0.
1	-0.39	-0.31	-0.40	-0.53	-0.50	-0.35	-0.46	-0.38	-0.53	-0.41	-0.31	-0.40	-0.36	-0.20	-0.17	-0.32	-0.
2	-0.19	-0.40	-0.35	-0.31	-0.39	-0.45	-0.37	-0.36	-0.45	-0.53	-0.44	-0.32	-0.34	-0.33	-0.32	-0.32	-0.
3	-0.05	-0.13	-0.08	-0.01	-0.14	-0.26	-0.40	-0.31	-0.35	-0.42	-0.43	-0.25	-0.23	-0.34	-0.31	-0.28	-0.
4	0.13	0.17	0.30	0.24	0.11	0.11	-0.00	0.05	0.02	-0.03	0.02	-0.01	0.03	-0.13	-0.09	-0.20	-0.
5	0.31	0.29	0.31	0.26	0.24	0.25	0.13	0.11	0.11	0.18	0.11	0.19	0.05	0.04	-0.01	-0.01	-0.
6	0.46	0.30	0.27	0.30	0.24	0.16	0.15	0.15	0.14	0.09	0.11	0.13	0.02	-0.02	-0.00	0.01	-0.
7	0.47	0.40	0.44	0.30	0.16	0.16	0.14	0.23	0.12	0.09	0.07	0.12	0.03	-0.06	-0.08	0.01	-0.
8	0.63	0.62	0.52	0.51	0.33	0.26	0.24	0.31	0.21	0.11	0.10	0.06	-0.01	0.08	-0.07	-0.07	0.
9	0.75	0.77	0.65	0.60	0.49	0.37	0.31	0.28	0.19	0.11	0.02	0.08	0.11	0.05	-0.03	0.07	-0.
10	0.86	0.87	0.79	0.61	0.51	0.37	0.34	0.30	0.21	0.13	0.10	0.14	0.06	0.00	0.11	0.07	-0.
11	0.89	0.94	0.78	0.59	0.32	0.34	0.42	0.32	0.14	0.17	0.11	0.11	0.13	0.09	0.07	0.16	0.
12	0.78	0.87	0.65	0.61	0.58	0.59	0.48	0.47	0.34	0.20	0.11	0.09	0.10	0.16	0.15	0.06	0.
13	0.60	0.60	0.62	0.61	0.73	0.77	0.63	0.54	0.42	0.24	0.12	0.13	0.16	0.12	0.13	0.10	0.
14	0.38	0.58	0.63	0.68	0.73	0.73	0.70	0.55	0.47	0.38	0.25	0.13	0.11	0.13	0.11	0.18	0.
15	0.29	0.39	0.35	0.50	0.61	0.66	0.69	0.60	0.45	0.39	0.40	0.21	0.21	0.20	0.09	0.08	0.
16	0.12	0.30	0.26	0.32	0.48	0.53	0.53	0.55	0.58	0.50	0.32	0.28	0.31	0.33	0.23	0.09	0.

THE THRESHOLD VALUE IS 0.5842

The overall computation time = computation times of stage 1 + stage 2. If we take a random sample of size n to be the subtemplate in the first stage, the computation time of the first stage = $n(M-N+1)^2$ additions $+n(M-N+1)^2$ multiplications. When M=32, N= 16, and n=16, the computation time for the first stage = 0.7 sec.

The computation time for the second stage is a function of the number of points that fall above the threshold value. This depends on the characteristics of the template. If X is the number of pixels which fall above the threshold value in the first stage, then the search of the second stage involves XN^2 additions and XN^2 multiplications. Using X=35 from Table 1, the computation time of the second stage is 1.2 secs. Adding the computation time of the first stage to the computation time of the second stage, we find the overall computation time, which is 1.9 secs. These times are about 1/3 of the time needed by the fFt algorithm and about 1/5 of the time needed by the one-stage approach.

When using this approach, we can take templates of any shape and any size. This is not true for the fFt where the template must be square and the number of pixels in each row or in each column a power of 2.

Another experiment was carried out for search area b of Figure 2.a and template b' of Figure 2.b. With α=0.05 and n=16, 2 false matches were obtained with average number of positions falling above the threshold value to be X=27. Computation time for the secend stage was obtained to be 1.0 secs and the overall computation time = 1.7 secs was obtained.

VI. CONCLUSION

Cross-correlation coefficient is a similarity measure which is widely used in template matching because of its superior accuracy over the sum of absolute differences. It is heavily used in preparation of depth maps [8], and in registration of satellite images [5]. These processes may involve hundreds of template matchings and so they are quite costly. A method to speed up the template matching process with cross-correlation has long been desired.

We have applied the two-stage template matching idea to the template matching with cross-correlation coefficient as the similarity measure and have demostrated reduction in computation time. The threshold value of the first stage was estimated using the subtemplate size and the false alarm probability. The validity of the process was then verified experimentally.

REFERENCES

[1] G. J. Vanderburg and A. Rosenfeld, "Two-Stage Template Matching," IEEE Trans. on Computers, Vol. C-26, No. 4, April 1977, pp 384-393.

[2] A. Rosenfeld and G. J. Vanderburg, "Coarse-Fine Template Matching," IEEE Trans. on Syst. Man, Cybern. Feb. 1977, pp 104-107.

[3] D. I. Barnea and H. F. Silverman, "A Class of Algorithms for Fast Digital Image Registration," IEEE Trans. on Computers, Vol. C-21, No. 2, Feb. 1972, pp 179-186.

[4] M. Svedlow, C. D. McGillem, and P. E. Anuta, "Experimental Examination of Similarity Measures and Preprocessing Methods Used for Image Registration," Symp. Machine Processing of Remotely Sensed Data 1976.

[5] Paul E. Anuta, "Spatial Registration of Multi-Spectral and Multi-Temporal Digital Imagery Using Fast Fourier Transform Techniques," IEEE Trans. on Geoscience Electronics, Vol. GE-8, No. 4, Oct. 1970, pp 353-368.

[6] R. A. Fisher, Statistical Methods for Research Workers, Hafner Publishing Company Inc., New York, 1948, pp 175-210.

[7] S. S. Gupta, "On Some Multiple Decision (Selection and Ranking) Rules", Technometrics, Vol. 7, No. 2, May 1965, pp 225-245.

[8] Martin D. Levine, Douglas A. O'handley, and Gary M. Yagi, "Computer Determination of Depth Maps", Computer Graphics and Image Processing, 1973, Vol. 2, pp 131-150.

Submitted To Journal of Photogrammetric Engineering and Remote Sensing

1983

*POINT PATTERN MATCHING BY SELECTIVE SEARCH**

Ardeshir Goshtasby
Dept. of Computer Science
University of Kentucky
Lexington, Kentucky 40506

&

George C. Stockman
Dept. of Computer Science
Michigan State University
E. Lansing, Michigan 48824

The optimal tranformation parameters for registration of two images can be estimated automatically from control points in a few seconds if the parameter space is searched selectively.

* Data for this work was provided by the Center for Remote Sensing, Michigan State University, East Lansing, Michigan 48824.

Abstract: Algorithms for matching two sets of points in a plane are given. These algorithms search in the parameter space and find the transformation parameters that can match the most points in the two sets. Since exhaustively searching for the best parameters is not affordable as the number of points in the sets become large, a subset selection method is given in order to reduce the search domain. Subsets are chosen as points on the convex hulls of the sets. The algorithms are tested on generated and real data and their performance is compared.

ABSTRACT

AN EVALUATION OF DIGITAL LANDSAT CLASSIFICATION PROCEDURES FOR LAND USE INVENTORY IN MICHIGAN

By

Richard Hill-Rowley

The major research objective of this study was to evaluate the informational value of LANDSAT digital data in the context of providing land use data to users in Michigan. Information on user needs was developed through an extensive survey focusing primarily on land use planners. Land categories were identified and subsequently modified in order to be compatible with processing of LANDSAT data.

Three test sites, each characterized by a distinct land use type (agricultural, urban and forest) were chosen to evaluate LANDSAT performance. For each of these sites LANDSAT data for August 16, 1979 were classified by means of three commonly available algorithms (maximum likelihood, minimum distance-to-means, grouping of cluster classes). Accuracy evaluation of the resulting classifications included examining the effects of generalization for geographic information system formats.

Conclusions derived from the study can be summarized in three major areas. Analysis of land use categories identified by questionnaire responses, in conjunction with limitations imposed by the

Page intentionally left blank

Page intentionally left blank

TABLE OF CONTENTS

RESEARCH report
452 JANUARY 1984
NATURAL RESOURCES
FROM THE MICHIGAN STATE UNIVERSITY AGRICULTURAL EXPERIMENT STATION EAST LANSING

Interpreting Michigan Forest Cover Types From Color Infrared Aerial Photographs

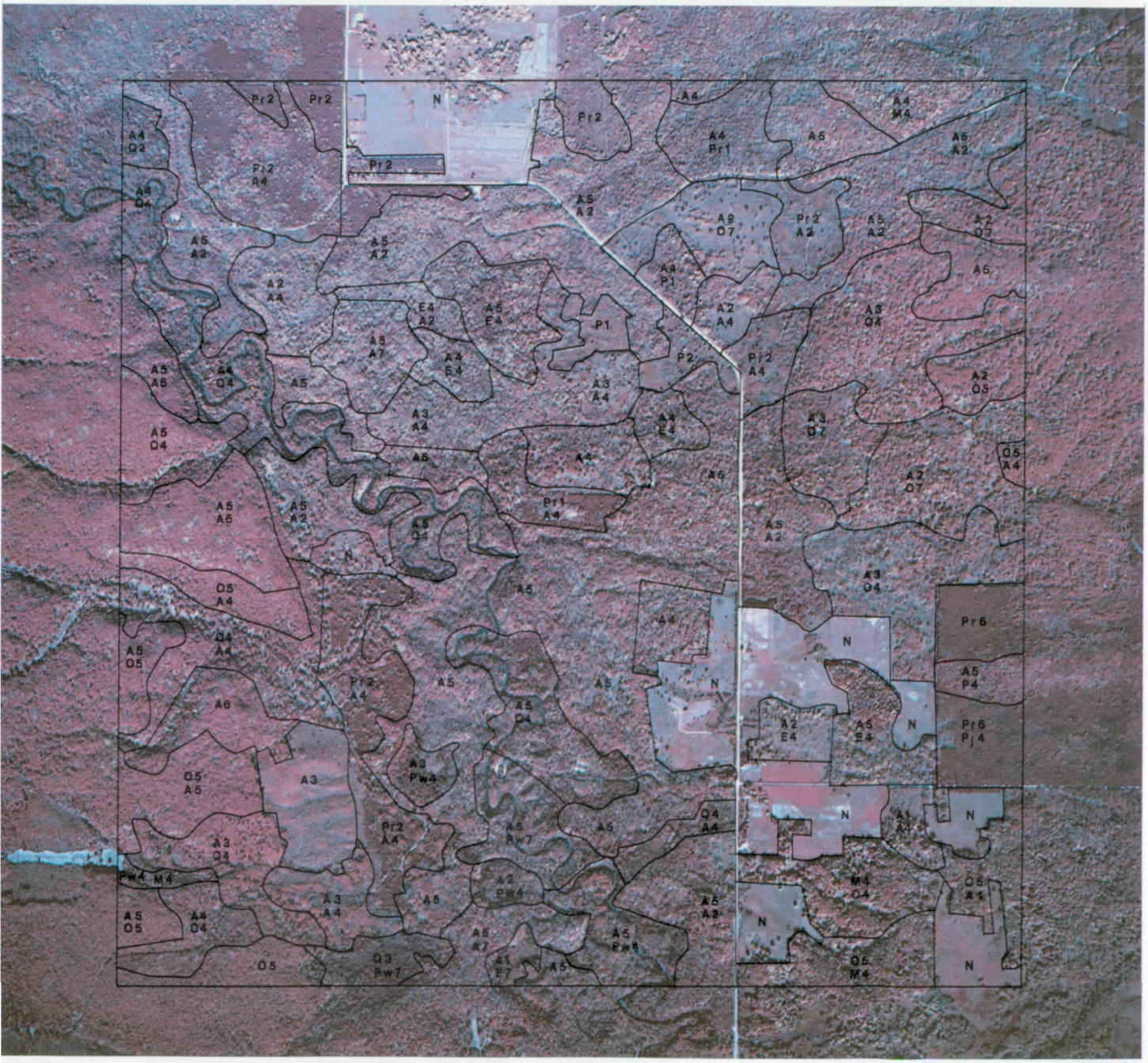

Interpreting Michigan Forest Cover Types From Color Infrared Aerial Photographs

William D. Hudson, Center for Remote Sensing/ Department of Forestry, Michigan State University

This research was supported by a National Aeronautics and Space Administration grant, NASA NGL 23-004-083, to Michigan State University, Center for Remote Sensing.

Introduction

The recognition of forest cover types and individual tree species from aerial photographs often provides needed inventory data with greater accuracy and at lower cost than by ground methods alone. Resource managers (or their staffs) who can extract information from aerial photographs have a powerful tool to aid their information needs.

This publication will provide an introductin to the identification of forest types and tree species from medium scale color infrared aerial photography. The material was originally compiled for use in a short course on the interpretation of color infrared airphotos for forest resource inventories. It was designed to be a practical reference on the techniques of airphoto interpretation and is used to support the lectures and exercises.

While the basic techniques of airphoto interpretation are easily learned, their effective use is normally acquired only by practice. Although considerable training and experience are required before one becomes proficient at delineations, a careful study of the materials in this publication should allow you to begin to make correct interpretations.

Several references exist on species identification that apply to the forests of Michigan. The interpretation of tree species from medium scale (1:15,840 to 1:20,000) panchromatic photography has been covered in Photographic Interpretation of The Species in Ontario (Zsilinszky, 1966). Although it covers tree species in Ontario, most also occur in Michigan. Included are detailed descriptions of identifying features, comparisons of similar species and illustrations of actual photographic stereopairs. Additional work on the forests of Canada, applicable to Michigan forest types, include generalized photo interpretation guides (Sayn-Wittgenstein, 1978) and a series devoted to the recognition of tree species on large scale photos (1:1,000 to 1:3,000) by crown characteristics (Sayn-Wittgenstein, 1960 and 1961).

The use of color aerial photography for identifying certain conifers and hardwoods of the northeastern U.S. has been dealt with by the U.S. Forest Service (Heller, Doverspike and Aldrich, 1964). Interpreting forest types in the Lake States with black-and-white infrared photography (1:12,000 to 1:15,840) is covered in two reports of the U.S. Forest Service (Chase and Korotev, 1947 and Region Nine, U.S. Forest Service, 1947). The latter consists of 49 photographic stereograms illustrating sample forest condition classes and species.

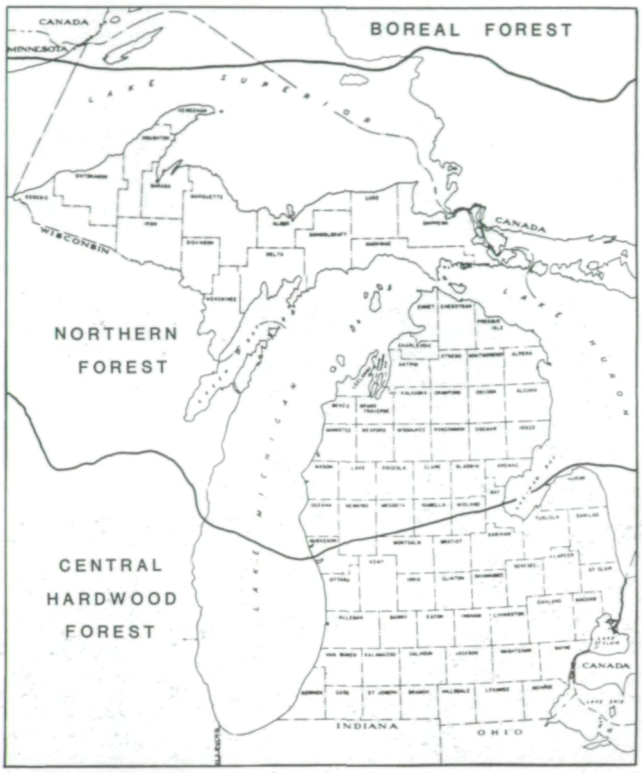

Figure 1. Generalized forest regions in Michigan (individual tree distributions, as compiled by the U.S. Forest Service (Little, 1971 and 1977), are available in the form of tree distribution maps).

The present publication covers interpreting medium scale (1:24,000) color infrared aerial photography for identifying common forest types and tree species of Michigan. This is an extension of a previous effort to develop techniques for mapping forest resources on a county-wide basis (Hudson, Amsterburg and Myers, 1976,).

The characteristics of 17 cover types (13 forest types or tree species and 4 non-forest cover types) and their interpretation are presented. For each type its occurrence is briefly described by forest region (Figure 1) and site requirements are given. Descriptions follow of those attributes of a tree or stand which are helpful when attempting to interpret the type from a vertical perspective. The description of common crown shapes has followed a system (Figure 2) developed by the Canadian

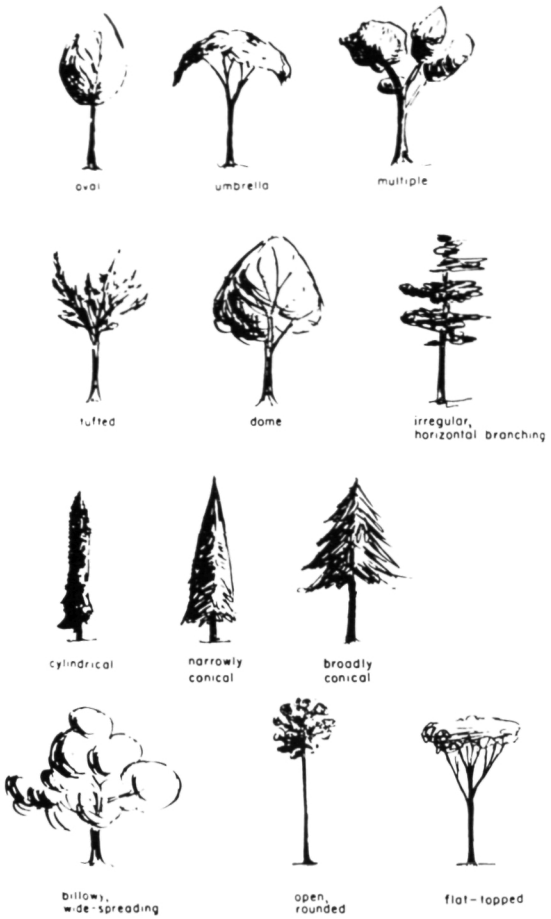

Figure 2. Several common crown shapes (reprinted by permission of the Canadian Forestry Service).

Forestry Service (Sayn-Wittgenstein, 1978). Identification of the forest type or species by using image characteristics (e.g. size, shape, shadow, color, texture, pattern, size or association) is then discussed. Individual types are accompanied by ground photos, sketches and stereograms[1] of "typical" stands.

General knowledge of forest ecology, and thorough knowledge of local environmental conditions, are very important in forest interpretation. With sufficient local experience and data, the interpreter may use phenological phenomena to help distinguish between species and groups. The following events are useful on a given survey: date of leaf flushing, description of immature foliage, date of flowering and fruiting, time of fall coloring, description of fall colors and time of leaf fall (these topics are covered in considerable detail in Sayn-Wittgenstein, 1961b and 1978).

A working knowledge of the ecological and silvicultural characteristics of the species in the area being studied is of great importance in the interpretive process. Knowing site requirements or preferred habitat of species or groupings will often narrow choices or eliminate species. The natural associations of certain species may suggest the presence of a second type, or eliminate the probability of a particular tree species. The tendency of certain species to form characteristic stands (i.e., pure, uneven-aged, coppice stands, etc.) will also be useful in the interpretive process.

[1]Copies of the stereograms, printed on color photographic paper, are available for purchase from the Center for Remote Sensing, 302 Berkey Hall, Michigan State University, East Lansing, MI 48824-1111.

White Pine

White pine[2] occurs throughout the Northern Forest and in portions of the Boreal and Central Hardwood Forest Regions. While more abundant in the Upper Peninsula (U.P.), it is also common in the northern Lower Peninsula. White pine grows on a wide variety of sites in natural stands. More than half of them are located in the western U.P.

White pine occurs as a component of other forest types, either as an overstory or scattered individuals. On moderately well drained, mesic sites, it is associated with sugar maple, yellow birch, beech, basswood and hemlock. On dry sites, such as dunes and outwash plains, it is found with red pine (where it may be a dominant or co-dominant component of the stand), jack pine, red oak, black oak, white birch and quaking aspen. On moist sites,

[2]Scientific names of tree species are given in the Appendix.

Figure 3. White pine illustrating characteristic branching habit.

Figure 4. Mature white pine stand, Allegan State Game Area.

small ridges or mounds in swamps and poorly drained sites, it may occur with white and black spruce, balsam fir, northern white-cedar, quaking aspen and red maple (Barnes and Wagner, 1981.).

In the western U.P., white pine is a frequent component of the northern hardwood, aspen and spruce-fir forest types. In the eastern U.P., it is more commonly found in the cedar, red pine and black spruce forest types. In the northern lower Peninsula, it is a common component of the oak and aspen forest types. White pine is a commonly planted species, though not as common as red or jack pine.

White pine is one of the tallest trees in Michigan and usually has a straight, undivided trunk. Branches along the stem are often large and occur at nearly right angles in a whorl-like arrangement. Those in the upper crown are smaller and sweep upwards (Figures 3 and 4).

When viewed from above, the large horizontal branches are very prominent, giving the crown an irregular star-shaped outline (figures 5 and 6). This distinctive shape is clearly displayed on trees which are over-mature, open-grown, or in mature stands where white pine towers above associated species (area 3 in Figure 58). Young white pines often have nearly conical or pyramidal shaped crowns.

Identification is possible by recognition of a shelf-like pattern displayed by shadows. Color varies from light purple to salmon but is always the "lightest" of the three pines (Figure 7.). Plantation white pine may be distinguished by its color, light brown to salmon, and its "ragged" or "fuzzy" texture, especially as compared to red or jack pine plantations (area 1 in Figure 58).

Figure 5. Schematic diagram of white pine illustrating vertical and horizontal views (Figures 5, 9, 14, 19, 24, 28, 32 and 36 reprinted by permission of the Canadian Forestry Service, from Sayn-Wittgenstein, 1960).

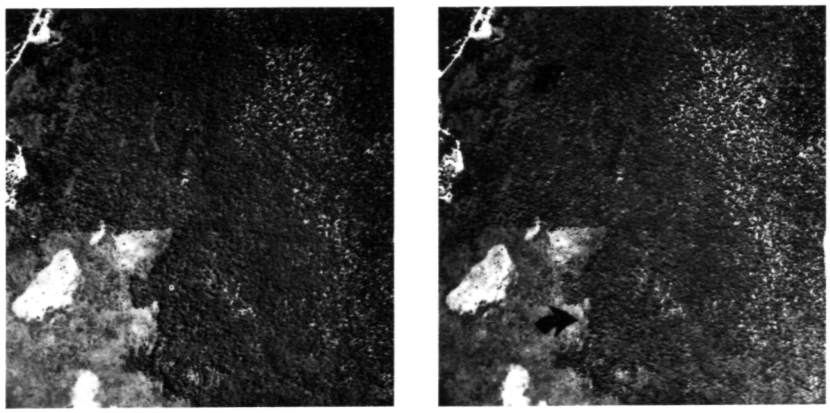

Figure 6. White pine stand, Kalkaska County.

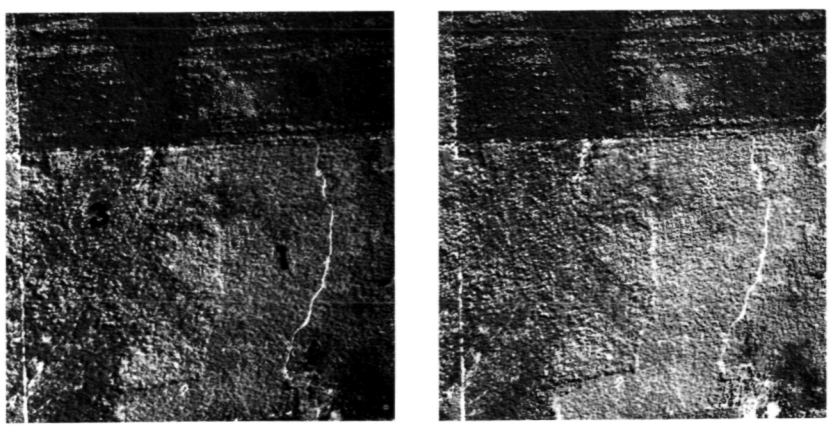

Figure 7. White (1), red (2), and jack pine (3) plantations illustrating relative tonal differences.

Red Pine

Red pine is primarily a tree of the southern Lake States, but does occur farther north with a scattered distribution. It is commonly found on level or gently rolling sand plains throughout the northern Lower Peninsula and portions of the U.P.

Red Pine grows in both pure and mixed stands. Commonly associated species include jack pine, aspen, white birch and northern pin oak on dry sites and white pine, red maple, red oak, balsam fir and white spruce on moist sites. Red pine is a frequent component of the aspen, white pine and jack pine forest types in the western U.P.; the jack pine cover type in the eastern U.P.; and the aspen-paper birch and oak forest types in the northern Lower Peninsula. Red pine is the most extensively planted species in Michigan.

Red pine has a straight, columnar trunk often clear of branches for one-half to two-thirds of its height. Large, horizontal and spreading branches form a broadly-rounded crown which is rather open (Figure 8).

As viewed from above, the crown appears circular, beyond which individual branches rarely protrude (Figures 9 and 10). Red pine may be distinguished by a honeycombed stand pattern and a saw-toothed profile (Zsilinszky, 1966) (Figures 11, 12 and 13). Color will be a reddish-brown or sometimes a light-true-brown, intermediate between white and jack pine. Red pine stands appear more uniform and less "jagged" than stands of white or jack pine (Figures 7, 13 and 58).

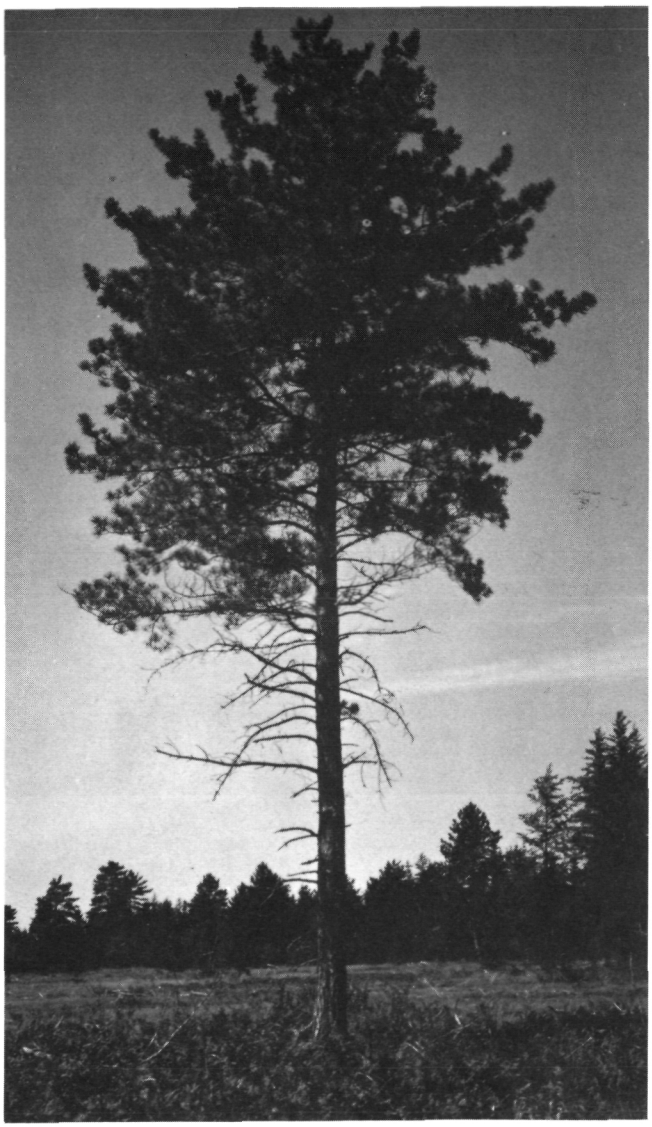

Figure 8. Red pine illustrating straight, undivided trunk and broadly-rounded crown.

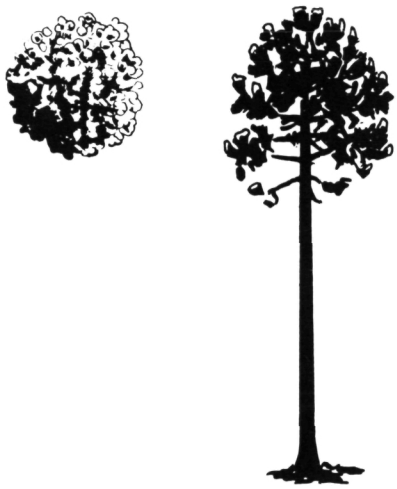

Figure 9. Schematic diagram of red pine illustrating vertical and horizontal views.

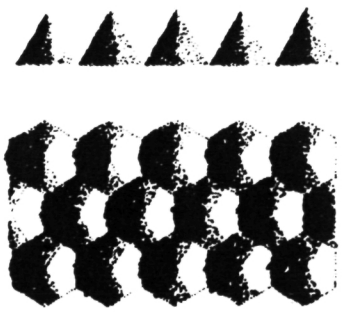

Figure 11. Schematic diagram of the saw-toothed stand profile and honeycomb stand pattern of red pine (reprinted from Zsilinszky, 1966).

Figure 12. Red pine plantation illustrating saw-toothed profile.

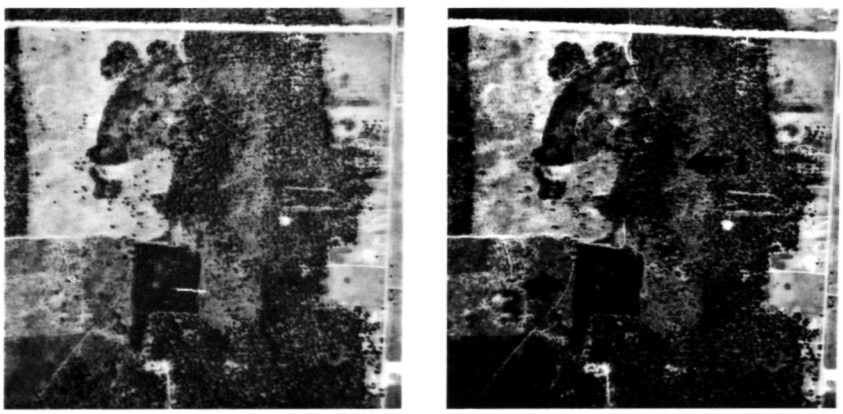

Figure 10. Red pine stands, Montmorency County; 1) natural stand, 2) plantation.

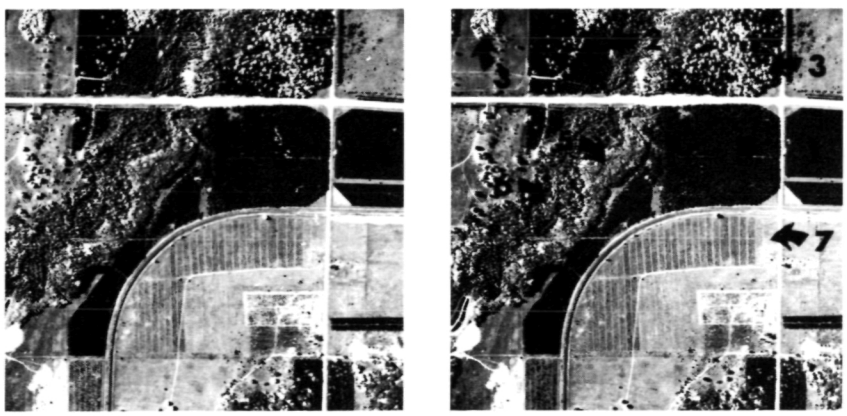

Figure 13. Forest cover types: 1) red pine plantation, 2) northern white-cedar, 3) northern hardwoods, 4) jack pine plantation, 5) aspen, 6) lowland hardwoods and swamp conifers and 7) Christmas tree plantation.

Jack Pine

Jack pine occurs extensively in Michigan, common in both the Boreal and Northern Forest Regions. This species is found on a variety of sites, but is most characteristic of dry, coarse, sandy outwash plains. It occupies large areas of these plains in both the U.P. and central portions of the northern Lower Peninsula.

Common, associated species include: red pine, northern pin oak, black oak and bigtooth aspen. Jack pine is often a component of the oak, aspen and red pine forest types. Farther north, jack pine may occur on more moist, sandy soils near swamps where it may be associated with black spruce and tamarack. Jack pine is a commonly planted species.

Jack pine normally forms a small, narrow crown of short branches with a roughly cylindrical shape (Figures 14 and 15). This is especially true of trees growing in closed stands. When open grown, the crowns tend to be rounded but irregular. When viewed from above, jack pine crowns appear irregularly rounded, fuzzy and relatively small and pointed (Figures 16, 17 and 18).

Pure jack pine stands appear hazy with a somewhat uniform texture, which contrasts with the more ragged appearance of spruce. Jack pine normally appears as a blue-black color, but may tend towards black or blackish-brown. It always has the darkest tone of the three pines (Figure 7). Plantations appear more irregular than red pine, but often more uniform than white pine (Figures 7 and 13).

Figure 14. Schematic diagram of jack pine illustrating a relatively small, pointed crown.

Figure 15. Jack pine stand illustrating typical crown shapes.

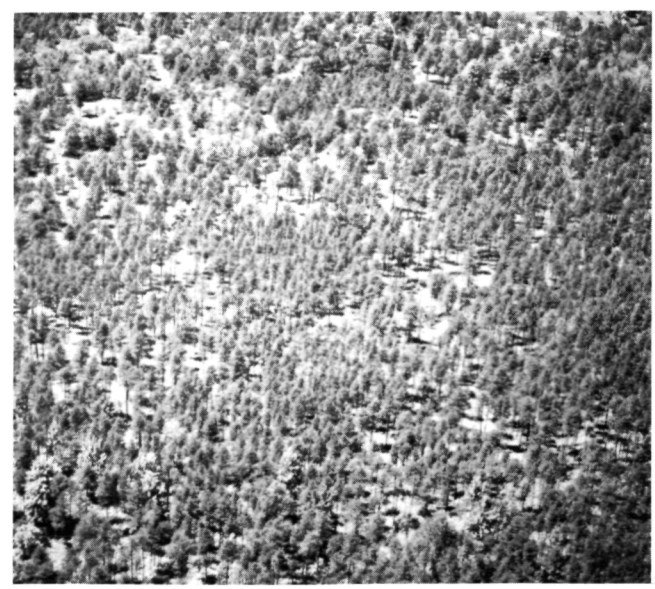

Figure 16. Oblique view of jack pine illustrating fuzzy appearance.

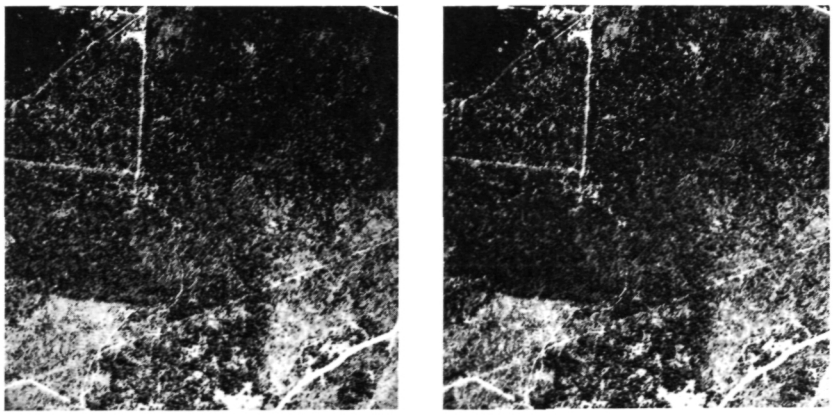

Figure 17. Jack pine stand, Kalkaska County.

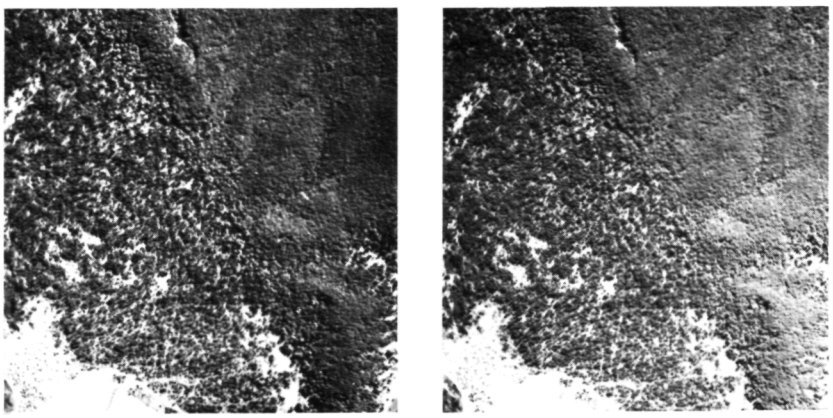

Figure 18. Jack pine stand, Crawford County.

Tamarack

Tamarack is widespread throughout the Boreal and Northern Forest Regions. It reaches the southern limit of its range in the northern portions of the Central Forest Region. It is usually confined there to small, relic stands in bogs and swamps.

In the northern part of its range, the northern Lower Peninsula and especially the eastern U.P., tamarack is a characteristic tree of wetland sites where it is either a pure type or in association with black spruce. On the more productive swamp sites, it may form part of the mixed conifer swamp type, a mixture of northern white-cedar, black spruce, balsam fir and tamarack - - none of which comprises a majority of the stand (Eyre, 1980). On upland sites, associated species include: balsam fir, white birch and aspen.

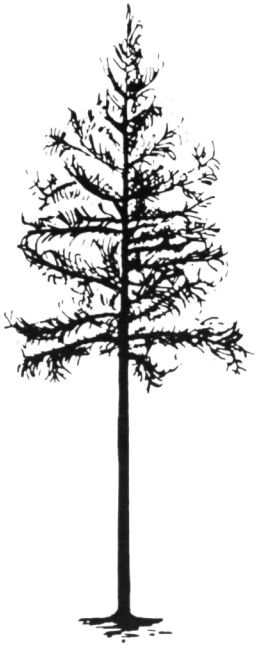

Figure 19. Schematic diagram of tamarack illustrating the characteristic open, pyramidal shape.

Being exceedingly intolerant of shade, tamarack frequently grows in the open or, if growing under forest conditions, it is usually dominant with its crown above the level of the crown canopy.

Tamarack is a medium-sized tree with a straight, undivided trunk. The crown consists of short horizontal branches forming an open, pyramidal shape (Figures 19 and 20).

Tamarack may be identified by its symmetrical, cone-shaped crown and light purplish-blue color (Figures 21 and 67). It is distinguished from black spruce, its common associate, by the somewhat broader crown and lighter color.

Figure 20. Tamarack illustrating typical crown shapes.

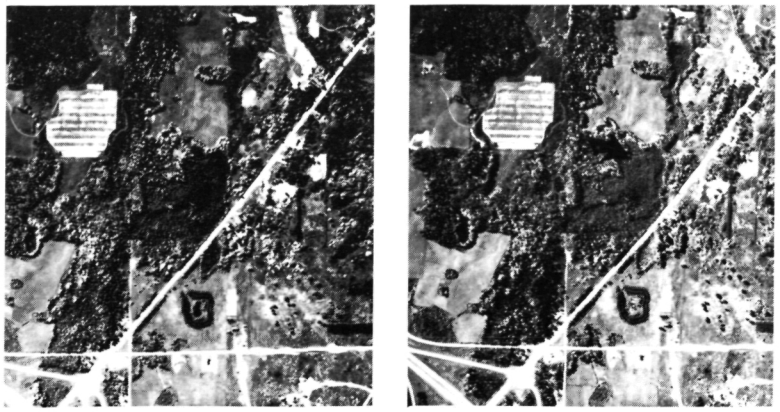

Figure 21. Tamarack, Wexford County.

Spruce-Fir

The spruce-fir forest type, although usually found in the Boreal Forest, occurs in both the Upper Peninsula and the northern Lower Peninsula. Balsam fir is typically the most abundant species of this cover type. White spruce, along with quaking aspen and white birch, are the most frequently occurring associated species.

The type is usually represented by pure stands of balsam fir, and less frequently white spruce, although it occupies a relatively small areal extent. Both species are components of the northern hardwood and aspen forest types in the Upper Peninsula and the cedar and aspen forest types in the northern Lower Peninsula. Balsam fir often occurs as an understory in the aspen and paper birch types. Although found on a variety of sites, this type is typical of mesic to moist conditions.

White spruce is a medium to large tree with a single, straight trunk. The crown is often large, dense and conical. The symmetrical crown forms more of a broader cone than black spruce or balsam fir (Figures 22, 23 and 24).

When viewed from above, spruce-fir stands may be identified by thier symmetrical, broadly conical and pointed crowns (Figures 24, 25 and 26). The type may display an irregular stand profile with a rough, uneven texture. Color will vary, depending on the site, from light brown to a deep purplish magenta (Figures 26 and 27).

Figure 22. White spruce illustrating broadly conical crowns.

Figure 24. Schematic diagram of white spruce (left) and balsam fir (right) illustrating vertical and horizontal views.

Figure 23. Balsam fir illustrating a slender, very symmetrical, cone-shaped crown.

Figure 25. Oblique view of the symmetrical, cone-shaped crowns of balsam fir.

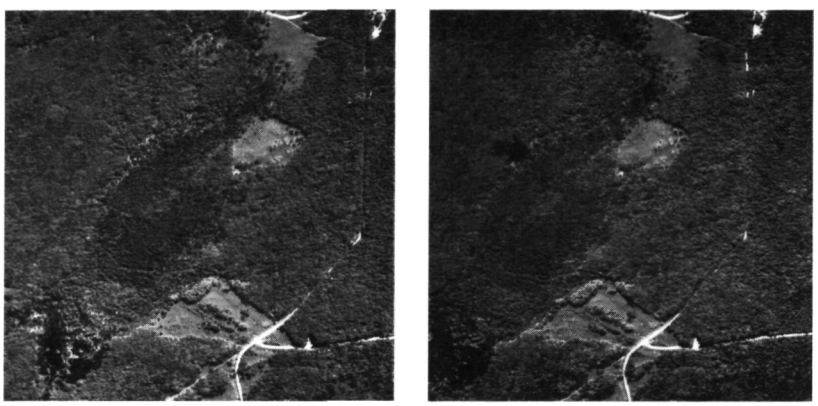

Figure 26. Spruce-fir forest type, Alger County; the surrounding forest type is northern hardwoods.

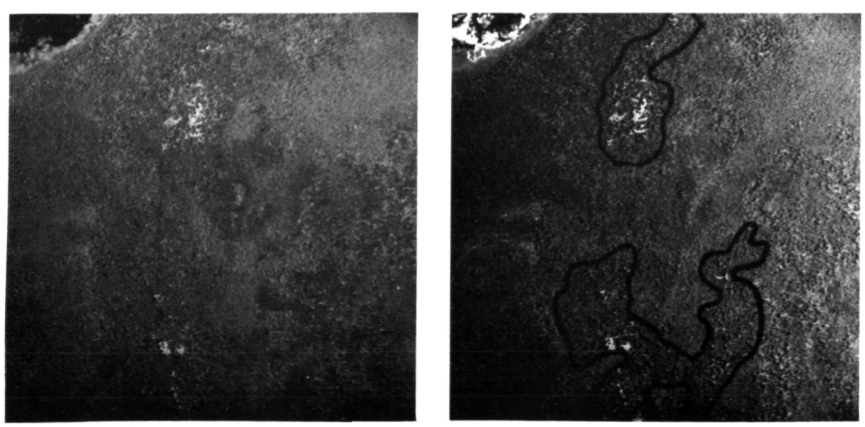

Figure 27. Spruce-fir forest type, Mackinac County.

Black Spruce

The black spruce forest type is fairly widespread and common in the northern part of its range, but is much less common in the southern parts of Michigan, being quite rare in the southern Lower Peninsula. The type grows on organic soils, sphagnum bogs and poorly drained swamps.

Black spruce often occurs in pure stands but may contain white pine, cedar and balsam fir as associated species. Black spruce is also found in the cedar, spruce-fir and aspen forest types in the Upper Peninsula. It may occur as a pure type in the northern Lower Peninsula, being most commonly found in cedar, spruce-fir and mixed conifer swamps.

Black spruce is a relatively small tree, seldom exceeding a height of 60 feet. It has a slender trunk with little taper, supporting a narrow, irregularly conical to nearly cylindrical crown (Figures 28 and 29).

Black spruce is recognized by its slender and almost cylindrical crown which appears fairly smooth (Figure 30). Stands appear quite regular, especially pure stands, with even or gradual changes in height. Color varies from light to dark but is always a bluish-black hue (Figures 43 and 52).

Figure 28. Schematic diagram of black spruce illustrating the narrow, nearly cylindrical crown.

Figure 29. Black spruce illustrating characteristic crown shapes.

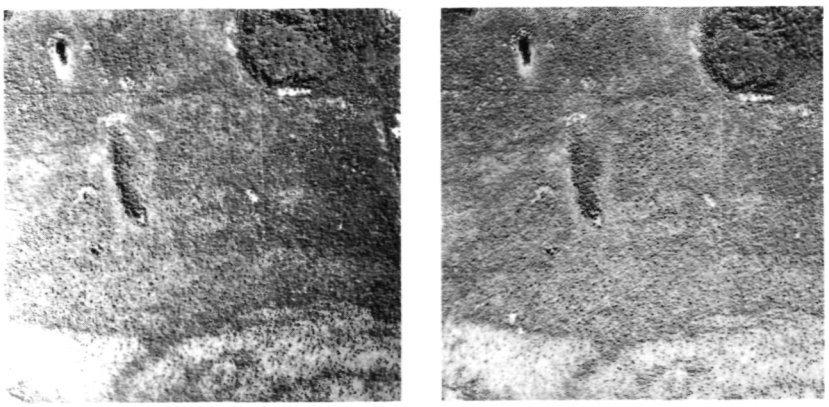

Figure 30. Black spruce stand, Delta County; the broadleaved trees on the higher sites are northern hardwoods.

Hemlock

Eastern hemlock occurs throughout the Northern Forest, but is most common in the western U.P. It occurs to some extent in the northern Lower Peninsula, but is restricted in the southern Lower Peninsula to cool, moist sites. It may form pure stands but is usually found in groups within the northern hardwood forest type. The type prefers moist flats and low-lying areas but is also found on drier sites. Commonly associated species include: beech, sugar maple, red maple and yellow birch.

Eastern hemlock is a large tree with a straight trunk supporting a broadly conical crown (Figure 31). The crown is broader than those of balsam fir and white spruce and has a less apparent taper (Figure 32). When viewed from above, hemlock crowns will appear irregularly rounded and somewhat star-shaped, although not as prominant as white pine (Figures 33 and 34). The type displays a rough texture and appears a deep purple magenta.

Figure 31. Hemlock illustrating the characteristic broadly conical crown.

Figure 32. Schematic diagram of hemlock illustrating a broad crown with little taper.

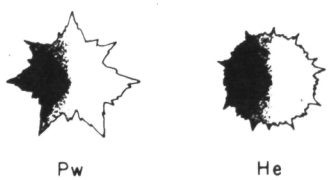

Figure 33. Schematic diagram comparing the crown shapes of white pine (Pw) and hemlock (He), reprinted from Zsilinszky, 1966.

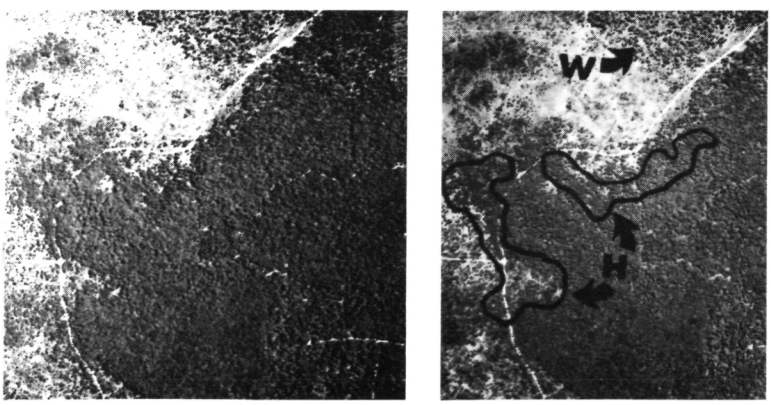

Figure 34. Hemlock (H) and white pine (W) stands, Luce County; the surrounding broadleaved forest is predominantly northern hardwoods.

Northern White-Cedar

Northern white-cedar occurs in the Boreal Forest, but is more common throughout the Northern Forest. It is most common in the eastern U.P. and the northern Lower Peninsula, but does occur in the western U.P. and even into the southern Lower Peninsula. The cedar type is primarily found on organic soils of swamps and along stream borders, but not in stagnant swamps or bogs. It also occurs on limestone uplands, especially adjacent to the Great Lakes.

Northern white-cedar grows in both pure stands and as a component of the mixed conifer swamp type. Commonly associated species include: balsam fir, black spruce, white pine, tamarack, black ash and red maple. Cedar may also form a component of the spruce-fir and lowland hardwood forest types.

Northern white-cedar is normally a small tree which seldom exceeds 50 feet in height. The tapering trunk normally supports a full dense crown, slightly conical, and has a rounded top (Figures 35 and 36). When growing in dense stands, as in a swamp, the individual trees display a variety of shapes and appear more "pointed" than open grown trees (Figure 37).

The cedar type is recognized by the dense, very smooth crown, though not as symmetrical as balsam fir. Stands may appear open with an irregular stand pattern (Figure 38). Cedar is normally a distinctive dark brown-magenta (Figures 58 and 13).

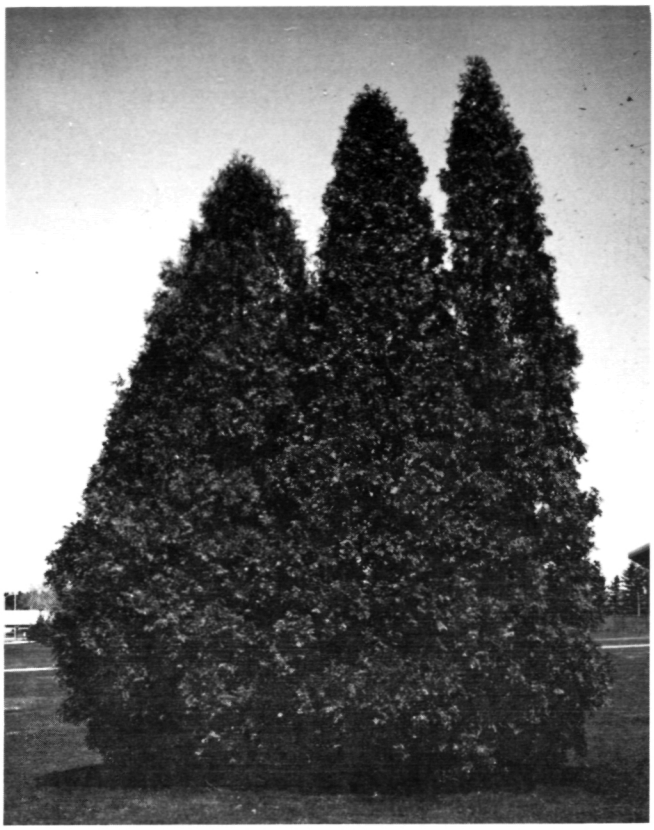

Figure 35. Northern white-cedar illustrating characteristic crown shapes.

Figure 37. Dense stand of northern white-cedar with "pointed" crown tips.

Figure 36. Schematic diagram of northern white-cedar illustrating vertical and horizontal views.

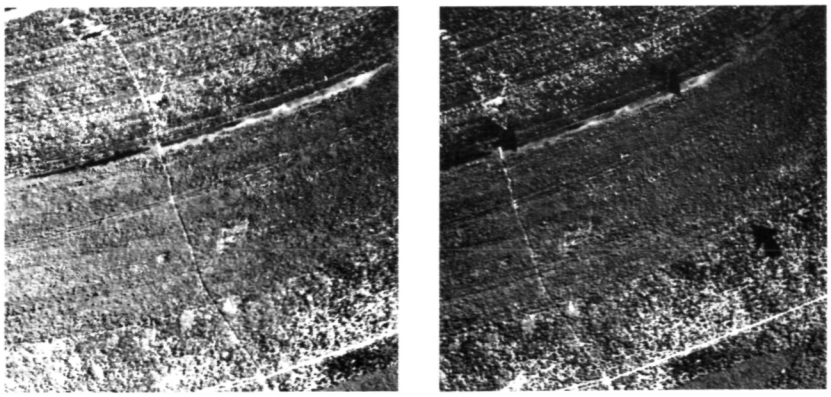

Figure 38. Northern white-cedar, Presque Isle County.

Aspen

The aspen type is very widespread throughout the Northern and Boreal Forests, and is commonly found in the Central Forest. Aspen is very common throughout Michigan, although the largest acreage is found in the northern Lower Peninsula. It is found on most sites except the driest sands and wettest swamps. Trembling or quaking aspen is found on a variety of soils. Bigtooth aspen is restricted to more mesic or dry sites.

Figure 39. Aspen illustrating the characteristic straight trunk and small, somewhat rounded crown.

The most common species found in association with aspen are paper birch, red maple and pin cherry, with balsam poplar often present on wetter sites. Quaking aspen is sometimes a component of the northern hardwoods, spruce-fir and lowland hardwood forest types while bigtooth aspen is commonly associated with both the northern hardwood and oak (especially in the northern Lower Peninsula) forest types.

Both of the aspens have single, straight trunks, with branching mainly confined to the upper reaches of the tree (Figure 39). Since they are intolerant species and occur in even aged stands, aspen displays a uniform stand pattern. Crowns are rounded, small (as compared to the tree's height) and consist of relatively few branches (Figures 40, 41, 42, 43 and 52.). Because of its thin foliage, aspens cast lighter shadows than most other hardwoods.

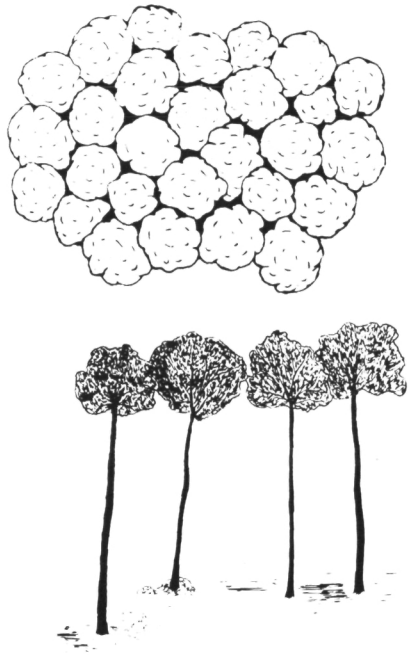

Figure 40. Schematic diagram of an aspen stand illustrating horizontal and vertical views.

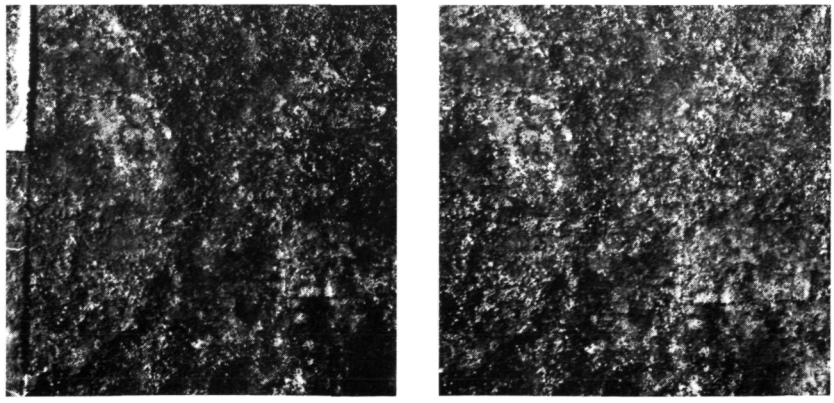

Figure 41. Aspen stand, Wexford County.

The stand structure is very systematic and a high density of stocking (many thousands of trees per acre) produces an unbroken, grainy texture (Figures 43 and 44). The tendency to form clones can result in a stand pattern which appears patchy or "clumpy" with single clones typically 1/10 to an acre in size. The aspen type normally appears a bright red or magenta; fall coloration produces pink and, eventually, white colors. Coloration may be patchy whenever clonal grouping is present.

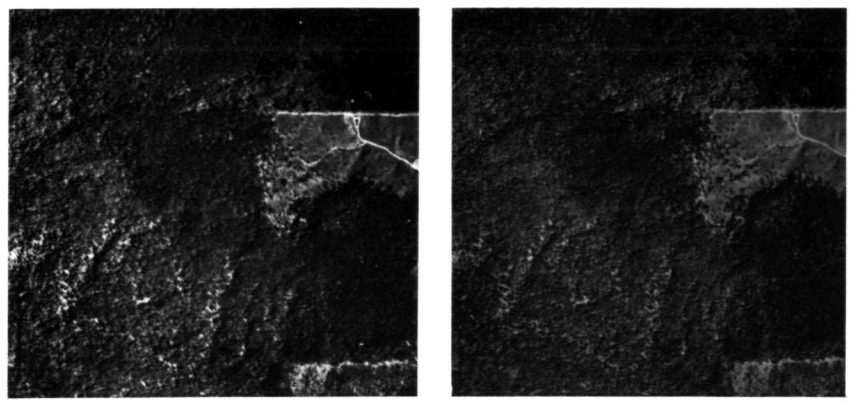

Figure 42. Aspen stand, Montmorency County.

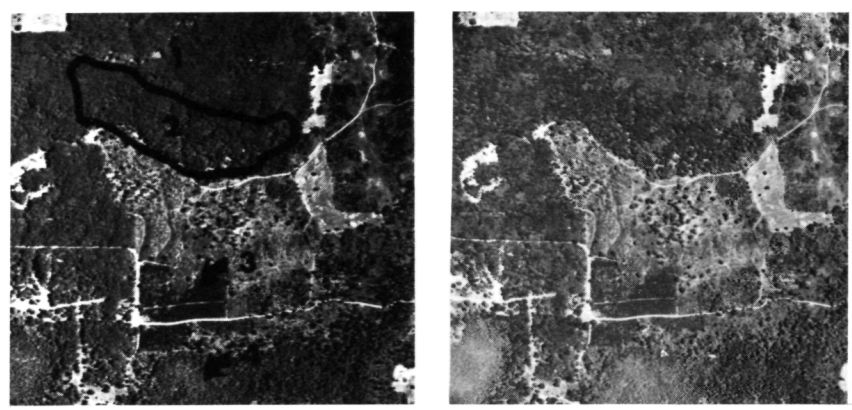

Figure 43. Forest cover types: 1) aspen, 2) oak, 3) red pine plantation and 4) black spruce; the cleared area, between 2 and 3, supports reasonably thick aspen reproduction.

Figure 44. Dense stand of aspen reproduction.

White Birch

White birch is found throughout the Boreal and Northern Forest Regions. In Michigan, it is most common in the northern half, reaching its southernmost limit in the southern Lower Peninsula. White birch grows on a variety of upland sites, and along lake and stream borders and as a pioneer on burned and clear-cut areas.

The type may occur as a pure stand or with the following associated species: quaking aspen, red maple, white pine and balsam fir. White birch is also a component of the northern hardwood, aspen, cedar and lowland hardwood forest types.

White birch has two distinct growth forms: single, straight stems (Figure 45) and multiple, often leaning clumps (Figure 46). Crowns may be ovoid to irregularly rounded and are usually smaller than those of aspen.

When occuring in pure groups or stands, the stand pattern is quite regular and even (Figure 47) or displays a "patchy" pattern due to coppice clumps. White birch appears bright red magenta or occasionally a reddish-pink.

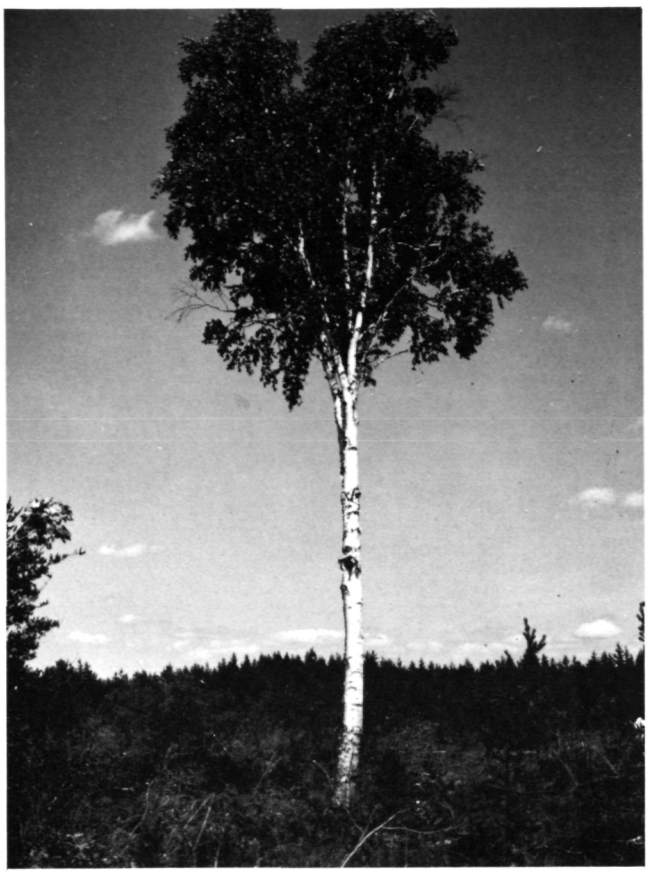

Figure 45. White birch illustrating a single, straight trunk.

Figure 46. White birch illustrating multiple, leaning clump form.

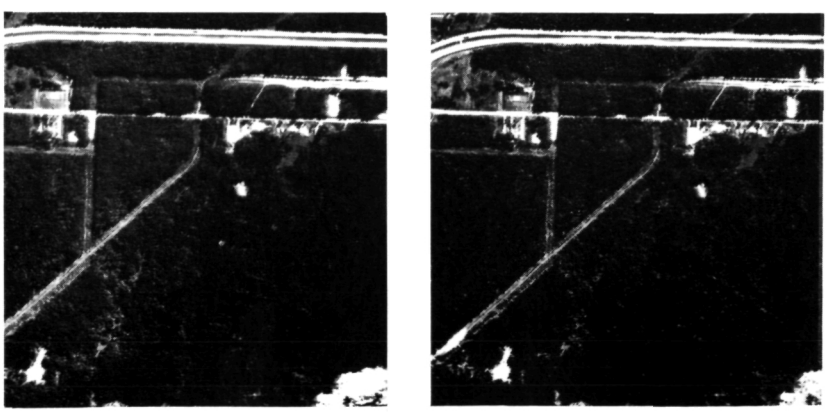

Figure 47. White birch stand, Emmet County.

Oak

The oak forest type is widespread in the Central Forest Region and the southern portion of the Northern Forest Region. Since most oaks reach the northern limit of their ranges in Michigan, the oak forest type is most abundant in southern Michigan. Oaks occur on a variety of sites, but are commonly found on mesic to dry upland soils. The composition widely varies, changing from the oak-hickory associations of the Central Forest in the southern Lower Peninsula, to a northern mixed oak complex, often referred to as "scrub oak," on the outwash plains of the northern Lower Peninsula (Arend and Scholz, 1969).

Principal species include northern red oak, white oak, black oak and shagbark hickory in the south with black oak, northern red oak, white oak and northern pin oak more abundant in the northern Lower Peninsula. Northern and central hardwoods are commonly associated species on the better sites, whereas red maple, aspen and jack pine are associates on the more droughty sites. The oak species also occur as components of both the northern hardwood and aspen forest cover types.

Most oaks are medium to large trees with straight trunks supporting a few large, spreading branches. The crowns are large to massive and relatively broad when compared to the trees' height (Figure 48). The larger branches are somewhat ascending, and the overall crown solid and somewhat round-topped (Figure 49).

Figure 48. White and Black oaks illustrating broad, spreading crowns.

Figure 49. Black oak illustrating ascending branches and round-topped crown.

Oak stands are recognized by their broad, solid crowns, even stand pattern and rounded or wavy texture (Figures 43, 50, 51 and 52). Occasionally a stand will display a rough, somewhat broken texture due to scattered, small openings in the stand. Oaks appear from light to deep red or magenta except during fall coloration when they appear a rusty-red brown (sometimes orangish-brown-red).

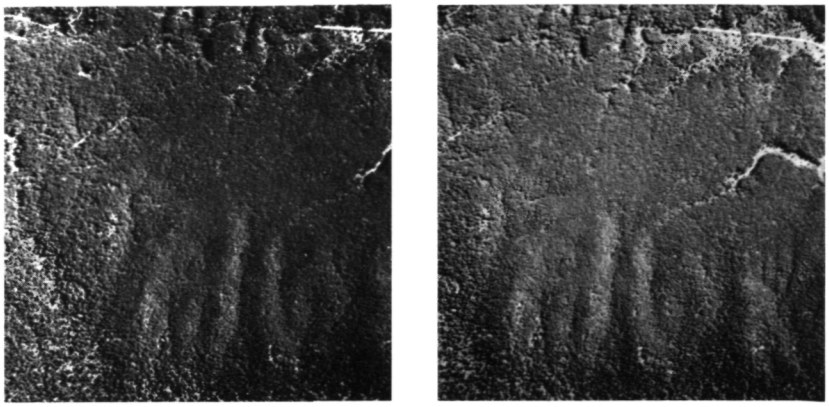

Figure 50. Oak stand, Crawford County.

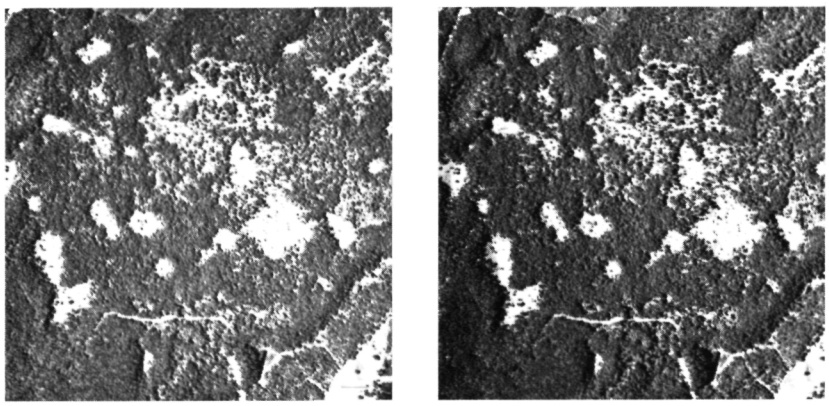

Figure 51. Oak forest cover type, Muskegon County.

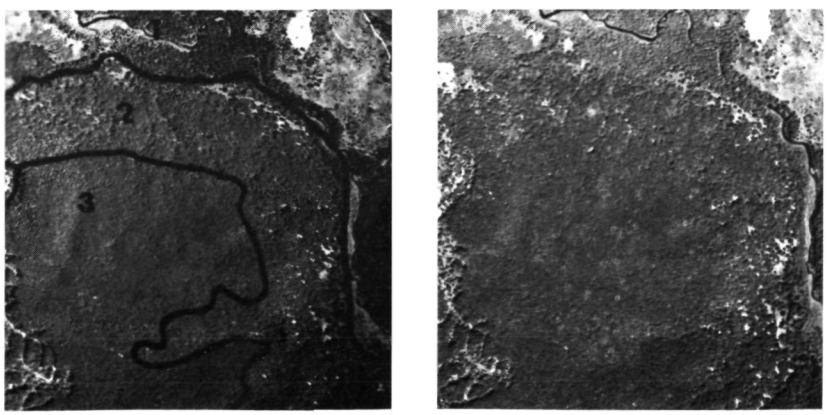

Figure 52. Forest cover types: 1) black spruce, 2) oak and 3) aspen.

Northern Hardwoods

Northern hardwoods is a broadly defined forest cover type used to describe several upland association. The major northern hardwood species is sugar maple in various mixtures including yellow birch, basswood, eastern hemlock and red maple. Sugar maple is dominant in most stands and is the most characteristic species. Other, associated species include: white ash, black cherry, red oak, white spruce, white pine and balsam fir.

The type is generally found on loamy soils with good fertility and moisture conditions, but may extend into sandy soils. The type covers extensive areas throughout Michigan, especially in the western U.P. Old-growth stands are typically uneven-aged, whereas many second growth stands are even-aged.

Because of the number of species and their associations, it is difficult to describe a typical stand. Most of the species are relatively shade tolerant and support a medium to large, irregularly rounded crown (Figure 53). Stand structure, especially in young, even-aged stands, appears solid and even (Figures 54 and 55). Although the crowns may be small and about the same size, they are irregular in outline when compared to aspen or white birch (Figure 56). Crown texture is a distinctive feature, especially when the stand is composed of a variety of species and/or tree and crown sizes, and appears rough with distinctive crown-edge shadowing (Figures 26, 57 and 58). The northern hardwood type displays variable colors within a stand, the colors ranging from shades of pink to dark red and creating a mottled effect (maples produce a distinctive pink color [Figure 30]).

Figure 53. Yellow birch illustrating a large, irregularly rounded crown.

Figure 54. Profile view of a northern hardwood stand illustrating the solid and even stand structure.

Figure 55. Schematic diagram of a northern hardwood stand illustrating horizontal (left) and vertical (right) views.

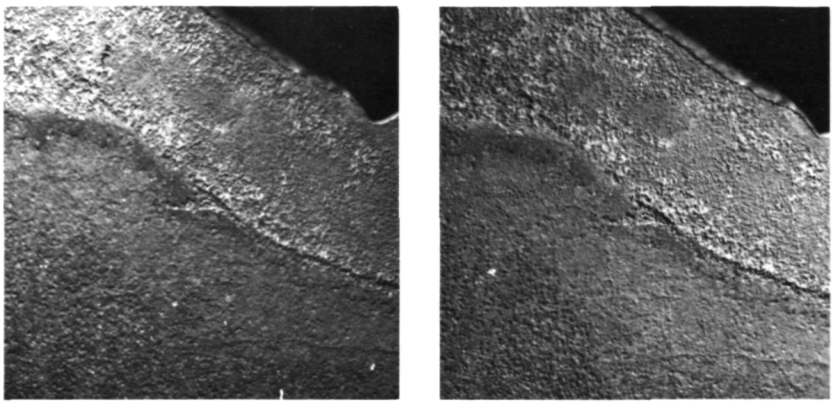

Figure 56. Northern hardwood stand, Alger County. Note the small but irregular crown shape.

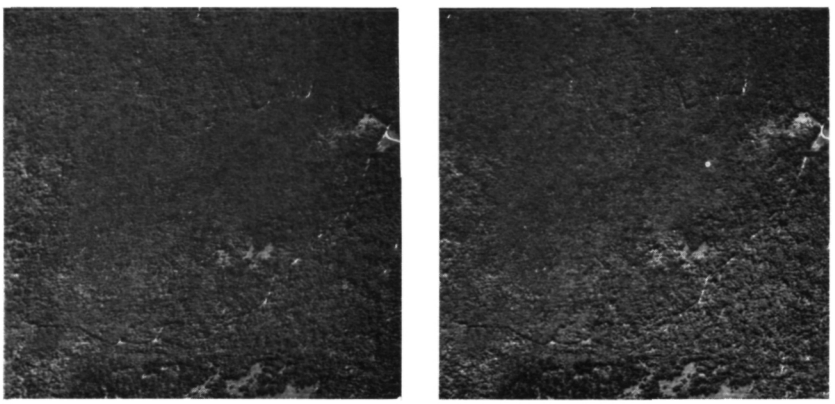

Figure 57. Northern hardwood stand, Alger County.

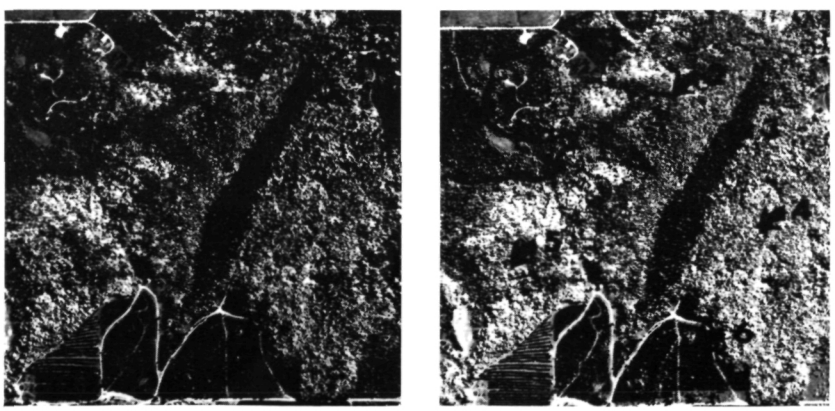

Figure 58. Forest cover types: 1) white pine plantation, 2) aspen, 3) scattered white pine over northern white-cedar, 4) northern hardwoods, 5) lowland hardwoods and 6) red pine plantations.

Lowland Hardwoods

Lowland, or swamp, hardwoods occur throughout the Northern Forest and into parts of the Central Forest. Occupying moist to wet mineral and muck or shallow peat soils, they are found in swamps, gullies and small depressions of slow drainage or in elongated areas along small sluggish streams, occasionally covering extensive areas. This type often grades into northern white-cedar on the wetter sites.

Principal species include black ash, elm, red maple and, in the northern Lower Peninsula, balsam fir. Common, associated species are: basswood, eastern hemlock, white birch, white pine, aspen, northern white-cedar, tamarack and black spruce. While the type is commonly found in the northern Lower Peninsula and the eastern U.P., it can be found in the southern Lower Peninsula or the western U.P. where site conditions are favorable.

The lowland hardwood species may be recognized by their large, ascending branches spreading from the trunk (Figure 59). When viewed from above, these branches display a characteristic forked or divided crown and produce a rough texture (Figure 60). The type is separated from aspen by its more broken and staggered stand pattern and from swamp conifers by the large, ascending branches and rounded crowns of the hardwoods (Figures 58 and 61).

The ground often appears as very dark colors beneath this type due to the open nature of the stands, soil moisture and under-story vegetation (Figures 60 and 62). Lowland hardwoods display a rough, uneven texture and vary in color from dark pink to purple (Figures 13 and 58). Because of their topographic location, lowland hardwoods are some of the first trees to show fall coloration (Figure 63). Bright shades of yellow, pink and greens are common of this type.

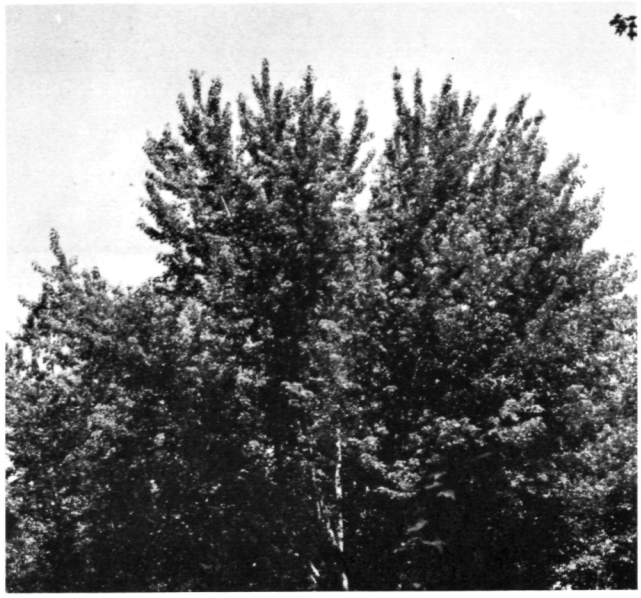

Figure 59. Red maple illustrating ascending branches, characteristic of many lowland hardwood species.

Figure 60. Schematic diagram of a lowland hardwood stand illustrating horizontal (left) and vertical (right) views.

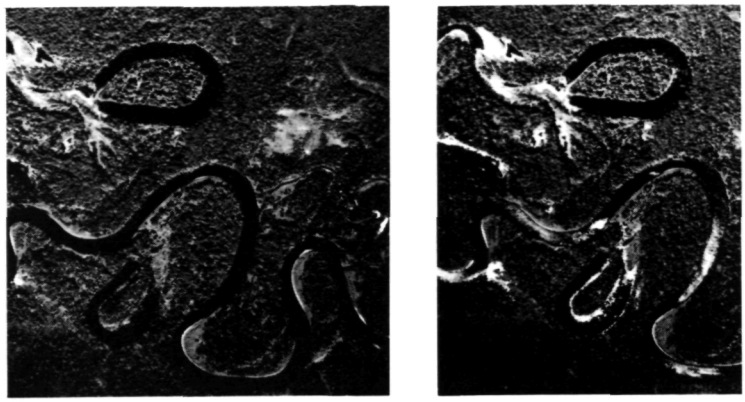

Figure 61. Lowand hardwood stand, Schoolcraft County.

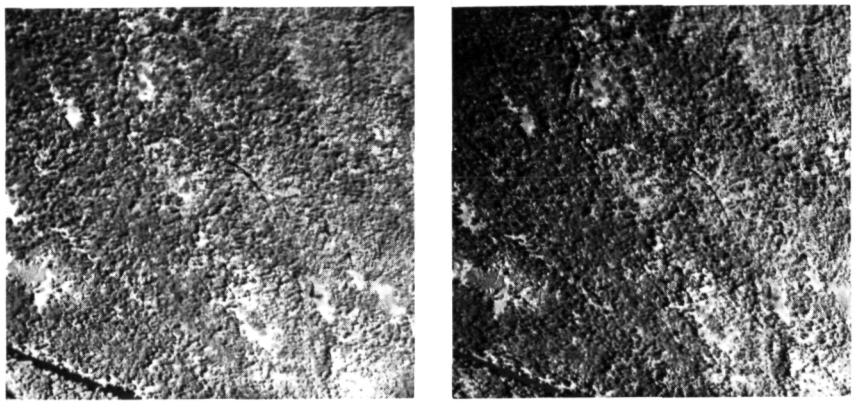

Figure 62. Lowland hardwood stand, Muskegon County.

Figure 63. Oblique view of lowland hardwoods showing fall coloration while the upland forest types are still predominantly green.

Nonforested Cover Types

Lowland Brush

Lowland brush (alder, dogwood, willow, etc.) often forms clumps of several crooked stems (Figure 64) which merge to form a continuous canopy. The crowns are indistinct and create a somewhat rough (wavy) texture (Figure 65). The canopy may be solid or broken by patches of open water, aquatic plants or scattered trees.

Lowland brush is distinguished from aspen reproduction by its topographic location, irregular stand pattern and lack of evidence of logging or other disturbance. This type normally appears in shades of "rusty-red" magenta.

Figure 64. Lowland brush illustrating characteristic stand profile.

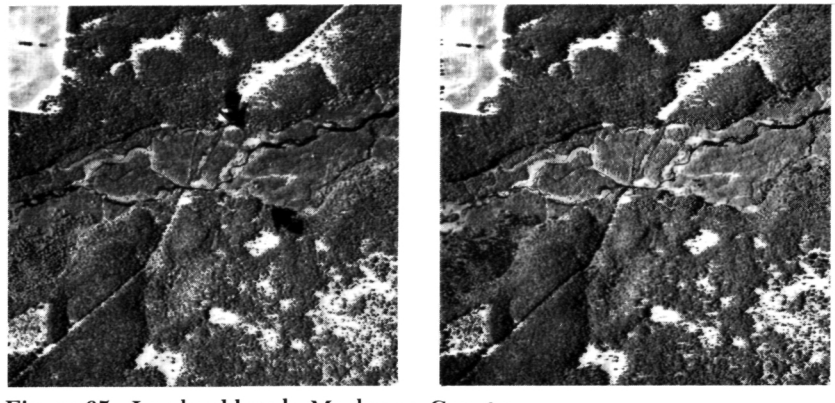

Figure 65. Lowland brush, Muskegon County.

Bog/Treed Bog

These areas of peat land or muskegs support mosses and low bog shrubs and occasionally a sparse stocking of tamarack, spruce, cedar, aspen or jack pine (Figure 66). Bogs follow the contour of a topographic low or depression and may contain open water in the middle. This type has a rusty-orange or rusty-light-brown color and presents a smooth to grainy texture (Figure 67).

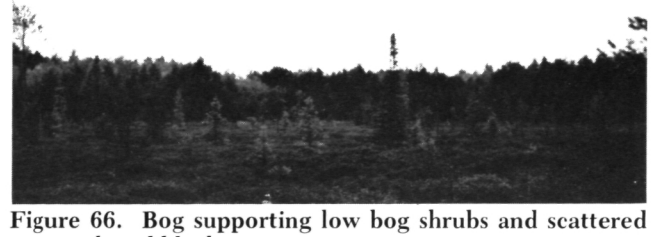

Figure 66. Bog supporting low bog shrubs and scattered tamarack and black spruce.

Figure 67. Bog, Missaukee County; the scattered trees are tamarack.

Upland Grass

These upland sites contain less than 10% stocking of tree species or shrubs and are dominated by either grass, ferns or blueberries (Figure 68).

Upland grass areas display an extremely smooth texture with no detectable pattern or shape (Figure 69). The color of natural grass is light magenta to light blue or cyan in contrast to the brighter red magenta of managed grass (Figure 70).

Figure 68. Upland grass with less than 10% stocking of trees or shrubs.

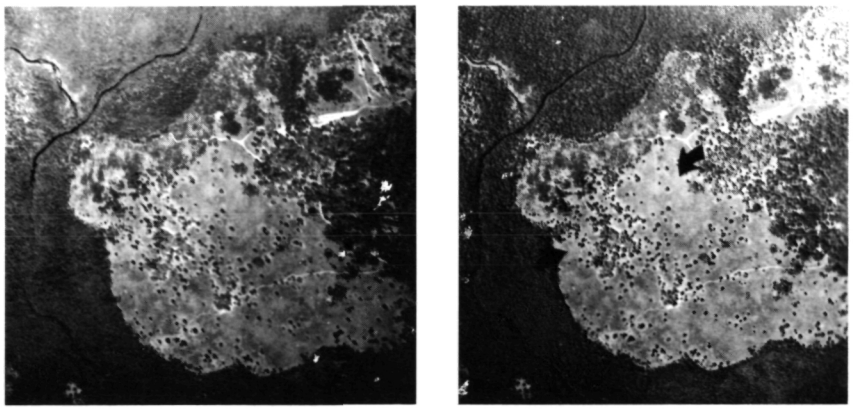

Figure 69. Upland grass, Montmorency County.

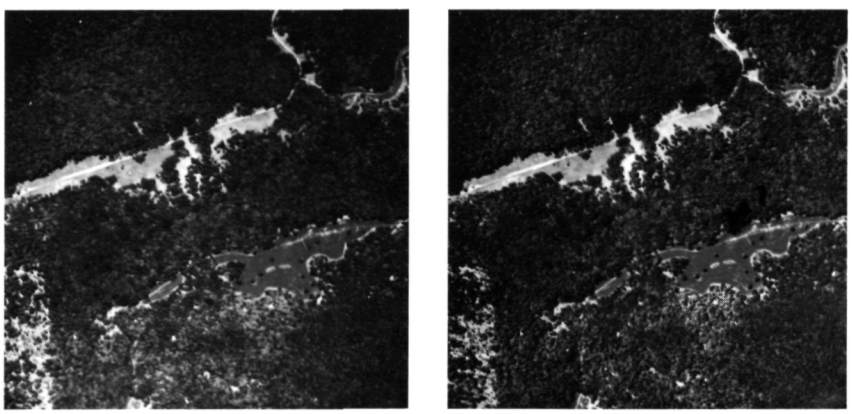

Figure 70. Comparison of natural grass (2) with an area of managed grass (1).

Upland Brush

These upland sites, mesic to dry, support at least 10% stocking of upland shrubs (briars, dogwood, sumac, etc.) (Figure 71). The upland brush type is moderately rough, may have slight shadow patterns and appears light pink to dark blue magenta (Figure 72).

Figure 71. Upland site with more than 10% stocking of upland shrubs (pin cherry and oak sprouts).

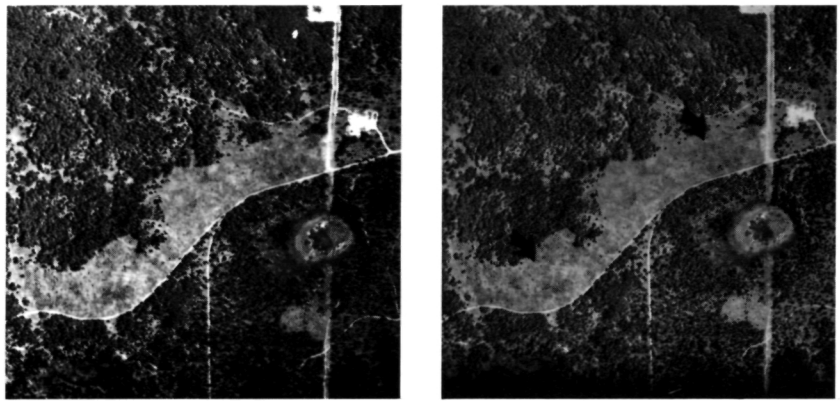

Figure 72. Upland brush, Kalkaska County.

References

Arend, J.L. and Scholz, H.F. 1969. Oak Forests of the Lake States and Their Management. North Central Forest Exp. Stn., St. Paul, Minn., U.S.D.A. For. Serv. Res. Paper NC-31.

Barnes, B.V. and Wagner, W.H., Jr. 1981. Michigan Trees. Univ. Mich. Press, Ann Arbor, Mich.

Chase, C.D. and Korotev, J.R. 1947. Key to Forest Types in Marinette County, Wisconson, on Infrared with Minus Blue Filter at 1:12.000. Autumn Pictures. U.S. Forest Service.

Eyre, F.H. (editor). 1980. Forest Cover Types of the United States and Canada. Society of American Foresters, Wash., D.C.

Heller, R.C., Doverspike, G.E. and Alrich, R.C. 1964. Identification of Tree Species on Large-Scale Panchromatic and Color Aerial Photographs. Agric. Handbook No. 261, U.S. Dept. Agric. For. Serv., Wash., D. C.

Hudson, W.D., Amsterburg, R.J., Jr. and Myers, W.L. 1976. Identifying and Mapping Forest Resources From Small-Scale Color-Infrared Airphotos. Research Rep. 304. Mich. State Univ. Agric. Exp. Stn., East Lansing, Mich.

Little, E.L., Jr. 1971. Atlas of United States Trees.-Volume I. Conifers and Important Hardwoods. Misc. Pub. No. 1146, U.S. Dept. Agric. For. Serv., Wash., D.C.

Little, E.L., Jr. 1977. Atlas of United States Trees. Volume 4. Minor Eastern Hardwoods. Misc. Pub. No. 1342, U.S. Dept. Agric. For. Serv., Wash., D.C.

Little, E.L., Jr. 1979. Checklist of United States Trees (Native and Naturalized). Agric. Handbook No. 541, U.S. Dept. Agric., For. Serv., Wash., D.C.

Region Nine, U.S. Forest Service. 1947. Stereograms, Sample Forest Condition Classes, Lake States Area, Modified Infra Red Photography. U.S. Dept. Agric. For. Serv., Region Nine.

Sayn-Wittgenstein, L. 1960. Recognition of Tree Species on Air Photographs by Crown Characteristics. Can. Dept. For., For. Research Branch Tech. Note No. 95.

Sayn-Wittgenstein, L. 1960b. Phenological Aids to Species Identification on Air Photographs. Can. Dept. For., For. Research Branch Tech. Note No. 104.

Sayn-Wittgenstein, L. 1961. Recognition of Tree Species on Air Photographs by Crown Characteristics. Photogrm. Eng. 27:792-809.

Sayn-Wittgenstein, L. 1978. Recognition of Tree Species on Aerial Photographs. Can. For. Serv., Dept. Environ., For. Manage. Inst., Int. Rep. FMR-X-118.

Zsilinszky, V.G. 1966. Photographic Interpretation of Tree Species in Ontario. Ontario Dept. of Lands and Forests.

Appendix

Common and Scientific Names[1] of Tree Species

balsam fir	*Abies balsaemea*	pin cherry	*Prunus pensylvanica*
balsam poplar	*Populus balsamifera*	quaking aspen	*Populus tremuloides*
basswood	*Tilia americana*	red maple	*Acer rubrum*
beech	*Fagus grandifolia*	red oak	*Quercus rubra*
bigtooth aspen	*Populus gradidentata*	red pine	*Pinus resinosa*
black ash	*Fraxinus nigra*	shagbark hickory	*Carya ovata*
black cherry	*Prunus serotina*	sugar maple	*Acer saccharum*
black oak	*Quercus velutina*	tamarack	*Larix laricina*
black spruce	*Picea mariana*	white ash	*Fraxinus americana*
elm	*Ulmus sp.*	white birch	*Betula papyrifera*
hemlock	*Tsuga canadensis*	white oak	*Quercus alba*
jack pine	*Pinus banksiana*	white pine	*Pinus strobus*
northern pin oak	*Quercus ellipsoidalis*	white spruce	*Picea glauca*
northern white-cedar	*Thuja occidentalis*	yellow birch	*Betula alleghaniensis*

[1] *Scientific names are based on Little, 1979.*

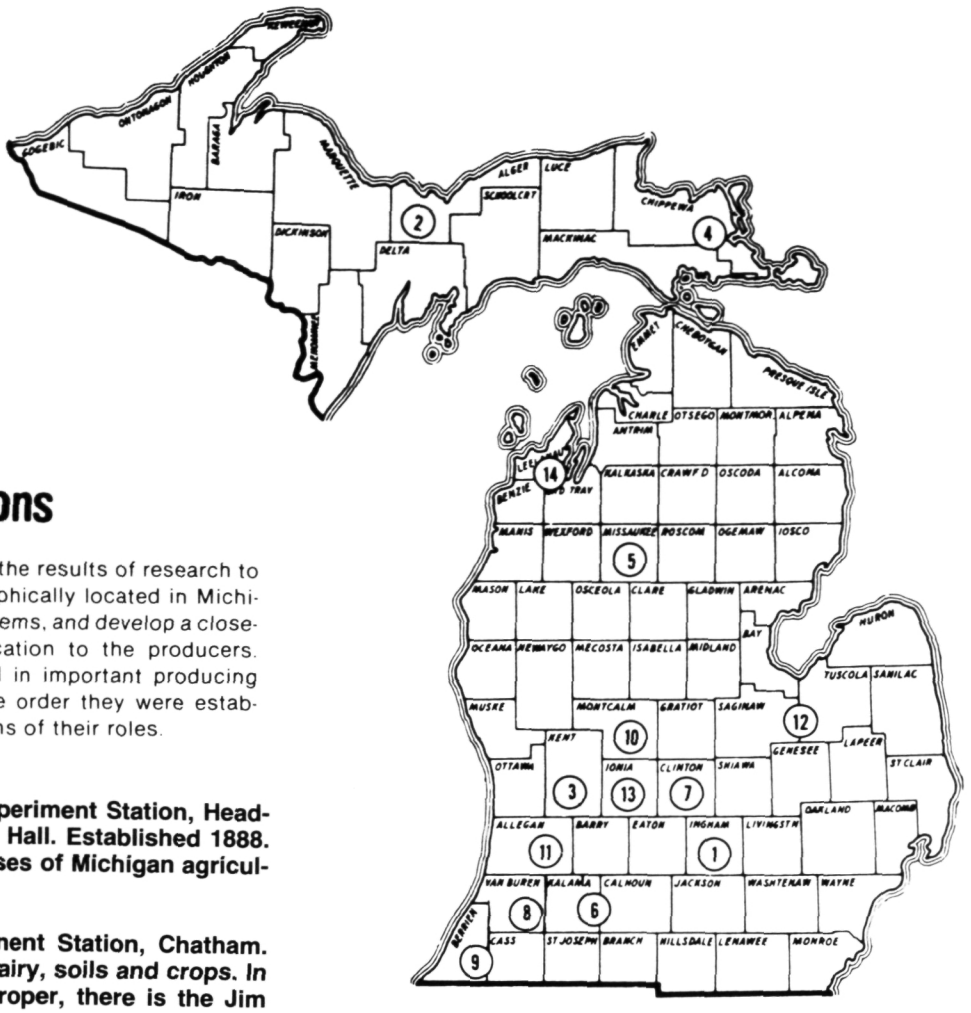

Outlying Field Research Stations

These research units bring the results of research to the users. They are geographically located in Michigan to help solve local problems, and develop a closeness of science and education to the producers. These 14 units are located in important producing areas, and are listed in the order they were established with brief descriptions of their roles.

1. **Michigan Agricultural Experiment Station, Headquarters, 109 Agriculture Hall. Established 1888. Research work in all phases of Michigan agriculture and related fields.**

2. **Upper Peninsula Experiment Station, Chatham. Established 1907. Beef, dairy, soils and crops. In addition to the station proper, there is the Jim Wells Forest.**

3. **Graham Horticultural Experiment Station, Grand Rapids. Established 1919. Varieties, orchard soil management, spray methods.**

4. **Dunbar Forest Experiment Station, Sault Ste. Marie. Established 1925. Forest, fisheries and wildlife management.**

5. **Lake City Experiment Station, Lake City. Established 1928. Breeding, feeding and management of beef cattle and fish pond production studies.**

6. **W. K. Kellogg Biological Station Complex, Hickory Corners. Established 1928. Natural and managed systems: agricultural production, forestry and wildlife resources. Research, academic and public service programs.**

7. **Muck Soils Research Farm, Laingsburg. Plots established 1941. Crop production practices on organic soils.**

8. **Fred Russ Forest Experiment Station, Decatur. Established 1942. Hardwood forest management.**

9. **Sodus Horticultural Experiment Station, Sodus. Established 1954. Production of small fruit and vegetable crops. (land leased)**

10. **Montcalm Experimental Farm, Entrican. Established 1966. Research on crops for processing with special emphasis on potatoes.**

11. **Trevor Nichols Experimental Farm, Fennville. Established 1967. Studies related to fruit crop production with emphasis on pesticides research.**

12. **Saginaw Valley Beet and Bean Research Farm, Saginaw. Established 1971, the farm is owned by the beet and bean industries and leased to MSU. Studies related to production of sugar beets and dry edible beans in rotation programs.**

13. **Clarksville Horticultural Experiment Station, Clarksville. Purchased 1974. First plots established 1978. Research on all types of tree fruits, small fruits, vegetable crops and ornamental plants.**

14. **Northwest Michigan Horticultural Experiment Station, Traverse City. Established 1979. Research and education for cherry and other horticultural crops in northwest Michigan.**

1-84-2.5M

ABSTRACT

A SYMBOLICALLY-ASSISTED APPROACH TO
DIGITAL IMAGE REGISTRATION
WITH APPLICATION IN COMPUTER VISION

By

Ardeshir Goshtasby

Analyzing a sequence of images from the same scene often requires image registration; that is, the process of determining the position of corresponding points in the images.

Two images taken from the same viewpoint from a two-dimensional scene can be registered if the position of at least two pairs of corresponding points in both images are known. However, images obtained at different viewpoints from a three-dimensional scene (such as stereo images) cannot be registered by knowing only the position of a few corresponding points in the two images, and a window search is often needed to individually determine the position of corresponding points.

Images from a two-dimensional scene that have translational, rotational, and scaling differences, are registered by first segmenting the images and determining

corresponding regions in both images. Corresponding regions are refined to obtain optimally similar regions. The centroids of corresponding regions are then used as corresponding points to determine the registration parameters. These centroids will correspond to each other regardless of translationsl, rotational, and scaling differences between the corresponding regions.

When registering stereo images of three-dimensional scenes, the images are segmented and a search is carried out for the position of points in one image that correspond to points on the region boundaries of the other image. Windows centered at region boundaries are used for the search because their high variances make searches more reliable than those using windows from homogeneous areas. To reduce the effect of geometric difference between the images in the window search process, window shapes are taken such that only parts of objects (and not objects and background) are used in the search. The position of corresponding points in two stereo images are used to determine disparity between these points. Depth of points in the scene can then be determined by knowing the disparity measures and the camera parameters.

Page intentionally left blank

Page intentionally left blank

TABLE OF CONTENTS

Adv. Space Res. Vol.2, No.8, pp.71-75, 1983
Printed in Great Britain.

0273-1177/83/080071-05$02.50/0

ASSESSMENT OF MODIFIED SURFACE TEMPERATURES AND SOLAR REFLECTANCE USING METEOROLOGICAL SATELLITE AND AIRCRAFT DATA

J. Bartholic*, S. Gage**, A. Goshtasby*** and C. Mason†

**Agricultural Experiment Station, **Department of Entomology, **Center for Remote Sensing, Michigan State University, East Lansing, MI 48824, U.S.A.*
†Department of Atmospheric and Oceanic Science, University of Michigan, Ann Arbor, MI 48104, U.S.A.

ABSTRACT

Changes in surface temperature resulting from the activities of man are evaluated using meteorological satellite (NOAA and HCMM) and aircraft data. Study sites were located in Florida and Michigan. Thermal data showed that day surface temperatures over large areas could be increased by 10-15°C by modifications resulting from agricultural practices. Changes in reflected solar radiation as a function of agricultural practices were detectable using HCMM data. 1/

INTRODUCTION

Through time, man is gradually modifying more of the earth's surface to optimize conditions for habitation. The changes are largely for crop production, animal grazing and utilization of biomass for cooking and heat. In this process forests are being converted to pastures and farmlands, grasslands are being grazed by domestic animals, new species of plants are being introduced and major portions of the surface are being drained or irrigated.

This process has evolved slowly over centuries, but has speeded up dramatically during this century. Increasing modification of the surface for food production has been an essential part of increasing the earth's carrying capacity from two billion at the turn of the century to over four billion at the present time. Further, these changes will be occurring at an increasingly rapid rate as the projected population of the earth doubles by the year 2020 [1].

Relatively few studies have assessed the magnitude of these changes or their impact on surface boundary conditions [2,4]. Many characteristics of the surface, including temperature, radiation and surface roughness, could be altered significantly. This paper shows that information available from the National Oceanic and Atmospheric Administration (NOAA) and NASA's Heat Capacity Mapping Mission (HCMM) satellites and airplane scanner data can help assess the impacts on surface temperature and radiation of man's modification of our planet.

METHODOLOGY

Several recently launched meteorological satellites have collected valuable data on reflected radiation in the .5 to 1.1 micron range. This band has the information needed for good estimates of solar reflectance from different surfaces [5]. Also, data from scanners sensing in the 10.5 to 12.5 micron range are available on several satellites which can be used to determine surface temperature. Accuracy and resolution of these systems is sufficient to characterize vegetative types and to provide answers about the magnitude of changes that might be expected with deforestation or other significant changes in existing vegetation.

NOAA satellite data provides one kilometer resolution in the thermal (10.5 to 12.5 microns). The satellite orbits over at approximately 1000 and 2200. The sun-synchronous HCMM satellite provides high resolution thermal data with a .6 km by .6 km resolution at nadir, in the 10.5 to 12.5 micron range. Also, the concurrent visible channel 0.5 to 1.1 microns with a dynamic range of approximately 100 percent albedo and resolution of .5 km by .5 km at nadir potentially will provide the essential data required to meet the objective of characterizing solar reflectance [6].

For the NOAA data, transparencies were used, digitized and analyzed on the Image 100 at the Kennedy Space Center. The HCMM data was obtained in both pictorial and digital forms. Ana-

---

1/Michigan Agricultural Experiment Station Journal Article Number 10531.

lysis was done at the Center for Remote Sensing and the Image Processing Laboratory at Michigan State University.

The digital HCMM reflected radiation data were used to find the relation between vegetation types and reflected values. The reflectance image was thresholded at different values and the regions showing the same reflectivity were isolated for each classification. The isolated regions were compared with an already classified Landsat image.

A Daedalus DS-1250 scanner with 8-14 microns thermal channel was flown to obtain high resolution inputs required to assist in the analysis. This data was acquired on analog tape then digitized and analyzed on the Image 100 at the Kennedy Space Center.

The study areas were mainly in Florida and Michigan. The NOAA satellite and aircraft data were obtained for Florida and HCMM data was used for analysis of the Michigan test site.

RESULTS

NOAA thermal satellite imagery for April 28, 1978 at about 1000 (Fig. 1) shows darker areas as warmer and lighter areas as cooler. The agricultural areas in the Mississippi Valley and the southern portions of the United States including Georgia, Alabama and South Carolina, plus major areas of Florida, are shown to be markedly warmer (darker) than the adjacent naturally vegetated areas. Separate analysis indicates that many of the darker areas are about 10-12°C warmer than the adjacent natural areas.

More detailed examination of the Florida peninsula is possible in Fig. 2 (note that warmer areas appear lighter, the reverse of Fig. 1). In April, many fields in north central Florida are tilled and crops do not yet cover a significant portion of the surface. These agricultural areas are in long, broad strips generally lying in a north-south direction and are much warmer. Some of the greatest thermal contrasts in southern Florida occur between the water conservation reserves in the Everglades and the adjacent agricultural areas that have been drained. The adjacent agricultural areas are to the north and just south of Lake Okeechobee. Both drainage and agricultural practices are affecting the surface conditions, causing temperatures to be significantly warmer than natural areas.

Image displays of aircraft thermal scanner data are shown in Figures 3A and 3B. Two dissimilar areas were chosen for study in the Taylor Creek watershed located north of Lake Okeechobee, Florida. The first area, shown in Fig. 3A, was primarily improved grass pastures used for grazing dairy cattle. The second area (Fig. 3B) includes pasture, marsh and a large citrus grove. The thermal data of Fig. 3A were obtained at 1222-1225 EST on April 28, 1978. Windspeed was 700 cm/sec, air temperature was 26.1°C and the relative humidity was 59 percent (dew point 11.1°C). Thermal data of Fig. 3B were obtained at 1432-1435 EST on April 26, 1978 and meteorological conditions were similar to those measured on April 28. These surface meteorological measurements were made at a height of 10m. A uniform general rain of about 3cm had fallen on the area two days prior to the flights. Soil moisture conditions were good for growth [3].

U.S. Highway 441 runs N-S through the image in Fig. 3A. To the east of the highway the effects of high dairy cattle population density are easily seen. In the irregularly-shaped areas heavy cattle traffic had eliminated plants. A mixture of sand and partially decomposed manure made up the surface cover. The surface temperatures in this area were greater than 42°C. Similarly, Field 1, which had apparently been cut for hay and then grazed heavily prior to April 28, showed little spring growth and temperatures were in excess of 42°C. Field 2 of the same species, primarily Pangola (Digitavia decumbeus) had been cut for hay but had not been grazed. It was in a healthy growing condition and ranged from 36-42°C. Field 3 was rather heterogeneous, containing patches of grass interspersed with broadleaved weeds and thinner stands of grass and ranged in temperature from 28-36°C. Evapotranspiration (ET) and heat flux values for Field 1 were 20 and 30 mw/cm^2, respectively, and for Field 3 with higher ET were 40 and 10 mw/cm^2 [3]. Wet areas with woody shrubs as the primary gound cover had the coolest temperatures in the scene with a range of 22-26°C.

In Fig. 3B the marsh vegetation was coolest (about 21-24°C) and the citrus ranged from 24-28°C. Pasture 1 was poorly managed and had temperatures from 31-38°C while Pasture 2 was not over-grazed and ranged in temperature from 24-31°C.

Fig. 4A shows the HCMM thermal infrared data over the northern lower peninsula of Michigan. This imagery is from September 26, 1979. Digital values showed that the agricultural areas were warmest when compared to other areas. Surface radiant temperature for agricultural areas average 20°C while the average radiant temperature for water was 8°C. The surface temperatures for other surface types fall between these two values. Average temperatures of surface types acquired from this scene are shown in Table 1. The distinct differences in temperatures between the surface types shows the relationship of surface temperature and surface types.

TABLE 1 Average Temperature for Different Surface Types as Obtained from HCMM Data on September 26, 1979 for the Northern Portion of the Lower Peninsula of Michigan

Surface Type	Average Temperature
Water	8°C
Swamp	15°C
Forest	17°C
Agricultural Areas	20°C

Fig. 4B is the HCMM reflectance image of the same scene. Again, digital values showed the dependency of reflectance to the surface types. Experiments showed that it is even possible to verify some vegetation types solely by their reflectance values. In Fig. 4B reflectance values between .07 and .08 are isolated in black, which show the coniferous areas very well (see the areas pointed to by the arrows). This was verified by referencing the Landsat classified image of August 1, 1975 [7], Fig. 4C. This shows that the HCMM satellite reflectance data can be used to characterize this earth surface parameter.

DISCUSSION

From the analysis of the satellite data, it is clear that man's activities have significantly altered massive portions of the earth's surface. These changes have, in turn, modified the planet's boundary temperatures. The change is not only large in area, but also in magnitude. Frequently 10-12°C warmer temperatures were found in agricultural areas when compared to the natural surface (Fig. 3 and 4). These modifications could significantly impact the thermal radiation leaving the earth's surface and the repartitioning of energy into sensible and latent fluxes.

Further, the aircraft thermal data vividly show (Fig. 3A and 3B) that even within the agricultural areas, as vegetation types are changed or overgrazing occurs, there can be further significant changes in the thermal regimes. These scenes showed overgrazed areas were greater than 42°C while well-watered nondormant pastures were approximately 30°C. For these temperature differences to occur, major differences in energy going into evapotranspiration must exist. Thus, the fluxes of vapor and heat are considerably different depending on how the surface is managed. These surface differences will ultimately impact the hydrological balance.

The impacts of these changes over the composite area of the Florida peninsula could potentially have significant impacts on local weather. Some evidence of this modification is visible in Fig. 5. Lake Okeechobee, which is a man-made lake, is shown to be modifying the cloud pattern over the southern portion of the Florida peninsula in this figure.

Modifications in a more temperate area are clearly shown by the example using HCMM data for the peninsula of Michigan. This analysis also showed that significant changes in reflectance could occur with changes in vegetation. Modifications in this reflectant component could have long term ecological implications since solar radiation is the main driving force for temperature increase, hydrological changes and biological processes.

CONCLUSION

Modifications of surface temperature and radiation were clearly observable from analysis of satellite data. Both the spatial distribution and magnitude of these changes can potentially be monitored using satellite data. Thus, some preliminary considerations for the habitability of areas of the earth can start to be developed. Of greatest concern, however, is that the population is expected to increase by an additional 50% by the turn of the century, so the process of change examined in this paper can be expected to accelerate in the years ahead.

REFERENCES

1. Council on Environmental Quality and Department of State. "The Global 2000 Report to the President: Entering the Twenty-First Century." Gerald O. Barney, Study Director. Washington, DC: Superintendent of Documents, U.S. Government Printing Office.
2. DiCristogaro, Donald Charles. "Remote Estimation of the Surface Characteristics and Energy Balance Over an Urban-Rural Area and the Effects on Surface Heat Flux on Plume

Spread and Concentration." M.S. Thesis, The Pennsylvania State University, November 1980.

3. Florida Water Resources Final Reports, Institute of Food and Agricultural Sciences, University of Florida. Jon F. Bartholic, Principal Investigator. Gainesville, Florida, NASA Contract NAS10-9398, 1979.
4. Gannon, P.T., Sr., J.F. Bartholic, R.G. Bill, Jr. "Climatic and Meteorological Effects of Wetlands." *Proceedings: National Symposium on Wetlands, American Water Resources* Association, 1978, pp. 571-588.
5. Gates, D.M. "Radiant Energy, Its Receipt and Disposal" in Agricultural Meteorology. Meteorological Monographs, Am Met Soc, Vol. 6, #28, 1965, pp. 1-26.
6. National Aeronautics and Space Administration. "Heat Capacity Mapping Mission (HCMM) Data Users Handbook for Applications Explorer Mission-A (AEM)." NASA, Goddard Space Flight Center, Beltsville, Maryland, October 1980.
7. Rogers, R.H. "Application of Landsat to the Surveillance and Control of Lake Eutrophication in the Great Lakes Basin," NASA, Goddard Space Flight Center, Beltsville, Maryland, Contract NAS 5-20942, September 1977.

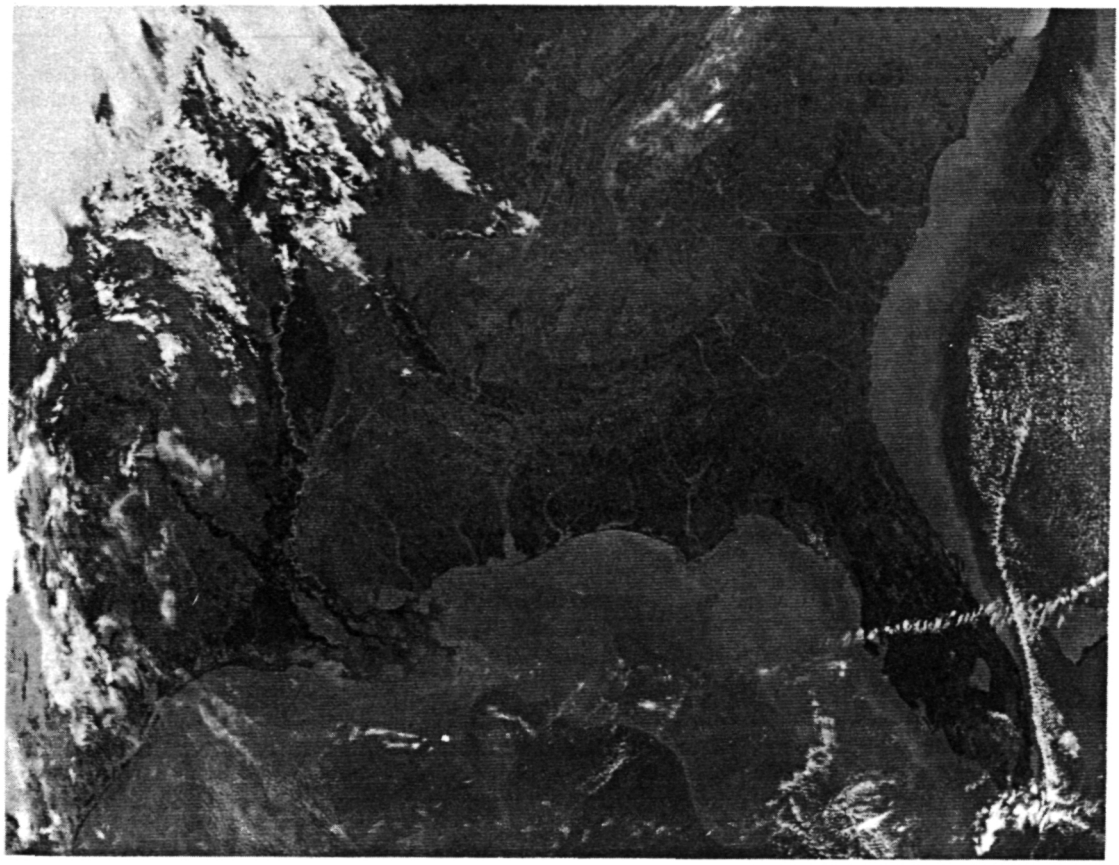

Fig. 1 Thermal scene for the eastern United States from NOAA satellite for 28 April '78 at about 1000.

Fig. 2 An expanded view of Fig. 1 showing mainly Florida.

A

B

Fig. 3 Images of aircraft thermal scanner data.

1=Field 1 3=Field 3
2=Field 2 4=Over Grazed
5=Barn

1=Pasture 1 3=Marsh
2=Pasture 2 4=Citrus

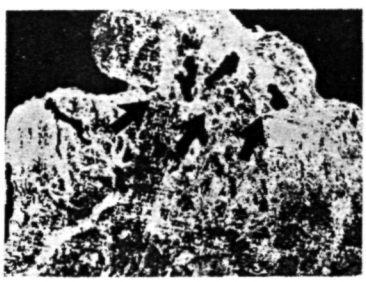

Fig. 4A

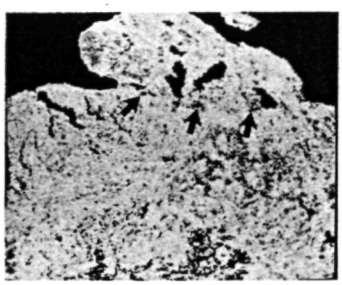

Fig. 4B

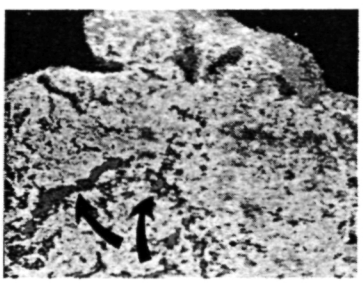

Fig. 4C

Fig. 4A HCMM Day-IR image of 26 Sept '79, Scene ID: A-A0518-18110-2.

Fig. 4B HCMM Day-Visible image of 26 Sept '79, Scene ID: A-A0518-18110-1.

Fig. 4C Classified Landsat data of 1 August '75 (2191-15453 and 2191-15460).

Fig. 5 A photograph from space looking south over the Florida peninsula.

NOTE: Arrows point to agricultural areas.